DISSERTATIONS IN
HEALTH SCIENCES

Sanna Suoranta

Skeletal and Neuroradiological Findings Related to Unverricht-Lundborg Disease (EPM1)

Publications of the University of Eastern Finland
Dissertations in Health Sciences

UNIVERSITY OF
EASTERN FINLAND

Skeletal and Neuroradiological Findings Related to Unverricht-Lundborg Disease (EPM1)

SUORANTA SANNA

Skeletal and Neuroradiological Findings Related to Unverricht-Lundborg Disease (EPM1)

To be presented by permission of the Faculty of Health Sciences, University of Eastern Finland for public examination at Kuopio University Hospital Auditorium, Kuopio,
on Friday, February 20th 2015, at 12 noon

Publications of the University of Eastern Finland
Dissertations in Health Sciences
Number 268

Departments of Clinical Radiology and Neurology,
Institute of Clinical Medicine,
School of Medicine, Faculty of Health Sciences,
University of Eastern Finland
Kuopio
2015

Kopio Niini Oy
Helsinki, 2015

Distributor:
University of Eastern Finland
Kuopio Campus Library
P.O.Box 1627
FI-70211 Kuopio, Finland
http://www.uef.fi/kirjasto

ISBN: 978-952-61-1705-8 (print)
ISBN: 978-952-61-1706-5 (PDF)
ISSNL: 1798-5706
ISSN: 1798-5706
ISSN: 1798-5714 (PDF)

Author's address:
Department of Clinical Radiology
Institute of Clinical Medicine
School of Medicine, Faculty of Health Sciences
University of Eastern Finland
Kuopio
Finland

Supervisors:
Professor Ritva Vanninen, M.D., Ph.D.
Department of Clinical Radiology
Institute of Clinical Medicine
School of Medicine, Faculty of Health Sciences
University of Eastern Finland
Kuopio
Finland

Professor Reetta Kälviäinen, M.D., Ph.D.
Department of Neurology
Institute of Clinical Medicine
School of Medicine, Faculty of Health Sciences
University of Eastern Finland
Kuopio
Finland

Reviewers:
Professor Riitta Parkkola, M.D., Ph.D.
Department of Radiology
University of Turku
Turku
Finland

Docent Jukka Peltola, M.D., Ph.D.
Department of Clinical Neurology and Rehabilitation
Tampere University Hospital
Tampere
Finland

Opponent:
Professor Osmo Tervonen, M.D., Ph.D.
Department of Diagnostic Radiology
Institute of Clinical Medicine
University of Oulu
Oulu
Finland

Suoranta, Sanna
Skeletal and Neuroradiological Findings Related to Unverricht-Lundborg Disease (EPM1)

Suoranta, Sanna
Skeletal and Neuroradiological Findings Related to Unverricht-Lundborg Disease (EPM1)
University of Eastern Finland, Faculty of Health Sciences
Publications of the University of Eastern Finland. Dissertations in Health Sciences 268. 2015. 106 p.

ISBN: 978-952-61-1705-8 (print)
ISBN: 978-952-61-1706-5 (PDF)
ISSNL: 1798-5706
ISSN: 1798-5706
ISSN: 1798-5714 (PDF)

ABSTRACT

Unverricht–Lundborg disease (EPM1) is the most common type of progressive myoclonic epilepsy clustered in Finland. It is caused by mutations in Cystatin B gene (*CSTB*) which is known to have role in neuroprotection and bone resorption. However, the exact pathogenesis of EPM1 and the role of *CSTB* in human function remain unknown. Despite the mutual genotype, the severity of the symptoms in EPM1 is heterogeneous. The main manifestations are observable in childhood or adolescence, which includes tonic–clonic epileptic seizures and progressively increasing stimulus-sensitive myoclonic jerks. An estimated one-third of the patients eventually become wheelchair-bound.

This study is a part of Finnish EPM1 clinical and molecular genetics consortium research. The main aim was to further deepen the understanding of the radiological findings of EPM1 and to connect these findings to the EPM1 patients' clinical phenotype. Altogether, 73 patients with EPM1 underwent 1.5 T head MR imaging in Kuopio University hospital during the period 2006–2010. MR images of the brain were examined by using the modern MR image analysis methods, cortical thickness analysis and texture analysis. Furthermore, the skeletal abnormalities of EPM1 patients were evaluated by quantitating calvarial MR findings and interpreting the x-rays and computed tomography studies collected from the medical records of the Finnish health institutions.

The results show that EPM1 patients exhibit thickening of the skull and various bone abnormalities that link the *CSTB* mutation to bone metabolism. In visual assessment of MR images, focal brain abnormalities were not found but cortical thickness analysis and texture analysis revealed subtle brain changes in patients with EPM1. The patients with the severe form of disorder exhibit regional thinning of the cerebral cortex, including areas involved in higher-order cognitive functions providing anatomical-biological background for cognitive variation in EPM1. Texture analysis revealed textural changes in thalamus and right putamen compared to the healthy controls supporting the thalamic and putaminal involvement in the pathophysiology of EPM1.

In conclusion, this study provides new and updated information on EPM1 patients' skeletal characteristics. Modern MR Image analysis methods provide new data from visually normal brain MR images that gave also new insights for the pathogenesis of EPM1.

National Library of Medical Classification: WL 385, WN 185, QU 500
Medical Subject Headings: Unverricht–Lundborg syndrome; Magnetic Resonance Imaging; Brain; Cystatin B/genetics; Myoclonic Epilepsies, Progressive; Phenotype; Bone Resorption

Suoranta, Sanna
Unverricht-Lundborgin taudin (EPM1) luusto- ja neuroradiologiset löydökset
University of Eastern Finland, Faculty of Health Sciences
Publications of the University of Eastern Finland. Dissertations in Health Sciences 268. 2015. 106 s.

ISBN: 978-952-61-1705-8 (nid.)
ISBN: 978-952-61-1706-5 (PDF)
ISSNL: 1798-5706
ISSN: 1798-5706
ISSN: 1798-5714 (PDF)

TIIVISTELMÄ

Unverricht-Lundborgin tauti (EPM1) on yleisin progressiivisen myoklonisen epilepsian muoto, ja sitä tavataan eniten maailmassa Suomessa. Taudin syynä ovat *CSTB*-geenin virheet, joilla tiedetään olevan merkitystä hermokudoksen suojauksessa ja luun metaboliassa, mutta EPM1:n tautipatogeneesi ja CSTB:n tarkka rooli ihmiselimistössä ovat vielä selvittämättä. Huolimatta yhteisestä genotyypistä, taudin oireiden vaikeus on vaihtelevaa. EPM1:n pääpiirteisiin kuuluvat lapsuus- tai nuoruusiässä puhkeava oireisto, epileptiset tajuttomuuskouristuskohtaukset sekä vähitellen pahenevat ärsykeherkät lihasnykäykset, joiden seurauksena noin kolmannes potilaista joutuu pyörätuoliin.

Tämä tutkimus on osa suomalaista, kliinistä ja molekyyligeneettistä EPM1-tutkimusta. Tutkimuksen tarkoituksena oli syventää sitä, mitkä EPM1:n radiologiset piirteet vaikuttivat sairauden vaikeusasteeseen. Kaiken kaikkiaan 73 potilaalle tehtiin aivojen 1.5 T magneettikuvaus Kuopion yliopistollisessa sairaalassa 2006–2010. Magneettikuvat jatkoanalysoitiin moderneilla magneettikuva-analyysimenetelmillä, korteksin paksuusanalyysillä sekä tekstuurianalyysillä. Lisäksi potilaiden luuston poikkeavuuksia tutkittiin suomalaisista terveydenhuollon yksiköistä kerätyistä natiivirröntgen- ja tietokonetomografiatutkimusta sekä mittaamalla kallon luuston paksuutta magneettikuvista.

Tulokset osoittavat, että EPM1-potilailla on kallon luuston paksuuntumista sekä erilaisia luustolöydöksiä, mikä liittää *CSTB*-mutaation luustometaboliaan. Visuaalisessa tarkastelussa pään magneettikuvista ei löytynyt fokaalimuutoksia, mutta korteksin paksuusanalyysi ja tekstuurianalyysi paljastivat vähäisiä aivomuutoksia EPM1-potilailta. Vaikeaa tautimuotoa sairastavilla potilailla oli merkittävästi ohuempi aivokuori muun muassa alueilla, jotka osallistuvat korkeampiin kognitiivisiin toimintoihin, mikä tarjoaa anatomis-biologista taustaa EPM1-potilailla havaittavaan vaihteluun kognitiivissa toiminnoissa. Tekstuurianalyysi paljasti potilailta teksturaalisia eroavaisuuksia talamuksessa ja putamenissa terveisiin verrokkeihin verrattaessa, mikä tukee talamuksen ja putamenin osuutta EPM1:n patofysiologiassa.

Yhteenvetona, tämä tutkimus tarjoaa uutta tietoa EPM1-potilaiden luuston ominaisuuksista. Modernit magneettikuva-analyysimenetelmät tuovat uutta tietoa visuaalisesti normaaleista aivojen magneettikuvista, ja tutkimustulokset lisäävät myös ymmärrystä EPM1:n patogeneesistä.

Yleinen Suomalainen Asiasanasto: epilepsia; magneettitutkimus - aivot; kuvantaminen - lääketiede

It's been a hard day's night!
RINGO STARR

Acknowledgements

This study was a part of EPI-MRI project organized by Kuopio Epilepsy Center, Kuopio University Hospital in collaboration with the Folkhälsan Institute of Genetics and Neuroscience Center, University of Helsinki. The work was carried out in the Departments of Clinical Radiology and Neurology, University of Eastern Finland and Kuopio University Hospital during the years 2010–2015.

First and foremost, I would like to express my appreciation to all the EPM1 patients who have participated in this study.

I wish to express my deepest gratitude to my principal supervisor Professor Ritva Vanninen, for giving me the chance to prepare this thesis and introduce me to the fascinating field of medicine, radiological imaging. I am truly grateful for the opportunity to have excellent research and work facilities, and the comfort of warm social evenings at the cottage with colleagues and friends. Her support and supervision to my colleagues and researchers in the Department of Radiology is invaluable. I am grateful to my supervisor, Professor Reetta Kälviäinen for providing me the opportunity to work in this unique field of research. Her tenacious expertise in Finnish epilepsy research and clinics is remarkable.

I appreciate the time from all of the co-authors, of this project. Their support and guidance provided me with an excellent foundation in research and without them this may not have been possible.

Professor Anna-Elina Lehesjoki has been unravelling the mysteries of genetics and I have been honored for her contribution to this thesis and critical review of the first article. I want to thank Professor Hannu Manninen, the Head of the Department of Radiology, for his contagious attitude for work and review of X-rays used in this thesis.

I wish to offer my sincere thanks to neuroradiologist Päivi Koskenkorva, Ph.D., for the expert advice and support. Her contribution has included the interpretation of MR images of the patients and her original work, created the foundation for my thesis.

It's been a pleasure to work with physicists Mervi Könönen, M.Sc., and Eini Niskanen, Ph.D. They have always made time for simple questions and guidance. I admire their cunning problem solving skills and their ability to provide a solution. Mervi was the initial one to help me with the cases concerning the computer applications. Eini has performed the cortical thickness analyses in this thesis. I want to thank physicist Kirsi Holli-Helenius, Ph.D., Department of Radiology, Tampere University Hospital, for introducing me into the realm of texture analysis. The collaboration has been fruitful and hopefully will continue.

My warmest thanks belong to my co-authors; Jelena Hyppönen, Ph.D., who has collected the clinical data of the patients in the study; neuropsychologist Marja Äikiä, Ph.D., who performed neuropsychological tests and interpreted the data; Rita Laitinen, M.D., for the

initial measurements of the skulls; and Professor Esa Mervaala for his enthusiastic work with clinical neurophysiology and collaboration in manuscript revision.

I want to thank the official reviewers of this thesis, Docent Jukka Peltola and Professor Riitta Parkkola for valuable comments and concerns. I wish to thank Ewen MacDonald and Nick Hayward for their revision of the manuscripts written in English. I want to thank Paul Pletnikoff, M.Sc., for revising the English literature review of this thesis; in addition, for his support and friendship.

My dearest thanks I dedicate to Tuula Bruun, for her secretarial guidance whenever necessary. Tuula has edited this thesis, as well as assistance in the submission of the manuscripts. It's been a pleasure to work with Taina Airola, she was the first person I had contacted when considering research in radiology. I also want to thank Anne-Mari Kulhomäki and Marika Miinalainen for their invaluable secretarial help.

I owe my warmest gratitude to all my colleagues; which include senior physicians, radiologists, nurses, radiographers and physicists, for their patience when I began radiology. I am privileged to work with such amazing people; we have shared laughter in the coffee room and the rush of the ER. I especially, want to thank Jari Karonen, Ph.D., the Head of the Department of Radiology in Mikkeli Central Hospital; firstly, for converting me towards radiology, and now, for offering me the best possible work facilities I could ever wish for.

I want to thank my fellow Ph.D. candidates in the Department of Radiology during this project; Mikko Taina, Antti Muuronen, Taavi Saavalainen, Amro Masarweh and Suvi Rautiainen, for academic support, listening and sharing the thoughts. I am blessed with a bunch of friends and I wish to thank you all; we have shared many joyful moments. I want to acknowledge "The Best Book Club Ever", for the not-always-so-critical revising of books and life, accompanied with good food and company. My special thanks belong to Suvi Ullgren, a longtime friend; Tia Väisänen, for supportive and critical conversations during the last years; and Annariina Tervaniemi, for sharing the first year of study together and currently sharing the first professional moments in work life together as well.

My dearest thanks go to my family, cousins and relatives. You have supported me from the very beginning of my life from the tiny village to the big world. I miss you Ahti and Tintti and I wish you could have shared this day with us. I want to thank my parents Ilkka and Sirpa and my little sisters Kirsikka & Anniina and their spouses. At last, my beloved infinite source of questions, nephew Paavo and niece Marja, you are the sunshine of my life!

This study was financially supported by EVO grants 5772751 and 5063523 from Kuopio University Hospital, Strategic Funding for the UEF-BRAIN consortium from University of Eastern Finland, Finnish Brain Foundation, Neuroradiologists of Finland, Radiological Society of Finland and Instrumentarium Research Foundation.

Mikkeli, January 2015

Sanna Suoranta

List of the original publications

This thesis is based on following original publications:

I Suoranta S, Manninen H, Koskenkorva P, Könönen M, Laitinen R, Lehesjoki A-E, Kälviäinen R, Vanninen R: Thickened skull, scoliosis and other skeletal findings in Unverricht-Lundborg disease link cystatin B function to bone metabolism: *BONE, 2012;51(6):1016-24.*

II Suoranta S, Äikiä M, Niskanen E, Hyppönen J, Koskenkorva P, Könönen M, Mervaala E, Vanninen R, Kälviäinen R: Regional cortical thinning associates with neurocognitive profile in Unverricht-Lundborg disease (EPM1): *Submitted.*

III Suoranta S, Holli-Helenius K, Koskenkorva P, Niskanen E, Könönen M, Äikiä M, Eskola H, Kälviäinen R, Vanninen R: 3D texture analysis reveals imperceptible MRI textural alterations in the thalamus and putamen in progressive myoclonic epilepsy type 1, EPM1: *Plos ONE, 2013, 8, 7, e69905.*

The publications have been adapted with permission from the copyright owners.

Contents

Abbreaviations

2D	two dimensional
3D	three dimensional
ACC	anterior cingulate cortex
AD	autosomal dominant
AED	anti-epileptic drug
ANCOVA	analysis of covariance
ApoE	apolipoprotein
AR	autosomal resistant
BA	Brodmann area
BMD	bone mineral density
CLASP	constrained Laplacian-based automated segmentation with proximities
COST	cooperation in science technology
CPS	complex partial seizures
CSF	cerebrospinal fluid
CSTB	cystatin B
CSTB	cystatin B gene
$Cstb^{-/-}$	cystatin B deficient
CT	computed tomography
CTH	cortical thickness
CV	coefficient of variation
DBS	deep brain stimulation
DLPFC	dorsolateral prefrontal cortex
DRPLA	dentatorubral–pallidoluysian atrophy
DTI	diffusion tensor imaging
DXA	dual x-ray absorptiometry
EEG	electroenceplahography
EPM1	progressive myoclonic epilepsy type 1
EPM2	Lafora disease
FDR	false discovery rate
FIQ	full scale intelligence quotient
FLAIR	fluid attenuated inversion recovery
GABA	gamma-aminobutyric acid
GM	gray matter
GMS	gray matter surface
HFI	hyperostosis frontalis interna
ICC	intraclass correlation coefficient
ICV	intracranial volume
INSECT	intensity-normalized stereotactic environment for classification of tissues

IQ	intelligence quotient
JME	juvenile myoclonic epilepsy
LD	Lafora disease
MERRF	Myoclonic Epilepsy of Ragged-Red Fibres
MPRAGE	magnetization prepared rapid acquisition gradient echo
MRI	magnetic resonance imaging
MRS	magnetic resonance spectroscopy
NCL	neuronal ceroid lipofuscinosis
PET	positron emission tomography
PIQ	performance intelligence quotient
PME	progressive myoclonic epilepsy
ROI	region of interest
SE	status epilepticus
SUDEP	sudden unexpected death in epilepsy
TA	texture analysis
TBSS	tract-based spatial statistics
TE	echo time
TLE	temporal lobe epilepsy
TMT	trail making test
TR	repetition time
ULD	Unverricht–Lundborg disease, EPM1
UMRS	unified myoclonus rating scale
US	United States
VBM	voxel-based morphometry
VIQ	verbal intelligence quotient
VLPFC	ventrolateral prefrontal cortex
VMPFC	ventromedial prefrontal cortex
VOI	volume of interest
WAIS-R	Wechsler adult intelligence scale revised
WM	white matter
WMS	white matter surface

1 Introduction

Unverricht–Lundborg disease, also known as progressive myoclonic epilepsy type 1 (ULD, EPM1, OMIM254800) is an autosomal-recessively inherited rare neurodegenerative disorder that belongs to the Finnish disease heritage with the highest incidence in the world (1:20 000) in Finland (Norio, Koskiniemi 1979, Kestilä, Ikonen & Lehesjoki 2010). It was first described by Unverricht 1891 in Estonia and Lundborg 1901 in Sweden, and it is still more common in Baltic Sea area as well as in Mediterranean areas until the present times. Sporadic cases are reported worldwide. (Kälviäinen et al. 2008)

EPM1 is caused by the loss-of-function mutations in Cystatin B gene (*CSTB*) found partly by the Finnish researchers in 90's (Lehesjoki et al. 1991, Pennacchio et al. 1996). Because of the neurodegenerative nature of EPM1 it can be concluded that the Cystatin B protein (CSTB) has a neuroprotective role. This has been proven in several molecular genetics studies. CSTB is also involved in bone resorption by inhibiting cathepsin K which is the main proteolytic enzyme in human osteoclasts (Laitala-Leinonen et al. 2006). However, the exact pathogenesis of EPM1 and the fundamental role of CSTB in human physiology remain unknown.

The onset age of EPM1 is 6–16 years, before that the child develops normally. The most typical and first symptoms are tonic–clonic epileptic seizures and stimulus-sensitive myoclonic jerks. Initially, findings in neurological examination can be obscure but within the next 5–10 years motor symptoms slowly progress. Eventually, diagnosis is based on typical EEG finding, clinical examination and gene characterisation. Tonic-clonic seizures are usually well controlled with anti-epileptic drugs (AEDs). The disease is slowly progressive and the severity of symptoms ranges from mild motor difficulties in some of the patients to severe incapacitation in one third of the patients. (Kälviäinen et al. 2008)

Imaging studies of EPM1 are sparse because of the rarity of the disorder. One of the original studies from the 70's reports thickening of the skull and scoliosis in some patients with progressive myoclonic epilepsy (Koskiniemi et al. 1974) but systematic assessment of bony structures in EPM has not been performed to date. It is interesting that despite the progressive neurological symptoms, the neuroradiological findings in visual assessment of EPM1 brain remain sparse. There can be widespread mild to moderate cerebral and cerebellar atrophy but usually no focal signal changes of the brain are seen in patients with EPM1. However, the first radiological group analysis of patients with EPM1 performed by voxel-based morphometry (VBM) indicated motor cortex and thalamic atrophy that correlated with the degree of severity in myoclonus (Koskenkorva et al. 2009).

This work continues the previous radiological research on EPM1 being a part of Finnish clinical and molecular genetic consortium study conducted by the Kuopio Epilepsy Center at Kuopio University Hospital and Folkhälsan Institute of Genetics at the University of Helsinki. This doctoral thesis is focused to further investigate radiological findings of patients with EPM1 and to combine the radiological findings with patients' clinical data and neuropsychological findings. The skeletal structures of EPM1 patients were systematically assessed from head MR images, x-rays and computed tomography studies. Brain structures were evaluated by using modern MR image analysis methods; cortical thickness analysis (CTH) and texture analysis. Recently, CTH analysis has been applied in brain research both to better understand human brain function and to characterize structural changes in various neurodegenerative disorders. Texture analysis is

an old method first invented for satellite image analysis. It collapsed into oblivion but has experienced new coming in the field of medical imaging and so far, has not been applied widely in clinical research.

2 Review of literature

2.1 UNVERRICHT–LUNDBORG DISEASE (EPM1)

2.1.1 Overview of EPM1 and other progressive myoclonic epilepsies

Progressive myoclonic epilepsies (PMEs) comprise a heterogeneous group of rare neurodegenerative disorders, characterized by myoclonus, epileptic seizures and progressive neurological impairment. PMEs are categorized into six disease groups: Unverricht–Lundborg disease (ULD, EPM1), Lafora disease (LD, EPM2), Neuronal Ceroid Lipofuscinoses (NCLs), sialidosis, Myoclonic Epilepsy of Ragged-Red Fibres (MERRF) and Dentatorubral–pallidoluysian atrophy. Disease progression and genetic aetiology are common features to all PMEs. They are usually inherited in autosomal recessive manner, and the genetic defects for PMEs have been identified (Table 1). MERRF makes an exception with maternal/mitochondrial inheritance. (Shahwan, Farrell & Delanty 2005) Due to rarity of the disorders research is challenging; in other words pathogenesis and the specific cure for various PMEs remains to be investigated.

Main characters of PMEs are presented in Table 1. NCLs comprise a group of 14 progressive encephalopathies where altogether five types are associated with PME (Shahwan, Farrell & Delanty 2005, Haltia, Goebel 2012). The onset age of PMEs is usually in childhood as in infantile forms of NCLs, or in puberty like in Lafora disease or EPM1, whereas MERRF and DRPLA can erupt at any age. Clinical manifestations of PMEs are varying. Usually ataxia, dysarthria and incoordination occur, in Lafora disease in early teenage years whereas in EPM1 an older age. Also the prognoses of various PMEs are variable with early cognitive decline and progressive dementia in Lafora disease leading to death at an early age whereas no premature death is seen in EPM1. Most of the PMEs are very rare occurring only in certain geographical spots like DRPLA that is rarely seen outside Japan. (Shahwan, Farrell & Delanty 2005) Furthermore, not only EPM1 but also CLN1, CLN3, CLN5, CLN8 have a background in Finnish disease heritage (Kestilä, Ikonen & Lehesjoki 2010).

Table 1. Basic characteristics of progressive myoclonic epilepsies modified from Shahwan 2005, including the information from the references, Orphanet[1] and OMIM.

Disease	Inheritance	Gene	Onset age (years)	Characteristic symptoms	Cognitive decline	Prognosis
Unverricht–Lundborg disease	AR	*CSTB*	6–16	Onset: Stimulus-sensitive myoclonic jerks, generalized epileptic seizures Later: ataxia, dysarthria & incoordination	Mild, late or absent	Mild & variable: no major impairment vs. wheel-chair bound, no premature death
Lafora's disease	AR	*EPM2A* *NHLRC1*	12–17	Various type of seizures; Early ataxia and dysarthria; Later intractable seizures, SE & continuous myoclonus	Early and relentless, major dementia	Poor: after the onset, the life expectancy is 10 years.
MERRF	Maternal	*MTTK*	Any age	Myopathy, neuropathy, hearing loss, dementia, short stature, optic atrophy	Variable: ID & dementia	Progressive but variable
NCL						
CLN1: Santavuori–Haltia disease	AR	*PPT1*	½–1	Psychomotor regression, visual failure, seizures, myoclonus	Rapid mental retardation	Poor: Death about 10 years after the onset
CLN2: Classical late infantile (Janský-Bielschowsky disease)	AR	*TPP1*	2.5–4	Intractable epileptic seizures, rapidly progressing ataxia and psychomotor regression	Rapid mental regression	Poor: After the onset, life expectancy is 5 years
CLN3: Juvenile classic (Spielmeyer–Sjögren disease)	AR	*CLN3*	4–10	Starts with visual failure → blindness, extrapyramidal symptoms, seizures are not the prominent symptoms	Dementia, psychiatric problems	Poor: Death about 8 years after the onset
CLN4: A & B, Adult (Kufs disease)	A: AR B: AD Sporadic	A: *CLN6* B: *DNAJC5*	< 30	A: Like in EPM1 B: Dementia and extrapyramidal signs, no myoclonus	ID & dementia; Changes in personality in B	Survival is 15 years after the onset
CLN5: Finnish-variant late infantile	AR	*CLN5*	5	Clumsiness, hypotonia, visual impairment , ataxia, epilepsy	Mental retardation	Poor: Life expectancy is 20 years

CLN6: Variant late infantile	AR	*CLN6*	5–7	Motor and visual impairment, recurrent seizures	Decline in intellectual function	Poor: Death in the mid-twenties
CLN8: Northern epilepsy variant	AR	*CLN8*	6–10	Frequent tonic-clonic seizures, myoclonus in late phase	Progressive cognitive decline	Disability; Shortened life expectancy
Sialidoses						
Type I (Normomorphic)	AR	*NEU1*	8–25	Mild: Cherry spots, visual loss	ID	No premature death
Type II (Dysmorphic)	AR	*NEU1*	0-12	Severe: Facial dysmorphism & bone dysplasia	Psychomotor retardation	Poor
DRPLA	AD	*DRPLA*	1–60	Variable: classical PME to pseudo-Huntington-like phenotype	Variable ID to dementia	Variable; mean duration is 13 years

[1]Orphanet is a web site providing information about orphan drugs and rare diseases; OMIM = Online Mendelian Inheritance in Man; AR = autosomal recessive; AD = autosomal dominant; SE = status epilepticus; ID = Intellectual disability; MERRF = myoclonic epilepsy of ragged red fibres; NCL = neuronal ceroid lipofuscinosis; DRPLA = dentatorubral-pallodoluysian atrophy

2.1.2 Unverricht–Lundborg disease

Unverricht–Lundborg disease or progressive myoclonic epilepsy type 1 (EPM1, ULD, OMIM254800) is the most common type of PME. It is clustered in Finland with a prevalence of 4:100 000 people and an incidence of 1:20 000 births per year (Norio, Koskiniemi 1979, Kälviäinen et al. 2008). EPM1 is also more common in Baltic Sea and Western Mediterranean regions. Sporadic cases of EPM1 are reported worldwide, and it has been suggested that EPM1 is underdiagnosed. (Kälviäinen et al. 2008, Eldridge et al. 1983, Moulard et al. 2002, de Haan et al. 2004) The genetic background of EPM1 was identified 20 years ago to localise in chromosome 21q22.3 and it is caused by the loss of function mutations in Cystatin B encoding *CSTB* gene (Lehesjoki et al. 1991, Pennacchio et al. 1996).

2.1.2.1 Clinical characteristics

Before the manifestation of EPM1, child's cognitive and physical development is usually normal. The age of onset is 6–16 years peak being around the 12–13 years and the first symptoms are tonic–clonic epileptic seizures and stimulus-sensitive and action-activated myoclonic jerks (Kälviäinen et al. 2008, Genton 2010).

Myoclonus denotes sudden, involuntary twitching of muscles without any rhythmical pattern and it can be classified according to the aetiology, clinical signs or anatomic origin of myoclonic jerks (Dijk, Tijssen 2010). In EPM1, asynchronous focal or multifocal positive muscular contractions occur mainly in the proximal muscles of the extremities. They can be action-activated or stimulus sensitive, provoked generally by light, but also any other stimuli like stress, noise and physical exertion. On occasion, myoclonus proceeds into serious continuous myoclonic jerks i.e. status myoclonicus with inability to respond and; a situation, which may be difficult to differentiate from a generalized epileptic seizure. Anatomic origin of myoclonus in EPM1 is considered to be cortical but evidence of multilevel origins exist as well (Kälviäinen et al. 2008). Myoclonus, is the first symptom in over a half of the affected individuals, and the most disabling symptom affecting the daily life of a patient with EPM1 (Koskiniemi et al. 1974).

Separate from myoclonus, the seizure type seen in EPM1 is almost exclusively generalized tonic–clonic seizure (Norio, Koskiniemi 1979, Koskiniemi et al. 1974). Few video-EEGs of absence, simple motor or complex focal seizures have been documented but they might be just poorly diagnosed seizures of myoclonic origin. On rare occasions, tonic–clonic seizures are not present. (Kälviäinen et al. 2008)

In the following years after the onset of EPM1, symptoms will slowly progress. Nonetheless, in some cases of EPM1, the symptoms are so mild that it can lead to a delay of the diagnosis. In addition, there is variation in the speed of progression and severity of symptoms among the patients with EPM1. An individual patient's symptoms may fluctuate in terms of good days and bad days for years. (Kälviäinen et al. 2008) Myoclonus progresses within 5–10 years reaching a plateau, and motor symptoms including dysarthria, ataxia, intention tremor and incoordination, will develop. One third of the patients lose their ability to walk and handle the daily routine which leads to severe incapability and makes the patients wheel-chair bound, in some of the cases as early as in the twenties. Furthermore, based on the longitudal study of 20 years it has been suggested that EPM1 would progress only in a limited period (Magaudda et al. 2006). At the onset, seizures are occasional increasing in frequency during the following 3–7 years while at the later stages of the disorder, seizures may cease entirely with a suitable medication (Kälviäinen et al. 2008). The cause of the variation in the severity of the phenotype of EPM1 remains unknown. However, the most recent studies have shown that the

compound heterozygous patients exhibit a more severe form of disorder than the homozygous patients (Koskenkorva et al. 2011, Canafoglia et al. 2012).

2.1.2.2 Prognosis

Compared to the other PMEs, EPM1 has a relatively good prognosis (Shahwan, Farrell & Delanty 2005). As late as the 1970's, patients spent the last years of their life bed-bound and died on average under age of 30 years (Koskiniemi et al. 1974). This was supported by the use of an established AED phenytoin, which seemed to aggravate the associated neurologic symptoms or even accelerate the cerebellar degeneration in EPM1 (Eldridge et al. 1983, Iivanainen, Himberg 1982). When phenytoin was abandoned, both the life expectancy and the quality of life in EPM1 increased. The oldest genetically verified Finnish patients with EPM1 have lived into their seventies, and premature deaths due to pneumonia or suicide are seen more seldomly in EPM1 currently. (Kälviäinen et al. 2008, Shahwan, Farrell & Delanty 2005) However, unexpected deaths (SUDEP, sudden unexpected death in epilepsy) are reported also in EPM1 (Khiari et al. 2009).

2.1.2.3 Diagnosis

Diagnosis of EPM1 is based on typical clinical findings in a previously healthy child or adolescent between 6–16 years (Table 2). In neurological examination, the clinical findings may be initially sparse. However, imperceptible myoclonus provoked by a stimuli (photic: bright light; sudden loud noise) or an action (clapping of the hand, testing the reflexes) can be noted. Later myoclonus becomes more evident, though it should be noted that the patient has not taken additional benzodiazepam or alcohol before the examination, which can dispel the real symptoms.

Table 2. Diagnosis of EPM1 modified from Kälviäinen et al. 2008.

A)	Previously healthy child with onset age of 6–16 years	
B)	Two of the following symptoms or findings	
	1) Myoclonus	Involuntary: stimulus-sensitive or action-activated
	2) Seizure	Generalized tonic–clonic
	3) Motor dysfunction	Mild difficulties in gross motor functions or coordination
	4) EEG	Marked photosensitive, generalized spike-and wave and polyspike and wave paroxysm in EEG. The EEG background activity varies from normal to mildly slowed and remains stable over time
	5) MRI	Normal or signs of cortical or central atrophy, no focal pathology
	6) Progression	Gradual progression of the symptoms, ataxia and myoclonus
C)	Gene test	

MRI is performed for the differential diagnostic purposes to verify seizure aetiology while at the time of the diagnosis, almost without exception, the brain MR image finding of a patient with EPM1 is normal (Kälviäinen et al. 2008).

The characteristic findings from an EEG may already be observed at the onset of EPM1 being more pronounced at the initial stages of the disorder. The typical findings include a normal or moderately slow background activity, and generalized fast spike or polyspike and wave discharges (Koskiniemi, Toivakka & Donner 1974, Ferlazzo et al. 2007). The discharges are provoked typically by photic stimulation, but they can also be provoked by other stimulus, or spontaneously. Also evidence of focal epileptiform EEG changes mainly from the occipital region have been observed (Kälviäinen et al. 2008). Similarly to the stabilization of tonic–clonic seizures, EEG changes may reduce over time while the background activity remains stable (Ferlazzo et al. 2007).

Eventually, genetic testing confirms the diagnosis of EPM1 (Kälviäinen et al. 2008). Gene testing should be performed, when there is considerable reason to suspect the diagnosis of EPM1 (symptomatic cases), not as screening test.

The main consideration in the differential diagnosis of EPM1 is juvenile myoclonic epilepsy (JME). JME is a relatively common form of genetic generalized epilepsy representing 10 % of all epilepsies (Kälviäinen 2007). It shares several resemblances with EPM1 including onset at 12–18 years, tonic–clonic seizures, occasional myoclonic jerks and similar epileptiform EEG findings. JME has a more benign outcome, so initially the mild cases of EPM1 can be misdiagnosed as JME. In JME neurological examination is, however always normal and myoclonic jerks do not interfere with daily functions. Eventually, other PMEs should be suspected in an affected individual if the symptoms are severe and progress more quickly than expected.

2.1.2.4 Treatment

Similar to other PMEs, there is currently no specific cure for EPM1 and the treatment remains palliative consisting of combination of symptomatic AEDs and antimyoclonic drugs, lifelong rehabilitation and comprehensive psychosocial support (Kälviäinen et al. 2008). Medication is a challenge, even if the majority of various AED's have a good response to convulsive seizures the response for the most disabling symptom in EPM1, myoclonus, stands poor. However, valproate is a drug of choice for seizures and myoclonus control, and it can be used as a monotherapy in mild cases (Norio, Koskiniemi 1979, Kälviäinen et al. 2008, Iivanainen, Himberg 1982). Normally, a more effective therapy is needed and valproate is added with clonazepam or newer drugs, piracetam, topimarate and levetiracetam (Kälviäinen et al. 2008, Shahwan, Farrell & Delanty 2005, Iivanainen, Himberg 1982). A recent single center study showed that polytherapy with valproate was in use by all patients with EPM1. Improvement in myoclonia was recorded for the majority of patients with either add-on piracetam, topiramate, or levetiracetam but add-on AED treatment was also often associated with significant adverse effects (Roivainen, Karvonen & Puumala 2014). It should be noted that there is a spectrum of other AED's (for example phenytoin, carbamazepine, oxcarbazepine, pregabalin), which can increase the symptoms of EPM1 and should be avoided (Kälviäinen et al. 2008, Shahwan, Farrell & Delanty 2005). In acute cases of generalized status myoclonus benzodiazepines, valproate and levetiracetam are used intravenously (Kälviäinen et al. 2008).

Based on suggested deficit in dopaminergic inhibitory neurotransmission, dopamine D2-receptor agonist ropinirole seemed to diminish motorical symptoms as an experimental add-on treatment in a case study of one patient (Mervaala et al. 1990, Karvonen et al. 2010). Third-generation AED brivaracetam has shown promising results in preliminary studies and is under investigation for treatment of myoclonus (Kälviäinen et al. 2008, Tai, Truong 2005).

2.1.3 Neuropsychological studies in EPM1

There are few studies of cognitive function in EPM1 found in literature. The first study by Koskiniemi et al. evaluated a population of 93 patients with stimulus-sensitive myoclonus, epileptic seizures, onset age 5–16 years, characteristic EEG and progressive course (Koskiniemi et al. 1974) that can now be considered as EPM1. They found that full scale Intelligence Quotient (FIQ) scores were variable alternating from 55 to 129. A negative correlation between age and FIQ was found.

Previously, it has been stated that the intellectual functioning in EPM1 is normal in most of the patients but mild to moderate intellectual dysfunction or mild dementia in single patients with EPM1 have also been reported (Magaudda et al. 2006, Mazarib et al. 2001, Chew et al. 2008). However, neuropsychological assessment of 20 patients with EPM1 revealed broad variability in cognitive functioning ranging from normal to moderately impaired where the mean of FIQ was 68. Attention and short-term memory were identified the main functions impaired but long-term memory, visual perception and visuospatial reasoning remained as less impaired cognitive domains. On the contrary to the Koskiniemi et al., no significant correlation was found between the duration of the disorder and FIQ scores (Ferlazzo et al. 2009). Furthermore, comparison between patients with EPM1 and patients with cryptogenic temporal lobe epilepsy or healthy controls found that particularly processing and executive functions were impaired in EPM1 (Giovagnoli et al. 2009).

Psychiatric disorders have not been widely investigated in EPM1. Mental disturbances are reported in individual patients with EPM1 including depression, anxiety, aggressiveness and mood lability. Particularly depression has been observed (Magaudda et al. 2006, Chew et al. 2008, Ferlazzo et al. 2009) and studies have also reported suicides following severe depression (Koskiniemi et al. 1974, Khiari et al. 2009).

2.1.4 Previous imaging studies of EPM1

2.1.4.1 Skeletal involvement in EPM1

Extracerebral imaging studies in EPM1 are sparse. As early as in 1970's Koskiniemi et al. reported thickening of the skull and thoracic scoliosis (Koskiniemi et al. 1974) from a series of 31 patients. Later Korja et al. reported hyperostosis frontalis interna -type of skull thickening from the head MRI of four EPM1 patients (Korja et al. 2007a). Thickening of the skull has also been reported in a case report of a patient with two different mutations, both EPM1 and myotonic dystrophy, who had a thick bony structure of the skull in MRI but no focal pathologic changes in the brain parenchyma were observed (Nokelainen et al. 2000).

2.1.4.2 Imaging of the brain in EPM1

Studies concentrating on radiological evaluation in EPM1 are still scanty (Table 3). Most of the EPM1 imaging studies list individual patients' findings rather than are based on group analysis.

In direct visual inspection of the brain, findings remain scarce in patients with EPM1. In CT or MR images, generalized brain atrophy or mild to moderate atrophic changes both in cerebrum and cerebellum have been reported in individual patients (Koskenkorva et al. 2009, Chew et al. 2008, Giovagnoli et al. 2009, Parmeggiani et al. 1997, Mascalchi et al. 2002, Korja et al. 2007b, Santoshkumar, Turnbull & Minassian 2008). Focal changes in the brain parenchyma are not commonly found in patients with EPM1. White matter lesions

are reported in 2 of 8 patients in a study describing the clinical characteristics of EPM1 (Chew et al. 2008). White matter changes were found in 8 patients from a total of 13 patients compared to the healthy controls and long-term epilepsy patients. Five of patients with EPM1 had T2-weighted high-intensity signal changes in basal ganglia especially in the right (Korja et al. 2010). However, most of the studies in patients with EPM1 report no focal changes in the brain parenchyma (Nokelainen et al. 2000, Mascalchi et al. 2002, Koskenkorva et al. 2012).

More recently, modern MR image analysis methods have been able to detect more specific changes in brain of EPM1 patients. A MRI-based morphometry evaluation of 10 homozygous patients with EPM1 has represented loss of neuronal volume in the brainstem; basis pontis, medulla and cerebellar hemispheres, whereas significant changes were not found in vermis, middle cerebellar peduncule and fourth ventricle compared to the controls (Mascalchi et al. 2002). The study also obtained magnetic resonance spectroscopy (MRS) of the pons and dentate, and showed significantly reduced *N*-acetylaspartate/creatine (NAA/Cr) and choline/creatine (Cho/Cr) ratios in the pons (Mascalchi et al. 2002). Another study with MRS has reported that the lactate concentration was increased in the cerebrospinal fluid (CSF) in one compound heterozygous patient (Koskenkorva et al. 2011).

Voxel-based morphometry (VBM) has shown loss of grey matter volume bilaterally in motor cortex, cuneus and thalami in patients with EPM1 compared to the healthy controls (Koskenkorva et al. 2009). Also, the right cuneus and left lateral orbital gyrus were involved. There was no difference in grey matter volume between the patients with shorter and longer duration of the disease. Furthermore, patients with EPM1 showed widespread cortical thinning compared to the healthy controls in cortical thickness analysis study (Koskenkorva et al. 2012). The affected areas included sensorimotor, visual and auditory cortices. The age-related thinning of the cortex was diffuse in healthy controls whereas in patients with EPM1 the thinning was confined to more limited areas, and also the duration of disease was negatively correlated with cortical thinning in same regions as the age effects in patients with EPM1. There was also a significant negative correlation between the scores measuring the severity of myoclonus (Myoclonus with Action score) and cortical thickness in patients with EPM1. In other words, the areas of regionally reduced cortical thickness were parallel with the severity of the action myoclonus symptoms.

Translational study in patients with EPM1 and *Cstb*$^{-/-}$ mice showed widespread changes in white matter resulting in axonal degeneration and white matter loss (Manninen et al. 2013). WM changes were especially seen in subcortical WM, thalamocortical system and cerebellum. The study provided new aspects of motor disability in EPM1 relating not only to the cortical changes but also deeper WM structures.

Finally, higher binding potential of the D2-like receptor antagonist ([11C]raclopride) in the thalamus, nucleus caudatus and putamen have been reported in a PET study of four patients with EPM1 compared to the healthy controls suggesting a dopamine depletion in the thalamostriatal area in EPM1 (Korja et al. 2007b).

Table 3. Brain imaging findings in EPM1.

	Modality	**Number of patients imaged (M/F)**	**Mean age (y)**	**Mean onset age/ Mean duration (y)**	**Disability: mild/ moderate/ severe**	**Imaging findings**
Parmeggiani et al. 1997	CT	2 (0/2)	23	7/16	NA	Normal in one sibling; in another, progressive cortical-subcortical atrophy
Mascalchi et al. 2002	MRI; proton MRS	10 (6/4)	29	11/29	6/3/1	Mild to moderate atrophy in 6 patients; loss of bulk of the pons, medulla and cerebellum in 10 patients
Korja et al. 2007	MRI	4 (1/3)	32	NA/21	0/3/1	Mild or moderate cerebral and cerebellar atrophy in 3 patients; Mild cerebellar atrophy in 1 patient
Chew et al. 2008	MRI	8 (4/4)	41	11/30	0/0/8	Cerebral atrophy in 2 patients; cerebellar atrophy in 2 patients
Santoshkumar et al. 2008	MRI	5 (2/3)	16	9/7	0/3/2	Cerebral atrophy in 3 patients; cerebellar atrophy in 2 patients
Giovagnoli et al. 2009	MRI	21 (8/13)	39	12/27	13/4/2	Mild atrophic changes in the brainstem, cerebellum and cerebral cortex in 8 patients
Koskenkorva et al. 2009	MRI; VBM	34 (18/16)	33	10/23	14/9/11	Mild to moderate cortical atrophy in frontal and/or parietal lobes in 23 patients; GM volume reduction on cortical motor areas, thalami and precuneus
Korja et al. 2010	MRI	13 (7/6)	35	NA/23	NA	White matter changes in 8 patients, 5 of them found in basal ganglia (T2)
Koskenkorva et al. 2012	MRI; CTH	53 (29/24)	35	11/24	NA	Thinning of the sensorimotor, visual and auditory cortices in group analysis
Manninen et al. 2013	MRI; DTI (TBSS)	19 (10/9)	35	NA/24	NA	Widespread alterations in subcortical WM, the thalamocortical system and the cerebellum in group analysis

2.1.5 Genetics and molecular basis of EPM1

2.1.5.1 Etiology of EPM1

EPM1 is caused by the mutations of the Cystatin B protein encoding *CSTB* gene (Pennacchio et al. 1996, Lalioti et al. 1997, Lafreniere et al. 1997) that result in substantially reduced *CSTB* gene and protein expression. EPM1 is inherited in autosomal recessive manner (Pennacchio et al. 1996) and the majority of EPM1 cases are homozygous for the expanded dodecamer repeat mutation in the promoter region of the *CSTB* gene (Virtaneva et al. 1997). However, some EPM1 patients are compound heterozygous for the dodecamer repeat expansion and the c.202C>T mutations with five known cases in Finland (Joensuu, Lehesjoki & Kopra 2008). So far, 14 loss of function mutations in the *CSTB* gene have been identified (Tegelberg 2013).

A few patients with a phenotype similar to EPM1 have mutations in the *PRICKLE1*, *SCARB2* or *GOSR2* genes (Bassuk et al. 2008, Corbett et al. 2011, Dibbens et al. 2009). Also, a new clinical phenotype resembling EPM1 has been reported where the *CSTB* mutation is not seen and the exact mutation is under investigation (Berkovic et al. 2005).

2.1.5.2 Cstb-deficient mouse model for EPM1

Cstb-knockout mouse model (*Cstb*$^{-/-}$) where the *CSTB* gene is inactivated causes a phenotype that recapitulates the key clinical features of EPM1 (Pennacchio et al. 1998). *Cstb*$^{-/-}$ mice show sufficiently the main aspects of EPM1 including myoclonic seizures and progressive ataxia but no tonic–clonic seizures or photoconvulsive response are seen. Initially, mouse model revealed apoptotic loss of cerebellar granule neurons whereas the signs of the apoptosis were sparse in the other parts of the brain (Pennacchio et al. 1998). Later studies have shown early microglia activation even in clinically normal young *Cstb*$^{-/-}$ mice and widespread gliosis followed by intense astrocytosis and progressive neuron loss in the cerebral cortex, cerebellum, thalamus and thalamocortical system (Shannon et al. 2002, Franceschetti et al. 2007, Tegelberg et al. 2012). Recently, a diffusion tensor imaging study reported that the diffusion changes in the white matter are similar in patients with EPM1 to those in *cstb*-deficient mice with the most remarkable changes found in the pyramidal tracts, thalamus and cerebellum (Manninen et al. 2013). Another recent study revealed early WM alterations in all major tracts and progressive non-uniform volume loss in the brain of *cstb*-deficient mice while brain volume increased in the control mice group (Manninen et al. 2014).

The pathological changes in hippocampus have remained controversial in literature of EPM1. Shannon et al reported massive apoptosis and gliosis within the hippocampal formation and entorhinal cortex whereas later stage mice had no activated microglia in hippocampi in a study of Tegelberg et al. (Shannon et al. 2002, Tegelberg et al. 2012). However, it has also been hypothesized that hippocampus plays a crucial role in the pathophysiology of EPM1. A significant loss of GABAergic interneurons has been found in the dorsal hippocampus associated to the more hyperexcitable hippocampi of *Cstb*$^{-/-}$ mice and higher susceptibility to seizures (Franceschetti et al. 2007). Macroscopically, the seizure-prone and seizure-resistant mice display similar neuropathologic changes (Pennacchio et al. 1998, Shannon et al. 2002).

2.1.5.3 *CSTB*, Cystatins and Cathepsins

CSTB encodes Cystatin B protein which is an endogenous inhibitor of cysteine proteases, cathepsins (Järvinen, Rinne 1982, Green et al. 1984). Experimental work has shown a neuroprotective role of *CSTB* and the contribution of both Cystatin B and Cystatin C to the pathophysiology of EPM1 (Pennacchio et al. 1998, Shannon et al. 2002, Lieuallen et al. 2001, Rinne et al. 2002, Houseweart et al. 2003, Lehtinen et al. 2009, Kaur et al. 2010).

Cystatin B and Cystatin C are the members of cystatin superfamily. They are expressed ubiquitously in human cells and have diverse roles in human physiology and disease processes including inflammation, cancer and neurodegeneration (Keppler 2006). Both Cystatin B and C inhibit cathepsins B, H, L, and S (Kopitar-Jerala 2006), Cystatin B also inhibits cathepsin D and probably cathepsin K (Laitala-Leinonen et al. 2006, Kaur et al. 2010, Yang et al. 2011).

Loss of Cystatin B function leads to enhanced cytosolic activity of cathepsins in EPM1 (Lieuallen et al. 2001, Rinne et al. 2002, Houseweart et al. 2003). Cstb-deficient mouse model for EPM1 showed that removal of cathepsin B from *Cstb*$^{-/-}$ mice strongly improves the EPM1 phenotype whereas removal of cathepsins L or S did not cause any changes to the phenotype of *Cstb*$^{-/-}$ mice (Houseweart et al. 2003).

An *in vitro* study has shown that CSTB is involved in bone resorption by regulating the intracellular Cathepsin K activity (Laitala-Leinonen et al. 2006). Cathepsin K is a major cysteine protease and has a critical role in bone resorption (Gelb et al. 1996, Saftig et al. 1998, Xia et al. 1999). In mice, overexpression of cathepsin K is related to enhanced osteoclastic bone resorption, osteopenia of metaphyseal trabecular bone, and increased cortical thickness and cortical bone mineral density in the diaphyseal regions (Kiviranta et al. 2001, Morko et al. 2005).

The role of Cystatin C in EPM1 is not as widely investigated as Cystatin B. It has been shown that the expression of Cystatin C is enhanced in the brains of *Cstb*$^{-/-}$ mice and the overexpression of Cystatin C rescues cerebral cortices and cerebellum from the cell death and gliosis (Kaur et al. 2010). In the light of present knowledge, Cystatin B and C and Cathepsin B, D and K have a contribution to the pathophysiology of EPM1.

2.2 OVERVIEW OF SKELETAL VARIABILITY IN HEALTH AND DISEASE

There are two types of bones based on the embryological origins: those with intramembranous ossification where the ossification takes place directly, and those with endochondral ossification with a cartilage precursor. The majority of the human bones, including long bones, vertebral column and skull base are developed through the endochondral ossification whereas the cranial vault (frontal bone, parietal bone, parts of temporal and occipital bones) and facial bones are developed via the intramembranous ossification. Although the embryology creates the basis for the skeleton, structural changes during the growth of the bone are an ongoing process. During the first year of life, almost the entire skeleton is replaced with continuum of 10 % remodelling per year. There are two major factors associated with bone remodelling, the osteoblasts and osteoclasts with various affecting factors both from genetic and environmental sources. Bone metabolism is a complicated and susceptible process varying from too effective bone resorption leading to osteoporosis, all the way to dysfunctional ossification that causes osteopetrosis. (Cohen 2006) Thus, seemingly small factors can disrupt the balance of bone metabolism leading to the pathogenesis of various skeletal diseases. This has been also recognized during drug development processes, for example for osteoporosis, with unexpected side-effects (Rachner, Khosla & Hofbauer 2011). In the following sections, the skeletal abnormalities studied in this thesis are reviewed.

2.2.1 Skull

The human skull, size, shape and cranial thickness have been investigated extensively. In recent history, by characterizing the morphology of the human skull, palaeanthropological, archeological, anthropological and other investigators have tried to explain human differences from behavioral and racial differences to intelligence. Intentions have not been always ethical (Greenblatt 1995). When it comes to human ancestors, subspecies of *Homo sapiens*, morphological differences of the skull are obvious. One topic for researchers has been to find correlations between cultural and sex differences and skull thickness. Early anthropological studies suggested that men have thicker skulls because of the size difference between men and women, but modern autopsy biopsy studies and one MRI study found no correlation between age, gender and body composition and thickness of the skull excluding hyperostosis frontalis interna (HFI) (Hershkovitz et al. 1999, Ross, Jantz & McCormick 1998, Hatipoglu et al. 2008). However, characteristics of the skull morphology are used to identify archeological findings, and recently, also modern radiological imaging methods are used to characterize calvarial and other skeletal structures of mummies (van Kaick, Delorme 2005). One of the characteristic skull findings is hyperostosis frontalis interna (HFI) (May et al. 2011).

Hyperostosis frontalis interna is a symmetrical protrusion on the inner table of the frontal bone (Hershkovitz et al. 1999). HFI is a sex- and age-dependent phenomenon of unknown aetiology that is highly related to the hormonal changes that vary over a lifetime, especially prolonged estrogen stimulus during the fertility has been suggested to be the reason to the HFI seen in postmenopausal females (Hershkovitz et al. 1999, Ross, Jantz & McCormick 1998). The overall prevalence of HFI is 5–12%, but it is notably higher among post-menopausal elderly women (40–60%). When both CT and MR imaging have become more frequent and routine, HFI has become a general incidental finding that by itself does not cause significant clinical disease (Hershkovitz et al. 1999). Thus, according to the present knowledge, HFI can be considered a separate, non-disease-related phenomenon.

Thickening of the skull is associated with many disorders, such as severe anaemia, polycythemia vera, myelofibrosis, hyperparathyroidism and myeloproliferative diseases such as lymphoma, multiple myeloma and myelodysplastic syndromes. (Ghanem et al. 2006, Nobauer, Uffmann 2005) Paget's disease is a relatively common entity with skull thickening and other bone findings, occurring in middle age (3–4% of those >40 years of age) (Smith et al. 2002).

In the 1970's an established AED, phenytoin was commonly used to treat epilepsy in Finland. Generalized thickening of the skull has been shown to associate with the long-term use of phenytoin (Kattan 1970). A more recent case report describes skull thickening and cerebral atrophy after thirteen years of phenytoin use (Chow, Szeto 2007). Finally, thickening of the skull has been reported in various inherited diseases that are reviewed in Table 9 (see page 50).

In this study, the paranasal sinuses of the patients with EPM1 were also evaluated. Paranasal sinus pathology is familiar for every physician because of common sinuitis. Hypoplasia of paranasal sinuses is a frequently mentioned entity but not much can be found from the literature about large paranasal sinuses which can be usually noted in acromegaly (Burgener, Kormano & Pudas 2008). However, large frontal sinuses are observed in some rare syndromes like Dyke Davidoff-Masson syndrome which is a neurological disorder characterized by marked hemiatrophy or hypoplasia of one cerebral hemisphere, contralateral hemiparesis and epileptic seizures (Table 9) (Atalar, Icagasioglu & Tas 2007).

2.2.2 Spine

Scoliosis, an abnormal curving of spine, is a common finding and a widely investigated spinal deformity: in a PubMed search it gives over 17000 hits. The literature reports prevalence rates for scoliosis that vary from 1% among school children to 8.3% among US adults aged 25–74 years and up to 35.5% among individuals older than 60 years (Carter, Haynes 1987, Hong et al. 2010, Ueno et al. 2011). It can be categorized into congenital, syndromatic or idiopathic. Abnormally formed vertebrae such as hemivertebrae, fused vertebrae and vertebral hypoplasia appearing early in development cause congenital scoliosis. Syndromatic or secondary scoliosis is associated with some other neuromuscular, skeletal or connective tissue disorder. Examples for syndromatic and/or congenital scoliosis are also widespread in patients affected by the syndromes shown in Table 9. Eventually, the most common form of scoliosis is idiopathic scoliosis where the cause remains unknown. Idiopathic scoliosis can be divided by the age of onset to the infantile, juvenile and adolescent forms. (Altaf et al. 2013) Several other types of vertebral anomalies exist, see Burgener & Kormano (Burgener, Kormano & Pudas 2008).

2.2.3 Other skeleton

Accessory ossicles of the foot are a relatively common congenital skeletal finding in normal population and the knowledge of accessory ossicles is beneficial when diagnosing fractures of the foot (Burgener, Kormano & Pudas 2008). The most common accessory ossicles are os tibiale externum with the estimated prevalence of 4–21% in healthy individuals. Other accessory ossicles like os trigonum and os peroneum are less prevalent (Mellado et al. 2003). In rare cases, there can be coalitions in the bones of the foot for example talonavicular and talocalcaneal coalitions (Burgener, Kormano & Pudas 2008).

Similar to the feet, many syndromes may also affect the hand**.** Arachnodactyly is seen in Marfan syndrome and it is defined when metacarpal index is more than 8. Metacarpal index is calculated by dividing the sum of the lengths by the sum of the widths of metacarpals II–V. In positive metacarpal sign the tangent of IV and V metacarpal heads passes through the head of the third metacarpal and it can be seen e.g. Turner's syndrome (Burgener, Kormano & Pudas 2008).

There are various other congenital anomalies in 206 bones of human skeleton including shortened and malformed limbs, absence of bones or part of them, and multiple deformities due the bone-connective-tissue-matrix problems (see Burgener et Kormano) but they are not included to the topic of this thesis.

Bone mineral density (BMD) describes the amount of mineral matter per cubic centimeter (g/cm3) that can be examined by dual x-ray absorptiometry (DXA). Osteopenia is a condition where bone mineral density is lower than normal (BMD is 80–120 mg/cm3 and T-score between -1.0 and -2.5). Osteoporosis means progressive bone disease where both bone mineral density and bone mass are decreased (BMD is < 80 mg/cm3 and T-score of less than -2.5). (Adams 2013) Several medical entities are related to the bone loss including endocrine diseases, rheumatoid artritis and other autoimmune disorders, cancers, malnutrition, smoking, excess use of glucocorticoids and chronic immobilization for example among the wheelchair users that increase the risk of osteoporotic fractures. (Rachner, Khosla & Hofbauer 2011) Osteoporosis is a problem in patients with chronic epilepsy and the association between low BMD and AEDs is strongly detected (Beerhorst et al. 2012).

2.3 BACKGROUND FOR STRUCTURAL BRAIN IMAGE ANALYSIS

2.3.1 Anatomy of cerebral cortex

Cerebral cortex is a crumpled and folded 6-sheet layer of grey matter forming numerous convolutions (gyrus) and crevices (sulcus) divided into right and left hemispheres and frontal, temporal, parietal and occipital lobes. With over 10^{10} neurons and various neurotransmitter connections to subcerebral areas e.g. thalamus and brainstem, cerebral cortex is a very complex structure that is largely responsible for higher brain functions e.g. memory, sensation and voluntary muscle movement. (Bear, Connor & Paradiso 2007)

Division of cerebral cortex can be comprehend and named several ways with three introduced here (Table 4). Anatomically cerebral cortex is named based on its gyri and sulci, every gyrus and sulcus has its own anatomic name (Duvernoy 1999). Functionally, cerebral cortex is basically divided into motor, sensory and association areas and smaller sophisticated functions of these parts are used to classify and name cerebral cortex. (Bear, Connor & Paradiso 2007) Brodmann's map from 1909 is a base of modern structural neuroimaging and understanding of function of human cerebral cortex (Zilles, Amunts 2010). Korbian Brodmann described total of 43 different areas that are based on both anatomical and functional cytoarchitecture and this classification is still a functional way to understand the cerebral cortex for researchers, physicians and radiologists (Figure 1).

During the embryogenesis cerebral cortex undergoes several developmental steps. This formation continues throughout the childhood and youth when finally at the age of 6–7 years gray matter volume starts to decrease and vice versa white matter volumes increase. (Kolb, Whishaw 2009). It seems that, GM loss, also known as brain maturation, starts in phylogenetically older brain areas. In other words the lower-order cortices develop before higher-order association cortices (Gogtay et al. 2004). It is commonly known that during aging the cerebral cortex becomes thinner (Salat et al. 2004, Fjell et al. 2009a, Thambisetty et al. 2010, McGinnis et al. 2011). Furthermore, the thickness of the cortex varies regionally. Cortical differences have been found between men and women but it seems that in the aging brain the sex does not matter (Luders et al. 2006, Sowell et al. 2007, Fjell et al. 2009b). It is crucial to know the anatomy and function of cerebral cortex to understand the possible underlying disease mechanisms. Yet, associations between cortical formation, function and thinning are poorly understood.

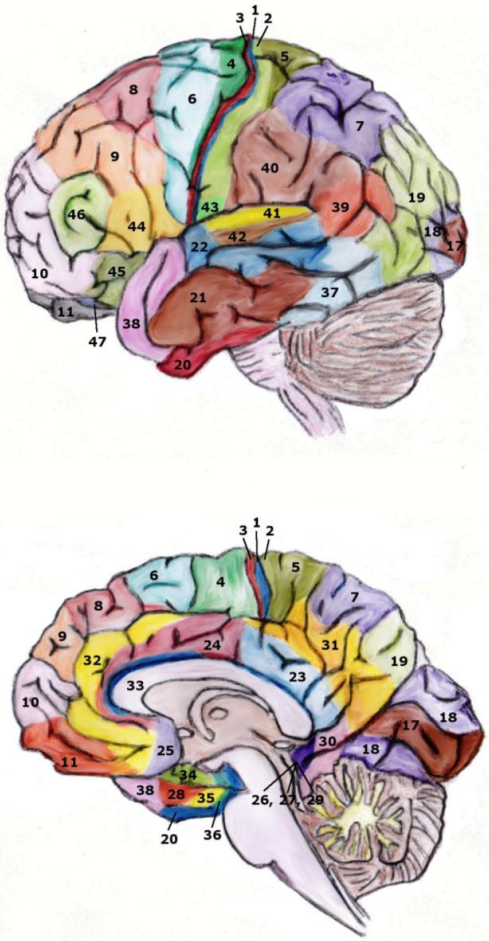

Figure 1. Brodmann's map illustrated in lateral and medial views.

2.3.2 Cerebral cortex and neurocognition

Cerebral cortex is a small part of a human brain, only 1.5–3.0 mm thick, and it is an essential for cognitive function. Humans and other intelligent species have larger brains and thicker cortices. Cerebral cortex contains areas that are involved in higher-order cognitive functions, a group of mental processes used for perception, processing and applying of new knowledge. (Kolb, Whishaw 2009) The basic aspects of cognition are same in human and other animals, many of cognitive functions like language, problem solving and learning, are the most developed in human being although the uniqueness of human brain has started to be to criticized (Herculano-Houzel 2012). Speech is a primary example of peculiar function of human cerebral cortex. Cognition and cerebral cortex have been widely investigated and debated with several theories on the organization of cognitive function.

2.3.3 Highlighted cortical areas involved in cognitive tasks

Posterior section of frontal lobe is responsible for motor skills (Bear, Connor & Paradiso 2007). In front of the primary motor cortex lies the premotor cortex that includes area BA6. Frontal eye fields (BA8) lie in or just before BA6 in the medial part of frontal lobe. BA8 includes the areas that participate in the control of saccadic eye movements (Amiez, Petrides 2009).

Anterior portion of frontal lobe comprises prefrontal cortex which retains the highest components of human behaviour (Kolb, Whishaw 2009). Dopamine plays an important role in the neurotransmission in prefrontal cortex and is involved in higher-order cognitive functions (Robbins, Arnsten 2009, Benchenane, Tiesinga & Battaglia 2011). In humans prefrontal cortex can be divided in ventrolateral, dorsolateral, orbitofrontal, ventromedial and frontopolar prefrontal cortex.

Ventrolateral prefrontal cortex, VLPFC (BA, 44, 45 and 47) receives detailed information of objects from the visual pathways in conjunction with motivational and emotional knowledge from subcortical areas and orbitofrontal cortex that is together committed for decision making or design of goal-directed behaviour (Sakagami, Pan 2007). VLPFC is considered to have significantly differing roles in two brain hemispheres e.g. verbal stimuli leads to activation of left VLPFC whereas visuospatial stimuli leads to the activation of right VLPFC (Levy, Wagner 2011).

Ventromedial prefrontal cortex (VMPFC) receiving signals from supplementary motor cortex, dorsal striatum and parts of parietal cortex, is also involved in goal-directed decision making and selection based on value of goals (O'Doherty 2011). VMPFC has been suggested to have an interesting role in emotional decision e.g. moral judgement between right and wrong (Koenigs et al. 2007).

Dorsolateral prefrontal cortex (DLPFC) involves mainly BA9 and 46 but also BA 6, 8 and 10 depending on reference. DLPFC is greatly involved in executive functions and working memory with dopamine modulation (Smith, Jonides 1999, Funahashi 2006, Arnsten 2009, Goldstein, Volkow 2011).

Frontopolar cortex (BA10) is suggested to function in cognitive branching enabling to hold primary goals in mind during the multitasking (Koechlin, Hyafil 2007). Orbitofrontal cortex (BA11) is a part of decision making, expected reward situations and adaptive learning (Schoenbaum et al. 2011).

Pars opercularis and pars triangularis in frontal lobe involve the Broca's area on the left. Wernicke's area is located in temporal lobe. Broca's area is crucial for producing speech and also involved in language comprehension, language processing and facial neuron control. Whereas, Wernicke's area is rather responsible for comprehension of language, semantic processing, language recognition and interpretation (Damasio, Geschwind 1984).

Anterior cingulate cortex (ACC) including BA 24, 32, and 33, is suggested to be ubiquitously active brain area involved in motor control, emotional self-control and in cognition by means of decision making (focused problem solving, error recognition and adaptive response to changing conditions) and it has been found to be involved in many psychiatric disorders (Allman et al. 2001, Paus 2001, Wallis, Kennerley 2011).

The posterior cingulate cortex (BA23, 31) is a part of the default mode network, a set of brain regions that are highly active during rest. It has been suggested that it has a role in creativity and creation of spontaneous thoughts, being relevant to major mental or cognitive disorders (Buckner, Andrews-Hanna & Schacter 2008). Posterior cingulate cortex is suggested also to be involved in eye movements, spatial attention and navigation (Kravitz et al. 2011).

Retrosplenial cortex (BA 26, 29, 30) projecting to the anterior thalamic nuclei and hippocampus is involved in episodic and spatial memory, navigation, imagination and planning for the future (Vann, Aggleton & Maguire 2009). Furthermore, neurocognitive studies and case reports indicate that patients with damaged retrosplenial cortex have spatial orientation deficit and difficulty acquiring new visual or verbal information (Maguire 2001).

Perirhinal cortex contributes to the higher-order visual perception and complex conjunctions of objects and storaging of this visual data in memory (Murray, Bussey & Saksida 2007). Fusiform gyrus is especially involved in the perception of faces (Kanwisher, McDermott & Chun 1997) but it also has highly selective neural populations for recognition of non-facial objects (Grill-Spector, Sayres & Ress 2006).

Finally, mice studies have shown that the piriform cortex is a highly seizure-prone region (Piredda, Gale 1985).

Table 4. Cerebral cortex named by functional, Brodmann and anatomical areas.

	Functional area	**Brodmann**	**Notes**	**Anatomical area**	
Frontal lobe					
Motor cortex	Primary motor cortex	BA 4		Precentral gyrus	Superior frontal gyrus
	Premotor cortex	BA 6	Association motor cortex	Superior frontal gyrus	
	Supplementary motor cortex	BA 6	including supplementary eye fields	Superior frontal gyrus	Middle frontal gyrus
	Supplementary motor cortex	BA 8	Frontal eye fields	Superior frontal gyrus	Middle frontal gyrus
Prefrontal cortex	Dorsolateral prefrontal cortex	BA 8			
	Dorsolateral prefrontal cortex	BA 9		Superior frontal gyrus	Middle frontal gyrus
	Dorsolateral prefrontal cortex	BA 46		Middle frontal gyrus	Inferior frontal gyrus
	Ventrolateral prefrontal cortex	BA 44	Broca's area	Pars opercularis	
	Ventrolateral prefrontal cortex	BA 45	Broca's area	Pars triangularis	
	Ventrolateral prefrontal cortex	BA 47		Pars orbitalis	Orbital sulcus
	Orbitofrontal prefrontal cortex	BA 47		Pars orbitalis	
	Orbitofrontal prefrontal cortex	BA 11	Anterior portion of orbitofrontal cortex	Orbital gyri Straight gyrus	Superior frontal gyrus
	Orbitofrontal prefrontal cortex	BA 12	Subcallosal area	Paraterminal gyrus	Orbital gyri
	Ventromedial prefrontal cortex	BA 10		Rostral middle frontal gyrus	Orbital gyri
	Frontopolar cortex	BA 10		Rostral superior frontal gyrus	Orbital gyri

Temporal lobe					
Superolateral	Primary auditory cortex (A1)& Auditory association cortex (A2)	BA 41		Transverse temporal gyrus	
	Primary auditory cortex (A1)& Auditory association cortex (A2)	BA 42		Transverse temporal gyrus	
	Superior temporal area	BA 22	Wernicke's area	Superior temporal gyrus	
	Temporopolar area	BA 38		Superior temporal gyrus	Middle temporal gyrus
	Middle temporal area	BA 21		Middle temporal gyrus	
	Inferior temporal area	BA 20		Inferior temporal gyrus	
Inferior	Occipitotemporal area	BA 37		Inferior temporal gyrus	Fusiform gyrus
Medial	Piriform cortex	BA 27		Parahippocampal gyrus	
	Posterior entorhinal cortex	BA 28		Parahippocampal gyrus	
	Anterior entorhinal cortex	BA 34		Parahippocampal gyrus	
	Perirhinal cortex	BA 35		Rhinal sulcus	
	Ectorhinal cortex	BA 36		Fusiform gyrus	
	Retrosubicular cortex	BA 48		Parahippocampal gyrus	
	Parainsular cortex	BA 52		Lateral sulcus	
Parietal Lobe					
	Primary somatosensory cortex (S1)	BA 1		Postcentral gyrus	
	Primary somatosensory cortex (S1)	BA 2		Postcentral gyrus	Postcentral sulcus
	Primary somatosensory cortex (S1)	BA 3		Postcentral gyrus	Central sulcus
	Secondary somatosensory cortex (S2)	BA 5		Superior parietal lobule	Postcentral gyrus

	Posterior parietal cortex	BA 7		Superior parietal lobule	Precuneus
	Inferior parietal lobule	BA 39	Part of Wernicke's area	Angular gyrus	
	Inferior parietal lobule	BA 40	Part of Wernicke's area	Supramarginal gyrus	
	Primary gystatory cortex	BA 43		Postcentral gurys	Precentral gyrus
Occipital lobe					
	Primary visual cortex (V1)	BA 17		Cuneus	
	Secondary visual cortex (V2)	BA 18		Lateral occipital gyri Lingunal gyrus	Cuneus
	Associative visual cortex (V3)	BA 19		Occipital gyri	Lingunal gyrus
	Visual area V4	BA 18/19		Occipital gyri	Lingunal gyrus
	Visual area V5	BA 19		Occipital gyri	Lingunal gyrus
Limbic lobe					
	Ventral anterior cingulate cortex	BA 24		Anterior cingulate gyrus	
	Dorsal anterior cingulate cortex	BA 32		Anterior cingulate gyrus	
	Pregenual cortex	BA 33		Anterior cingulate gyrus	
	Ventral posterior cingulate cortex	BA 23		Posterior cingulate gyrus	
	Dorsal posterior cingulate cortex	BA 31		Posterior cingulate gyrus	
	Subgenual cortex	BA 25		Subcallosal area	
	Retroplenial cortex	BA 26		Isthmus of cingulate gyrus	
	Retroplenial cortex	BA 29		Isthmus of cingulate gyrus	
	Retroplenial cortex	BA 30		Isthmus of cingulate gyrus	
Insula					
	Insular cortex			Long gyrus of insula	Short gyri of insula

2.3.4 Thalamus and basal ganglia

Thalamus is an oval-shaped relay centre of diencephalon between subcortical areas and the cerebral cortex. Thalamus consists of 50-60 nuclei that project via afferents and efferents to the well-defined cortical areas. With the exception of olfactory system, every sensory system includes a thalamic nucleus that contralaterally receives specific sensory signals and sends back information to different thalamic nuclei via basal ganglia. (Herrero, Barcia & Navarro 2002) These signalling pathways are known as cortical-striatal-pallidal-thalamic-cortical circuits that include motor, oculomotor, dorsolateral prefrontal, lateral orbitofrontal and anter cingulate circuits. (Green, Ostrander 2009)

Pathology in thalamus leads to disturbances in motor and sensory systems, as well as central pain or anaesthesis in the opposite side of the body. (Herrero, Barcia & Navarro 2002). More specifically, lesions confined to the specific nuclei have been associated with asterixis (Lee, Marsden 1994), cheiro-oral syndrome (Shintani, Tsuruoka & Shiigai 2000) or choreiform and dystonic movements associated with myorhythmia (Lera et al. 2000). Lesions of both thalamus and basal ganglia are related to dystonia (Lee et al. 1994). Importance of thalamus in fine motor control is well demonstrated by deep brain stimulation (DBS) of ventral intermediate nucleus of thalamus used as treatment in essential tremor that is the most common movement disorder in the world (Zesiewicz et al. 2013). Eventually, thalamus is best known for its multiple functions both in sensory and motor aspects, but thalamus is also involved in cognitive functions for example the regulation of awareness, attention, memory and language (Smythies 1997, Buchel et al. 1998, Johnson, Ojemann 2000).

Basal ganglia are a group of nuclei located at the base of forebrain. Basal ganglia are named in several ways that leads to difficulty to memorize parts of it (Figure 2). Putamen together with caudate nucleus and nucleus accumbens forms striatum which is the major part of basal ganglia. Basal ganglia are a part of extrapyramidal motor system regulating automatic and voluntary movements, movement initiation and spatial working memory, and processes of behaviour, learning and planning (Herrero, Barcia & Navarro 2002, Graybiel 2005, Yin, Knowlton 2006). Putaminal pathology is related to motor stereotypies like fine resting tremor, hyperkinetic movement disorders like Huntington disease and hypokinesia disorders including Parkinson's disease (Herrero, Barcia & Navarro 2002, Turner, Desmurget 2010). All these disorders also possess cognitive impairment and basal ganglia are also related to behavioural disorders like schizophrenia and obsessive compulsive disoders (Herrero, Barcia & Navarro 2002, Green, Ostrander 2009). Interestingly, microstructural and volumetric abnormalities of the putamen have been observed also in juvenile myoclonic epilepsy (Keller et al. 2011) which share some similar clinical characters with EPM1.

To summarise, the thalamus and striatum are important not only in motor control, but also in higher-order cognitive and behavioural processes.

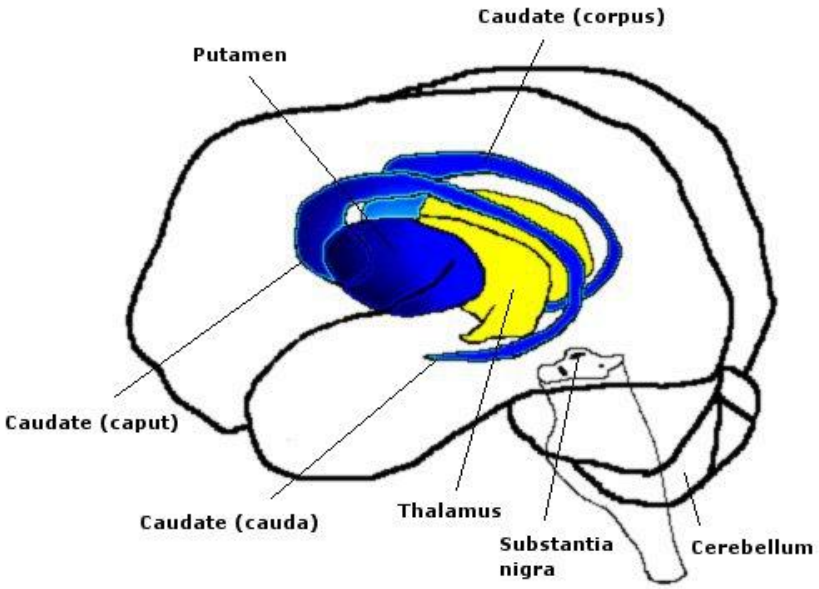

Figure 2. Thalamus and basal ganglia are located symmetrically within the middle of the brain.

2.4 MODERN ANALYSIS METHODS FOR MRI OF THE BRAIN

2.4.1 Cortical Thickness Analysis

Subtle pathological changes of the neurological diseases are characteristically too complex or diffuse to be detected by human visual system in MR images because of limitations on the resolution of MRI. (Ashburner et al. 2003) In recent years, new software has brought improved tools to investigate cerebral cortex in detail. Cortical thickness analysis (CTH) enables an automated and objective method to detect subtle changes in the brain *in vivo* using MR imaging (Fischl, Dale 2000).

There are several methods developed for the CTH analysis. A widely used CTH analysis is conducted by using the pipelining method developed at the McConnell Brain Imaging Centre, Montreal Neurologic institute, McGill University Montreal, Canada (http://www2.bic.mni.mcgill.ca).

In CTH, when the basic protocol is gone over step by step (Figure 3), the individual MR image volumes are; first, spatially normalized to the same stereotactic template (Mazziotta et al. 2001), secondly, intensity inhomogeneities are corrected (Sled, Zijdenbos & Evans 1998) and lastly, extracerebral voxels are removed with a stereotactic brain mask (Smith 2002).

Following with, the magnitude of the partial volume effect is estimated for each voxel (Tohka, Zijdenbos & Evans 2004) and brain tissue is divided into grey matter (GM), white matter (WM), and CSF (Zijdenbos 1998). The brains are automatically divided into two separate hemispheres and the inner and outer surfaces of the cortex are extracted by using automated segmentation (Kim et al. 2005) followed by identification of white matter surface (WMS) i.e. the surface between WM and GM and grey matter surface (GMS) i.e. the surface between GM and CSF. The thickness of the cortex is defined with a t-link

metric at each linked node as the distance between WMS and GMS and as a result a CTH map can be acquired (Lerch, Evans 2005). For further analyses, the thickness calculations are performed on each subject's native space and are then transformed back to the standard space for the group analysis. Finally, the data are smoothed to improve the signal-to-noise ratio and statistical power (Chung, Taylor 2004).

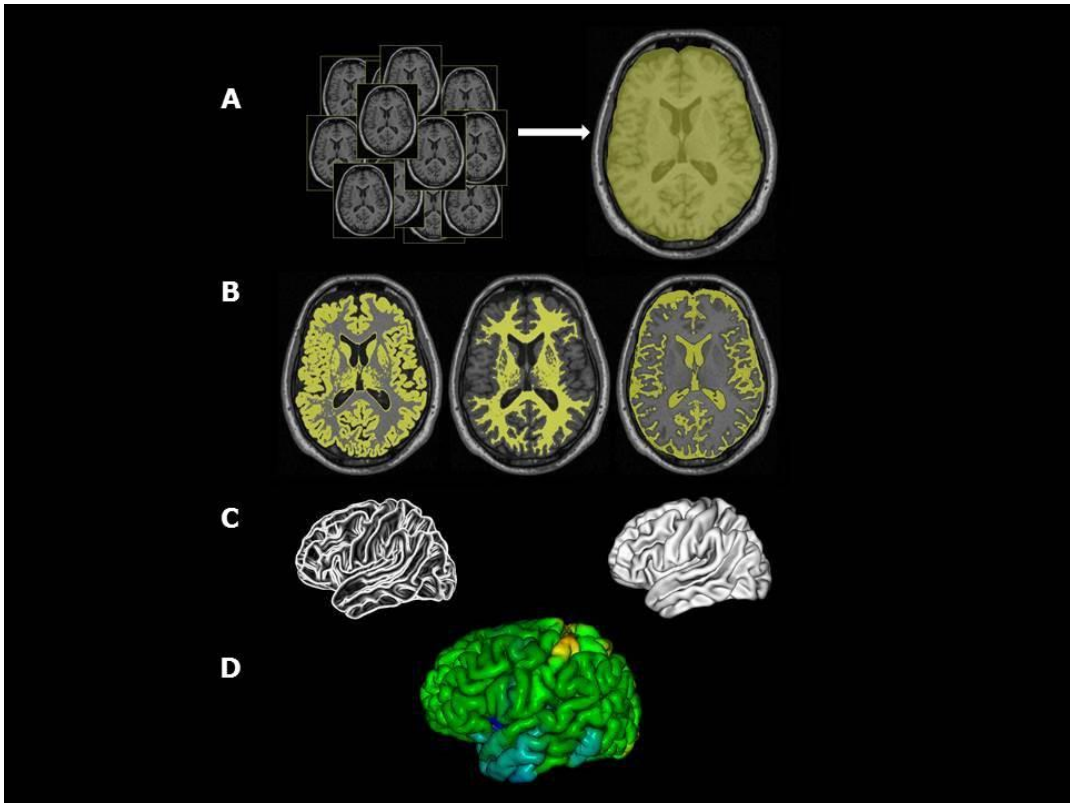

Figure 3. In short, the steps of CTH. A) Individual MR images are registered to the standard space and corrected for artefacts before the final brain mask is created. B) Brain tissue is divided into GM, WM and CSF. C) Inner (WM/GM) and outer (GM/CSF) surfaces of the cortex are extracted. D) Finally, the results are visualized in colors.

2.4.2 Cortical thickness in diseases

CTH analysis has been applied both to investigate neuroanatomy and individual variation in cerebral cortex and to explore how various diseases are related to the cortical alterations. One of the first applications of CTH analysis was in Alzheimer's disease (Lerch et al. 2005) where widespread cortical thinning was demonstrated in patients with AD compared to the healthy controls. Afterwards, several research projects on the effects of aging, mild cognitive impairment and AD, has been published (Julkunen et al. 2009, Vuorinen et al. 2013). CTH has been applied also in other common neurodegenerative

diseases like in frontotemporal dementia, multiple sclerosis and Parkinson disease (Calabrese et al. 2010, Lyoo, Ryu & Lee 2011, Hartikainen et al. 2012).

Several psychiatric related disorders have been linked in the cerebral cortex. Regional cortical thinning has been found in different parts of frontotemporal areas in schizophrenia, obsessive-compulsive disorder, psychopathy and violent antisocial personality disorder (Kuperberg et al. 2003, Kuhn et al. 2012, Ly et al. 2012, Narayan et al. 2007). Morphometric alterations of cerebral cortex have been studied even in white collar criminals (Raine et al. 2012).

In epilepsy, CTH has been applied to detect possible cortical differences in different neuropsychological phenotypes. In a temporal lobe epilepsy (TLE) study patients were divided in three cognitive clusters and were compared with each other and with healthy controls (Dabbs et al. 2009). The patients with the most impaired cognition exhibited the most significant cortical thinning that was evident throughout the cerebral cortex compared to the healthy controls. The most impaired cluster also had thinner cortex than the minimally impaired patient cluster in the bulk of parietal lobe and cuneus, and unilatelar parts of temporal and frontal lobes.

Correlation between cognitive scores (IQ, executive function and verbal episodic memory) and cortical thickness were studied in patients with only TLE and TLE with interictal psychosis and healthy controls. Cortical thickness differed between groups but no correlations were found between cortical thickness and cognitive scores in the groups (Gutierrez-Galve et al. 2012).

Tosun et al. compared patients with childhood absence epilepsy with healthy children and found abnormal age-related thinning in the right posterior central gyrus and posterior part of the superior temporal gyrus, lingual gyrus, and paracentral gyrus and thickening in the parts of left hemisphere (Tosun et al. 2011b). Patients with epilepsy had same mean VIQ and PIQ scores in the average range and the study findings suggested that patients with epilepsy use different brain regions to perform these cognitive functions compared to healthy controls.

Tosun et al. studied complex partial seizures (CPS) and found that patients with below average IQ's showed significantly greater cortical thinning with age than the control group, widespread in both the left and right hemispheres, however they also had thicker cortex in some parts of the brain (left fronto-temporal cortex, left lateral occipital cortex, right fusiform cortex) with older age than the normal group (Tosun et al. 2011a). They concluded that there is disruption of cortical thickness expression associated with intelligence in children with CPS.

Recently it has been found that valproate is related to overall decrease in brain volume, white matter volume and parietal lobe thinning (Pardoe, Berg & Jackson 2013). The study was performed by comparing valproate users, non-users and healthy controls in two different types of epilepsy, intractable focal epilepsy and child-hood onset epilepsy.

Finally, it has been demonstrated that carriers of ε4 allele of apolipoprotein E gene, a risk allele for Alzheimer disease, have significant cortical thinning of entorhinal cortex compared to non-carriers, which may be identifiable already in childhood (Shaw et al. 2007). This finding demonstrates that there may be a lot of intrinsic and extrinsic factors which affect the thinning or thickening of the cerebral cortex and topography of the cortex varies individually (Krubitzer, Seelke 2012).

2.4.3 Texture Analysis

2.4.3.1 Introduction to the texture analysis

There are several definitions for texture in literature. Texture is an arrangement and interrelationship of parts in an object. It can be described for example as irregular, fine, coarse, smooth or rippled (Haralick 1973). Texture is present everywhere; it can be seen in the images, touched from the textiles and heard in music. In images, including medical imaging, texture is a surface property that has a peculiar arrangement, but the ability of human vision to detect these pictorial details is limited (Julesz 1973). Differences in textures help to discriminate between various objects and help to develop applications to detect subtle differences between them (Figure 4).

Texture analysis (TA) is a method for evaluating the textural features of an object. Initially, it was developed for the evaluation of aerial photographs (Kaizer 1955, Hall et al. 1971), and shortly after it was applied to the medical imaging (Hall et al. 1971, Chien 1974). The basic idea of texture analysis is to provide advanced, non-visible information about areas of interest in an object or image. Thus, in radiology TA enables detection of differences between tissues and classifies them automatically. It can be applied in any digital image and numbers of studies have reported applications in x-ray, computed tomography, ultrasound and magnetic resonance imagining. (Castellano et al. 2004, Holli 2011, Harrison 2011) Eventually, TA can be a useful tool for computer-aided diagnosis (CAD), a set of electromedical procedures to help physicians and radiologists to interpret medical images (Tourassi 1999). Besides the medical imaging and biomedical surface inspection, TA is applied in industrial use in a shape of robots that use "the machine vision", one of the hot topics in research and computer image analysis (Szczypinski et al. 2009). For example, in food industry, robotic machine vision can assist to detect differences between various substances and can find contaminated or defective food, and in forest industry texture analysis can help to identify wood species from each other.

Figure 4. Examples of different kind of textures.

2.4.3.2 Texture analysis methods and texture features

In medical imaging texture analysis is a method for assessment of the position and intensity of pixels (2D picture elements) or voxels (3D volume elements) and their grey-level intensity in a digital image. Thus, every pixel or voxel has a peculiar coordinate and grey-level value. Texture features are mathematical parameters based on the distribution of pixels or voxels, which qualify the texture type and structure of the object. Texture methods process the information of pixel/voxel distribution resulting in texture parameters. (Castellano et al. 2004)

There are four major categories of texture methods given in the literature:

- **Statistical methods** were the original way of calculating the texture features introduced in the 1970's (Haralick 1973). First-order statistics calculate image properties from the features of individual pixel or voxel whereas second-order statistics describe the properties of pixel or voxel pairs. Higher order statistics represent image properties calculated from three or more pixels. Statistical methods include histogram-, absolute gradient-, autocorrelation function-, run-length matrix- and co-occurrence matrix-based texture parameters. (Castellano et al. 2004, Tuceryan, Jain 1998) Co-occurrence matrix-based features seem to be usable for discriminating image properties and they are the most commonly used in medical image analysis (Haralick 1979).
- **Geometrical or structural methods** define texture by using the local mathematical expressions i.e primitive elements from which another expression is derived. This means that a square object is represented in terms of the straight line shapes. Basically, these methods are better for the synthesis of an image than for its analysis and are not used as widely than the other texture methods. (Castellano et al. 2004, Tuceryan, Jain 1998)
- **Model-based methods** use sophisticated mathematical models to describe an image by generating an empirical pixel-weighted model of each pixel. In other words, these methods both describe and synthesize the texture of an image. (Tuceryan, Jain 1998) Model-based methods comprise autoregressive (AR) models (Haralick 1979), Markov random fields and fractal features (Tuceryan, Jain 1998). A mutual character of these models is that they make estimates of pixel or voxel intensities where the texture parameters are derived. The calculations of these parameters are very complex that causes computational limitations for these methods.
- **Signal-processing or transform methods** filter information from an image by executing the frequency analysis of its texture. Frequency analysis is based on that there is a characteristic distribution of pixels or voxels in an object and these pixels/ or voxels and their combinations occur in an image with varying frequencies. Fourier transform is one of the best known signal-processing applications. Also, Gabor and Wavelet transform-based methods are widely used in image texture analysis. (Castellano et al. 2004, Tuceryan, Jain 1998)

2.4.3.3 Software packages for texture analysis

There are various texture analysis softwares, also freely available on Internet. One of these is a product of European cooperation, MaZda MRI texture analysis software package. MaZda was initially developed for MR image analysis by Materka and co-workers (Institute of Electronics in the Technical University of Lodz, Poland) being a part of the Quantitation of Magnetic Resonance Image Texture project (COST B11 project, 1998–2002)

conducted by European Cooperation in Science and Technology (COST). (Szczypinski et al. 2009)

Before the texture analysis is performed, the suitable images must be picked and converted into the right format if necessary. The 2D version of Mazda reads image file formats that the common manufacturers use including .bmp, .ima, .img, .xim, .dicom, .dcm and unformatted (.raw). The 3D version of MaZda reads the dicom (.dcm; .dicom), Windows bitmap (.bmp) and floating point 3D data (.bmf), and unformatted (.raw).

First the appointed image (2D) or image package (3D) is opened in the MaZda program, then the regions of interest (ROI) in 2D or volumes of interest (VOI) in 3D are placed in an image by manually or semi-automatically drawing them on the image (Figure 5). Before the texture parameter calculations, image grey level intensity normalization computation is performed for each region or volume of interest. There are method limiting image intensities in the range $[\mu-3\sigma, \mu+3\sigma]$, where μ is the mean grey level value and σ the standard deviation. This method has been shown to intensify differences between two classes when comparing image intensity normalization methods in texture classification (Collewet, Strzelecki & Mariette 2004).

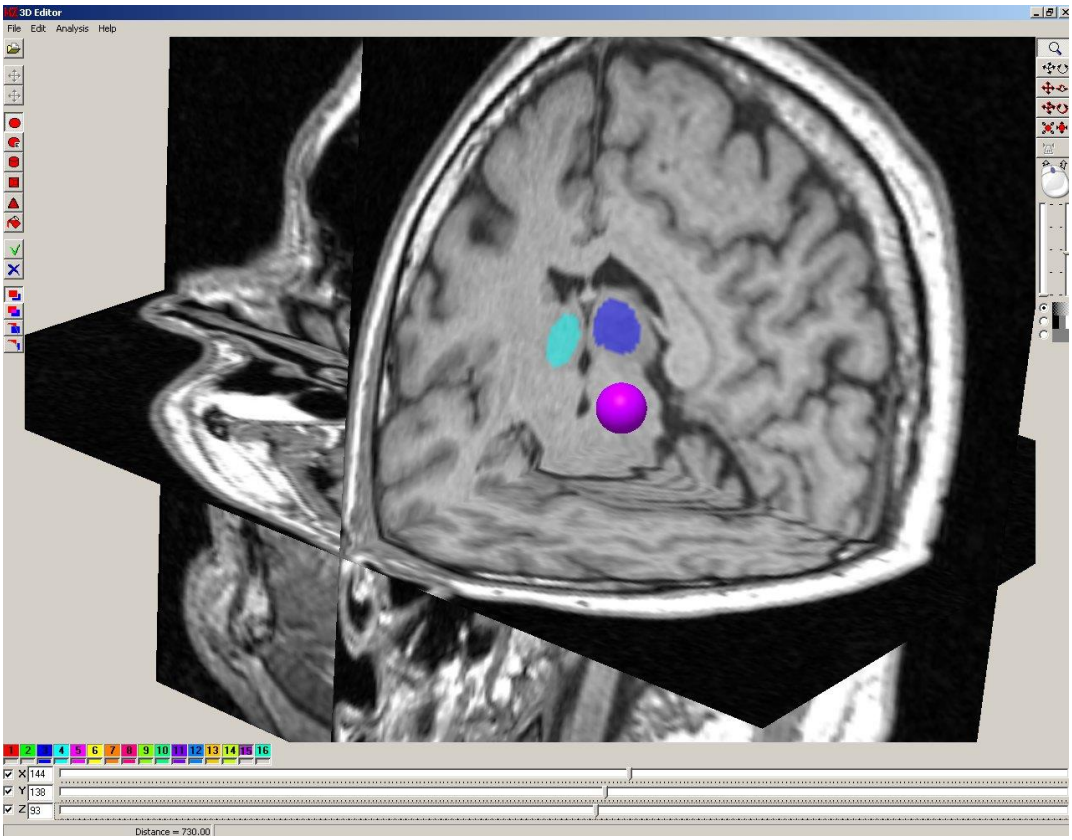

Figure 5. A view of MaZda during the ROI drawing. The blue areas represent an active ROIs ready for the further analysis and the red ball is an inactive ROI.

After these steps, the texture parameter calculations are conducted.

MaZda version 4.60 calculates almost 300 texture parameters based on histogram, gradient, run-length matrix, co-occurrence matrix, autoregressive model and wavelet-derived parameter feature sets (Szczypinski et al. 2009). Most of the parameters are pure mathematical definitions but some of the texture parameters have also a descriptive meaning (see also Table 13 on page 71).

- Histogram
  - Histogram-based statistics assess the global distribution of pixels/voxels with specific grey level tones (Castellano et al. 2004). Several statistical properties can be calculated from the histogram. The mean is the average intensity level of the image, variance assesses the roughness of an image, skewness describes the histogram symmetry and kurtosis describes the flatness of the histogram. (Materka, Strzelecki 1998)
- Gradient
  - The spatial variation of grey-level values across the image is described by the gradient. Thus, high values mean that the grey level varies suddenly from black to white whereas when variation of grey levels is smooth, the gradient value is low (Castellano et al. 2004). Gradient based parameters are mean, variance, skewness, kurtosis and percentage of pixels with non-zero gradient.
- Run-length matrix
  - A gray level run is a set of consecutive picture points i.e. when two or more pixels/voxels have the same value in a present direction (Galloway 1975). RLM-based parameters assess the number of runs and they describe the coarseness or smoothness of an image.
    - Long and short run emphases assess the proportions of runs. The value of short run emphasis is larger in more coarse images and the value of long run emphasis is larger in smoother images.
    - Gray level non-uniformity calculates how uniformly the runs are distributed among the gray levels; smaller values indicate that the distribution of runs is more uniform.
    - Run length non-uniformity gets low values if the runs are evenly distributed over all runs lengths.
    - Run percentage or fraction of image runs has low value in images with the most linear structure.
- Co-occurrence matrix
  - Entropy indicates the complexity and randomness within the image. It is inversely correlated with angular second moment. Images with more gray levels have higher average entropy and lower average angular second moment (Haralick 1973). When the image is not texturally uniform then the value of entropy is higher, whereas, the higher value of angular second moment feature indicates that the intensity varies less in the image is more homogenous.
- Autoregressive model parameters take in consideration also the neighbouring pixels/voxels, in consequence each pixel grey level value is a weighted sum of values from neighbour pixels (Castellano et al. 2004). In MaZda, Theta (model parameter vector, 4 parameters) and Sigma (standard deviation of the driving noise) can be calculated.
- Wavelet transform is a section of signal analysis or signal processing that deals with a complex time varying and spatially varying physical properties of an

object, signals. Signals can be from sound, electromagnetic radiation or like in this case, image. Wavelet-derived parameters analyse the frequency content of a variously scaled picture signal. (Castellano et al. 2004) They are complex mathematical patterns and MaZda generates parameters based on Haar wavelet groups (energy of the wavelet coefficients in subbands) (Szczypinski et al. 2009).

2.4.3.4 Texture analysis applications in medical imaging

MR images contain a huge amount of pictorial and textural information, and in a PubMed search on texture analysis, the majority of literature has been applied in MRI, but also x-ray and CT applications can be found. Texture analysis has been experimentally applied in several medical conditions and syndromes, for example: to detect osteoporotic changes (Link et al. 1999); to differentiate benign soft tissue tumours from malignant tumours (Juntu et al. 2010); to classify brain tumours (Herlidou-Meme et al. 2003) to detect textural changes in mild brain injury (Holli et al. 2010b); to classify liver lesions (Mayerhoefer et al. 2010); to assess the degree of liver fibrosis (Kato et al. 2007); to provide a prognostic factor in colon CT in patients with colorectal cancer (Ng et al. 2013); to characterize different breast cancer types (Holli et al. 2010a); and to correlate with the histopathologic finding of non-small cell lung cancer (Ganeshan et al. 2013). Publications are also found in the most common brain diseases, which include Alzheimers disease (Zhang et al. 2012), Parkinson disease (Sikiö et al. 2011), schizophrenia (Ganeshan et al. 2010) and multiple sclerosis (Zhang 2012). The following chapters focus mainly on neuroradiological MRI applications of texture analysis.

Texture analysis in epilepsy

In epilepsy research, TA has been applied in temporal lobe epilepsy (TLE), focal cortical dysplasia and juvenile myoclonic epilepsy (JME) (Yu et al. 2001, Bonilha et al. 2003, Jafari-Khouzani et al. 2010, Alegro et al. 2012, Antel et al. 2003, Bernasconi et al. 2001, de Oliveira et al. 2013).

In patients with unilateral temporal lobe epilepsy (TLE) with ipsilateral hippocampal sclerosis (n= 23) 2D TA was applied to characterize abnormalities on MR images of hippocampi (Yu et al. 2001). The study showed abnormalities in apparently normal contralateral hippocampi that remained normal in visual assessment. Furthermore in mesial TLE (n=19) textural differences were found between both proven hippocampal sclerosis and contralateral side, and between normal hippocampi in almost all texture parameters (Bonilha et al. 2003). The most significantly differing parameters were short run emphasis, fraction of image in runs, difference of entropy and sum entropy. No changes were found between proven hippocampal sclerosis and contralateral hippocampi. Additionally, study on mesial TLE (n=36) was able to show that the analysis of mean and standard deviation of 1.5 T fluid attenuation inversion recovery (FLAIR) images was able to detect the lateralization of the epileptic focus with an accuracy of 98 %. Whereas, for wavelet texture features, the accuracy was 94 % (Jafari-Khouzani et al. 2010). The most recent article continued the study of accuracy in mesial TLE (n=12) combined with histological data from recently removed hippocampi. MRI texture parameters were able to classify the hippocampal tissues according to the clinical history (Alegro et al. 2012).

In focal cortical dysplasia studies from Antel, Bernasconi and co-workers first-order statistics- and co-occurrence matrix-based TA parameters were applied in detection of focal lesions in cerebral cortex (Antel et al. 2003, Bernasconi et al. 2001). Automated co-occurrence matrix-based TA classifier was able to identify 17 lesions from 20 manually labeled lesions (Antel et al. 2003).

In a recent study, TA was applied in juvenile myoclonic epilepsy (n=24) that has the same characteristic symptoms as EPM1: age onset from 12 to 18 years, myoclonus and tonic–clonic seizures. The parameters based on co-occurrence matrix were used in 2D image slices in 3 segments in right and left thalamus, no other structures or other texture features were evaluated in this study (de Oliveira et al. 2013). The study reported a difference in right thalami and the differing features included contrast, difference variance, difference entropy, sum of squares, and inverse difference moment from distances 3–5. No changes were found in left thalami.

Texture analysis of inherited neurodegenerative disease

Machado-Joseph disease or spinocellar ataxia type 3 is a rare autosomal dominantly inherited neurodegenerative disorder which causes progressive cerebellar ataxia and motor dysfunction. TA based on co-occurrence matrix was applied in Machado-Joseph disease patients (n=18) where ROIs were placed in image slices of corpus callosum, thalamus, putamen and caudate nuclei (de Oliveira et al. 2012). The most significant textural changes between controls and patients were found in caudate nuclei and left thalamus in line with previous histopathological and imaging studies. The authors pointed out that single feature textural differences were crucial for detection of differences.

Three-dimensional texture analysis applications

Theoretically, three-dimensional (3D) texture analysis provides more comprehensive data analysis of biological tissue texture properties and enables calculation of texture parameters in several directions. However, the literature on 3D TA applications in brain research is still sparse (Zhang et al. 2012, Kovalev, Kruggel & von Cramon 2003, Mahmoud-Ghoneim et al. 2003, Chen et al. 2007, Kocinski et al. 2012, Georgiadis et al. 2009).

Thus far, literature on texture analysis in radiological research is limited. The majority of the published studies are based on small study groups. Nonetheless, recent studies in the field of radiology have shown promise in the feasibility of TA also in medical imaging.

3 Aims of the study

The general aim of this thesis was to identify and characterize radiological findings of patients with EPM1 and to find possible correlations between radiological findings and phenotype of EMP1. More specifically, the aims were:

I To study the possible skeletal abnormalities of patients with EPM1 by measuring the regional calvarial thicknesses from three-dimensional MR images and by evaluating the skeletal structures of the patients from clinical X-rays and CTs.

II To evaluate regional cortical thinning and its possible relation to neurocognitive function in EPM1 by cortical thickness analysis (CTH).

III To investigate possible imperceptible structural differences in thalamus and other deep gray matter tissue in patients with EPM1 in comparison with healthy controls by using three-dimensional MRI-based texture analysis.

4 Thickened skull, scoliosis and other skeletal findings in Unverricht-Lundborg disease link cystatin B function to bone metabolism

ABSTRACT

Purpose
Unverricht-Lundborg disease (EPM1) is a rare type of inherited progressive myoclonic epilepsy resulting from mutations in the cystatin B gene, *CSTB*, which encodes a cysteine cathepsin inhibitor. Cystatin B, cathepsin K, and altered osteoclast bone resorption activity are interconnected *in vitro*. This study evaluated the skeletal characteristics of patients with EPM1.

Methods
Sixty-six genetically verified EPM1 patients and 50 healthy controls underwent head MRI. Skull dimensions and regional calvarial thickness was measured perpendicular to each calvarial bone from T1-weighted 3-dimensional images using multiple planar reconstruction tools. All clinical X-ray files of EPM1 patients were collected and reviewed by an experienced radiologist. A total of 337 X-ray studies were analyzed, and non-traumatic structural anomalies, dysplasias and deformities were registered.

Results
EPM1 patients exhibited significant thickening in all measured cranial bones compared to healthy controls. The mean skull thickness was 10.0 ± 2.0 mm in EPM1 patients and 7.6 ± 1.2 mm in healthy controls ($p<0.001$). The difference was evident in all age groups and was not explained by former phenytoin use. Observed abnormalities in other skeletal structures in EPM1 patients included thoracic scoliosis (35% of EPM1 patients) and lumbar spine scoliosis (35%), large paranasal sinuses (27%), accessory ossicles of the foot, and arachnodactyly (18%).

Conclusions
Skull thickening and an increased prevalence of abnormal findings in skeletal radiographs of patients with EPM1 suggest that this condition is connected to defective cystatin B function. These findings further emphasize the role of cystatin B in bone metabolism in humans.

4.1 INTRODUCTION

Progressive myoclonic epilepsies (PMEs) comprise a multiform group of rare, usually inherited neurodegenerative syndromes marked by myoclonus, epilepsy and progressive neurological deterioration (Shields 2004). Progressive myoclonic epilepsy type 1 or Unverricht-Lundborg disease (EPM1, ULD, OMIM 254800) is the most common single cause of PME. EPM1 has the highest prevalence in Finland (incidence 1:20 000 births per year, about 200 diagnosed cases), but it is also prevalent elsewhere in the Baltic Sea region and in the Western Mediterranean area. Sporadic cases of EPM1 have been reported

worldwide (Kälviäinen et al. 2008).

Clinically, EPM1 is characterized by stimulus-sensitive myoclonus and tonic-clonic epileptic seizures. The age of onset is age 6–16 years, and the progressive symptoms typically include ataxia, balance and motor dysfunctions, dysarthia and dysphagia. About one-third of EPM1 patients become severely incapacitated, but the clinical symptoms can be so mild that there is a delay in the diagnosis. Accordingly, typical clinical manifestations and neurophysiological findings in a child that previously appeared to be healthy eventually lead to the clinical diagnosis of EPM1, which can then be confirmed by mutation analysis (Kälviäinen et al. 2008).

Clinical studies of EPM1 have concentrated on the neurological and neurophysiological findings. There are few imaging studies, and most of them have focused on the brain. MRI studies reveal mild to moderate cerebral and/or cerebellar atrophy, loss of neuronal volume in the brainstem and changes in the basal ganglia (Koskenkorva et al. 2009, Chew et al. 2008, Mascalchi et al. 2002, Korja et al. 2007b, Santoshkumar, Turnbull & Minassian 2008, Korja et al. 2010).

Mutations in the *CSTB* gene, which encodes cystatin B, are responsible for the primary defect in EPM1 (Pennacchio et al. 1996). The result of these mutations is substantially reduced *CSTB* gene and protein expression in the majority of cases (Joensuu, Lehesjoki & Kopra 2008). Some patients with a phenotype similar to EPM1 have mutations in the *PRICKLE1*, *SCARB2* or *GOSR2* genes (Bassuk et al. 2008, Corbett et al. 2011, Dibbens et al. 2009). Although the CSTB protein has been reported to act as an inhibitor of cysteine cathepsins (Green et al. 1984, Leist, Jaattela 2001), its physiological function remains largely unknown. Studies in mice implicate oxidative stress and early microglial activation as factors that contribute to EPM1 pathogenesis (Tegelberg et al. 2012, Lehtinen et al. 2009).

Interestingly, CSTB has also been suggested to play a role in bone resorption (Laitala-Leinonen et al. 2006). Thus far, few studies have documented bone findings in EPM1 patients. Koskiniemi et al. first described thickening of the skull and thoracic scoliosis in EPM1 patients in 1974 (Koskiniemi et al. 1974). Subsequently, thickening of the calvarium in four EPM1 patients was interpreted as hyperostosis frontalis interna (HFI) (Korja et al. 2007a). HFI is considered a benign symmetric nodular protrusion of the inner table in the frontal bone with an unknown etiology (She, Szakacs 2004). We hypothesized that in addition to the previously reported thickening of the frontal bone, EPM1 may be associated with more extensive calvarial changes and possibly with other skeletal changes. To investigate this hypothesis, we examined bone structures in a series of 66 patients with genetically verified EPM1. Three-dimensional MRI was used to evaluate possible hyperostosis or other abnormalities in the cranial bones in detail, and the perpendicular skull thickness was measured in the frontal, parietal, temporal and occipital areas. Fifty healthy subjects served as controls. In addition, we retrospectively evaluated all clinical bone X-rays of these 66 EPM1 patients to identify any structural abnormalities.

4.2 PATIENTS AND METHODS

4.2.1 Study design

For this study, 66 EPM1 patients were evaluated at Kuopio University Hospital between 2008 and 2010. The patient group included 35 men and 31 women, with a mean age of 33 ± 12 years (range, 12–65 years), who were participating in an ongoing clinical and molecular genetics study at the Kuopio Epilepsy Center, Kuopio University Hospital. This study was jointly administered by the Folkhälsan Institute of Genetics and Neuroscience Center at the University of Helsinki. The patients had either participated in an earlier molecular genetics study or were referred to the Kuopio Epilepsy Center during the study. Of the EPM1 patients, 61 were homozygous for the dodecamer expansion mutation, while 5 were compound heterozygous for the expansion and the R68X mutations. The control group included 50 healthy subjects, 26 men and 24 women, with a mean age of 41 ± 15 years (range, 18–75 years). The ethics committee at the Kuopio University Hospital approved the study, and written informed consent was obtained from all participants.

4.2.2 Clinical assessment of patients with EPM1

The medical histories of EPM1 patients were determined from medical records and by interviewing the patients and their relatives. The mean onset age was 10 ± 3 years (range, 5–25 years), and the mean duration of the disorder was 23 ± 11 years (range, 4–44 years). All of the patients were treated with antiepileptic drugs (AEDs). Table 5 lists the EPM1 patients' medications.

Table 5. Antiepileptic medications (AED) taken by the 66 EPM1 patients.

Medication (*n*)		**Number of AEDs (*n*)**		**Former phenytoin use (*n*)**	
Valproate	65	Monotherapy	1	Several years	2
Clonazepam	48	2 AEDs	19	Temporarily	17
Levetiracetam	45	3 AEDs	25	Never	43
Topimarate	14	4 AEDs	19	Unknown	4
Piracetam	12	5 AEDs	2		
Lamotrigine	10				
Clobazam	3				
Phenobarbital	3				

4.2.3 MRI and data analysis

The subjects underwent MR imaging (1.5 T, Siemens Avanto, Erlangen, Germany), and the structures of their skulls were evaluated from T1-weighted 3-dimensional images (MPRAGE, TR 1980 ms, TE 3.09 ms, flip angle 15°, matrix 256 x 256, 176 sagittal slices, slice thickness 1.0 mm, in-slice resolution of 1.0 mm x 1.0 mm).

Skull dimensions and local skull thickness were measured in the middle of each calvarial bone on a picture and archiving communication system workstation (Sectra workstation IDS5, version 11.1.P3; SectraImtec AB; Linkoping, Sweden) using the multiple planar reconstruction tool to achieve orientations perpendicular to the bone. A single

observer (SS) who was blinded to the subject's status (patient or control) measured the calvarial dimensions in all patients and controls according to a fixed measuring paradigm (Figure 6). To assess the repeatability of the measurements, a second observer (RL) measured the skull thickness in 75 individuals. The following measurements were performed: 1) internal and external dimensions of the skull in the coronal, sagittal and caudocranial directions; and the thickness of the 2) frontal bones (bilateral), 3) parietal bones (bilateral), 4) occipital bones (bilateral) and 5) temporal bones (bilateral) at the coronal level of the external auditory meatuses.

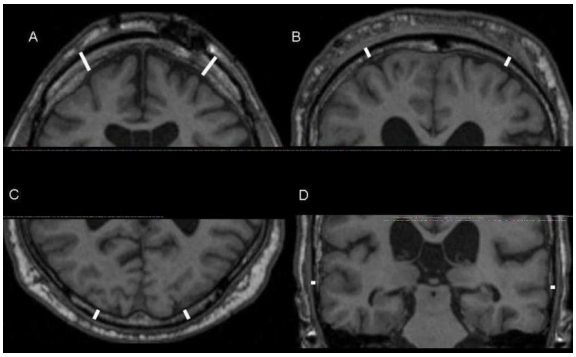

Figure 6. The mean thickness of each cranial bone was evaluated by calculating the average of the bilateral measurements of A) frontal bones from the coronal plane between the sagittal suture and the coronal suture; B) parietal bones from the coronal plane at the thickest point; C) occipital bones from the axial plane circa 20 mm above the AC-PC line between the sagittal suture and lambdoidal suture; and D) temporal bones at the coronal level of the external auditory meatuses.

The total intracranial volume (ICV) of the brain was evaluated using optimized voxel-based morphometry (VBM) with the VBM2 toolbox (http://dbm.neuro.unijena/vbm/) in SMP2 (Wellcome Department of Imaging Neuroscience, London, UK; www.fil.ion.ac.uk/spm) running under Matlab 6.5 (The MathWorks, Inc., Natick, MA) (Koskenkorva et al. 2009). Briefly, customized template and prior probability maps were created from T1-weighted 3-dimensional images, and then the primary VBM steps were performed, including normalization of the original magnetic resonance images and segmentation of normalized images. The absolute volumes of gray matter (GM), white matter (WM) and cerebrospinal fluid (CSF) were calculated from the segments. Finally, the GM, WM and CSF compartments were added to obtain the total ICV. The absolute volumes of these compartments and the ICV of 34 EPM1 patients were published previously (Koskenkorva et al. 2009).

4.2.4 X-ray and computed tomography (CT) analysis

The X-ray files of all 66 EPM1 patients were obtained from the patients' medical institutions and reviewed by an experienced radiologist (HM) and a resident (SS). X-ray films suitable for analyzing bones, spine or joints were identified in 61 patients. A total of 337 X-ray images were analyzed, and structural anomalies, dysplasias and deformities were registered. Osteoarthritis and other degenerative joint findings and fractures were

excluded from the evaluation. CT scans were evaluated when available to determine bone features in greater detail.

4.2.5 Statistical analysis

All statistical analyses were performed with the statistical software SPSS 17.0 for Windows (IBM SPSS Inc., Chigaco, IL). Differences were considered to be statistically significant when the P value was <0.05. The independent sample t-test was used for comparisons between groups, and correlation coefficients were calculated by Pearson's correlation test. The mean thickness of a cranial bone was determined by calculating the average of the bilateral measurements. Analysis of covariance (ANCOVA) was employed to determine the influence of different factors (age, onset age, duration of the disease, height, ICV) on the skull thickness of EPM1 patients, with gender and former phenytoin use as independent variables. Clinically relevant and potential predictors that showed statistically significant associations with the mean skull thickness in univariate analyses were included in ANCOVA. The intraclass correlation coefficient (ICC) was used to assess reproducibility and agreement of measurements between two readers (SS and RL) in 75 random subjects. (Landis, Koch 1977). The intraobserver reproducibility between skull thickness measurements was excellent. The intraclass correlation coefficient was 0.929. The mean skull thicknesses for 75 random subjects were 9.7 ± 2.1 mm (Observer A) and 9.4 ± 2.2 mm (Observer B), and no significant statistical difference in the mean values of the Observer A and B was found.

4.3 RESULTS

EPM1 patients exhibited significant calvarial thickening in all measured cranial bones compared to healthy controls (Table 6). The mean skull thickness was 10.0 ± 2.0 mm in EPM1 patients and 7.6 ± 1.2 mm in healthy controls ($p<0.001$). The most remarkable alterations were in the frontal bone (11.4 ± 3.1 mm vs. 6.6 ± 1.7 mm, $p<0.001$), parietal bone (9.4 ± 2.3 mm vs. 7.1 ± 1.6 mm, $p<0.001$) and temporal bone (2.4 ± 0.8 mm vs. 1.6 ± 0.5 mm, $p<0.001$). The mean intracranial volumes were 1706 mL ± 200 mL in EPM1 patients (n=60) and 1949 mL ± 185 mL in controls (n=28) ($p< 0.001$).

Table 6. Cranial bone thicknesses (mm) in 66 EPM1 patients and 50 control subjects.

	Men		**Women**	
	Patients	**Controls**	**Patients**	**Controls**
Frontal bone	12.2 ± 2.7***	6.8 ± 1.5	10.4 ± 3.4***	6.3 ± 1.9
Parietal bone	9.9 ± 2.2 ***	7.5 ± 1.4	8.9 ± 2.2 ***	6.7 ± 1.8
Temporal bone	2.5 ± 0.8 ***	1.7 ± 0.5	2.4 ± 0.8 ***	1.5 ± 0.4
Occipital bone	7.0 ± 1.8*	5.9 ± 1.6	6.2 ± 1.6 ***	4.8 ± 1.3
External sagittal skull	184.8 ± 8.3	181.9 ± 8.3	178.1 ± 7.7	176.2 ± 6.9
Internal sagittal skull	165.4 ± 8.0	164.3 ± 8.5	159.6 ± 7.3	159.7 ± 6.0
External coronal skull	139.7 ± 5.5	140.0 ± 4.7	133.0 ± 4.7	134.6 ± 5.7
Internal coronal skull	125.4 ± 5.1**	129.9 ± 5.0	119.9 ± 5.7 ***	125.3 ± 5.1
External CC skull	90.2 ± 4.6*	92.9 ± 5.3	85.5 ± 4.1	86.5 ± 3.8
Internal CC skull	81.5 ± 4.2***	86.1 ± 4.8	79.1 ± 4.1*	81.4 ± 3.4
Mean skull thickness	10.6 ± 1.9***	8.0 ± 1.2	9.4 ± 2.0***	7.2 ± 1.2

* $p \leq 0.05$ ** $p \leq 0.01$ *** $p \leq 0.001$ compared to control group

The difference in skull thickness between patients and controls was evident in all age groups (Figure 7). In addition, men had thicker skulls than women both in the healthy control group (8.0 ± 1.2 mm vs. 7.2 ± 1.2 mm, p=0.012) and in the group of patients with EPM1 (10.6 ± 1.9 mm vs. 9.4 ± 2.0 mm, p=0.023). The thickness of the skull increased with age in EPM1 patients (r=0.363, p=0.003) but not in healthy controls (r=0.160, p=0.268) (Figure 7). In women in the control group, the mean thickness of the frontal bone reached that of men in the control group as a result of aging, but this was not observed in EPM1 patients (Figure 8).

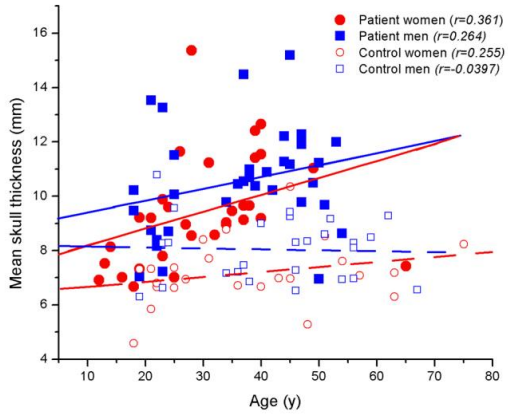

Figure 7. Mean skull thickness of EPM1 patients and healthy controls. The mean skull thickness was determined by calculating the average of the bilateral measurements and the differences between the external and internal skull dimensions. The thickness of the skull increased with age in EPM1 patients (r = 0.363, p = 0.003) but not in healthy controls (r = 0.160, p = 0.268).

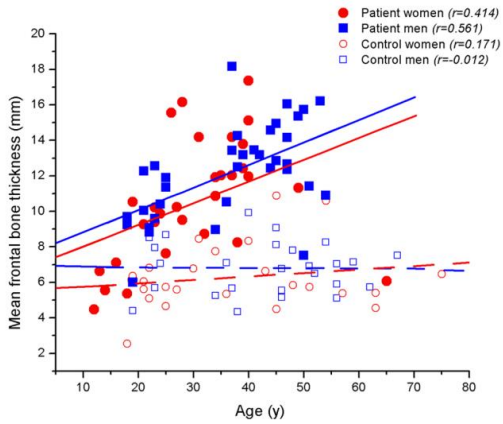

Figure 8. Mean frontal bone thickness of EPM1 patients and healthy controls. The mean frontal bone thickness was notably higher in EPM1 patients. Also, there was a slight increase in frontal bone thickness in female controls, possibly indicating hyperostosis frontalis interna.

Morphologically, the thickening was generalized; there were no distinct regional or focal findings. However, the inner table was affected in particular. Digital head CT scans were available for 15 patients, and evaluation of the skull indicated osteoporotic bone structure in the skulls of these patients (Figure 9).

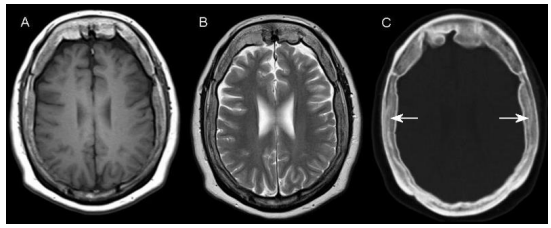

Figure 9. Representative images showing calvarial bone structure in a 28-year-old female patient. A) T1-weighted and B) T2-weighted MRI images. C) Head CT scan of the same patient showing marked and diffuse skull thickening and decreased bone density especially in the frontal bones. Note also the laminar appearance of the temporoparietal calvarium (arrows).

The mean skull thickness was significantly correlated with age ($r=0.363$, $p=0.003$), duration of the disease ($r=0.430$, $p<0.001$) and height ($r=0.292$, $p=0.017$). There was no correlation between the mean skull thickness and onset age ($p=0.153$, $r=-0.381$) in EPM1 patients; therefore, onset age was excluded from the final ANCOVA model. There was no significant statistical correlation between mean skull thickness and total ICV in the EPM1 patient group ($r=-0.215$, $p=0.099$). No significant correlation was found between the mean skull thickness and ICV in male EPM1 patients ($r=-0.324$, $p=0.066$). In contrast, in the female patients the ICV was significantly associated with the mean skull thickness ($r=-0.517$, $p=0.006$) and was thus included in the final ANCOVA model.

Since age is a common confounding factor that correlates strongly with duration of the disease and height, and since height correlates strongly with both duration of the disease and ICV, these parameters were excluded from the final ANCOVA model. Eventually, the duration of the disease and ICV were included in an analysis of covariance with gender and former phenytoin use as independent variables. As shown in Table 7, the adjusted model predicted mean skull thickness fairly well ($R^2=0.362$, adjusted $R^2=0.299$, $p<0.001$). The interaction between gender and former phenytoin use was not significant ($F(1,51)=1.078$, $p=0.304$). Gender, ICV and duration of the disease had a significant effect on the mean skull thickness, while former phenytoin use did not. Type III sums of squares showed the contribution to the prediction, with duration of the disease (ß=0.078) being the most effective variable followed by ICV (ß=-0.004) and gender (ß=0.748).

Table 7. ANCOVA results for predicting mean skull thickness.

Factor	Type III sum of squares	df	Mean Square	F value	p	ß
Corrected model	79.970	5	15.994	5.782	0.000	-
Duration of the disease	26.479	1	26.479	9.572	0.003	0.078
Total ICV	21.118	1	21.118	7.634	0.008	-0.004
Gender	14.927	1	14.927	5.396	0.024	0.748[1]
Former phenytoin use	0.430	1	0.430	0.155	0.695	-
Gender* Former[2] phenytoin use	2.983	1	2.983	1.078	0.304	-
Error	141.085	51	2.766			

[1]male EPM1 patients, [2]interaction effect

(R^2 = 0.362, adjusted R^2=0.299)

Table 8 summarizes the structural findings determined by examining the X-ray files. Skeletal changes were observed in 37 (61%) EPM1 patients. Thoracic (35%) and lumbar spine (35%) scoliosis was common in the EPM1 patient group. Accessory ossicles of the foot were also recorded, and the presence of os tibiale externum (68%) was remarkably high. Large paranasal sinuses (27%) were another common finding. Four patients had arachnodactyly.

Table 8. Prevalence of bone abnormalities on X-rays.

Prevalence in our data			Prevalence in literature	
	Patients (n)	Percentage (%)	Reference	Percentage (%)
Scoliosis				
Thoracic Spine	15/43	34.9	Ueno et al. 2011 (children)	1.0
Lumbar Spine	7/20	35.0	Carter et al. 1987 (25–74 years)	8.3
			Hong et al. 2010 (>60 years)	35.5
Accessory ossicles in lower extremities				
Os tibiale externum	19/28	67.9	Mellado et al. 2003	4.0-21.0
Os peroneum	6/28	21.4	Mellado et al. 2003	9.0
Other	6/39	15.4		
Other				
Large paranasal sinuses	8/27	29.6		
Arachnodactyly	4/22	18.2		

Furthermore, 13 patients had some other bone abnormality, including talonavicular coalition (n=1/29 cases in which the evaluation was possible), talocalcaneal coalition (n=1/29), abnormal femur angle (n=1/11), abnormal distal head of the humerus (n=1/10), abnormal metaphysis of the humerus (n=1/10), several exotoses in the tibia, talus and hallux (n=1/18), Erlenmeyer flask deformity in the femur (n=1/24), positive metacarpal sign (n=2/22), tapering occipital bone (n=1/15), double promontorium and extra sacral hemivertebrae S1 (n=1/20), hemivertebrae in the upper thoracic spine (n=1/43), apophysis in the lumbar vertebrae L1 and L5 (n=1/20) and Klippel-Feil fusion in the cervical spine (anterior segments of C2-5 and C3-4 in posterior segments) (n=1/18).

There was a correlation between the number of bone abnormalities and the mean skull thickness in patients with EPM1 (r=0.427, p=0.006). No correlation was found between the number of bone abnormalities and patient age, duration of the disease or age of onset. Further, there was no difference in the number of bone abnormalities in men vs. women or former phenytoin users vs. non-users.

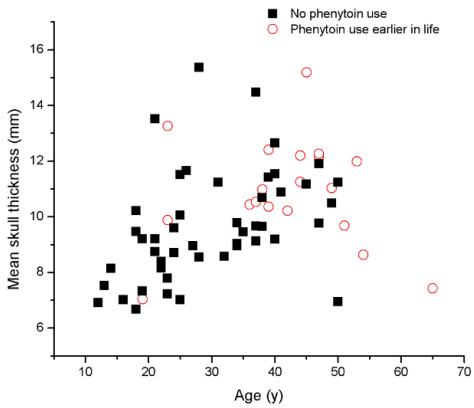

Figure 10. Mean skull thicknesses of former phenytoin users (*n*=19) and non-users (*n*=43) showed that former phenytoin use did not increase the skull thickness in EPM1 patients.

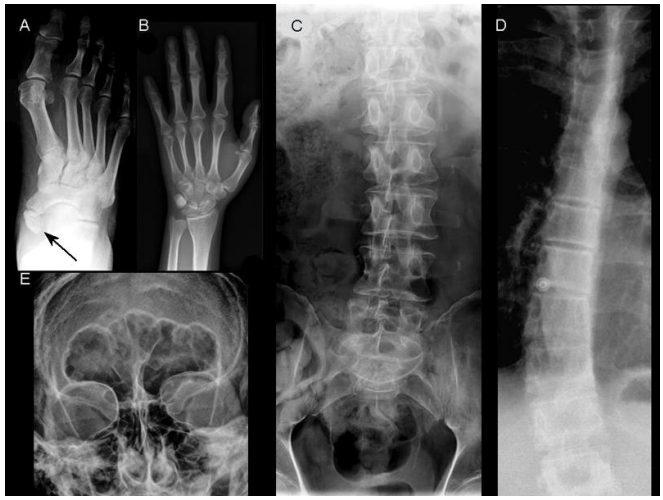

Figure 11. Representative images of skeletal findings in EPM1 patients. A) Os tibiale externum of a 47-year-old male patient. B) Arachnodactyly (MCI=10.4) of a 25-year-old female patient. C) Lumbar spine scoliosis of a 47-year-old male patient. D) Thoracic spine scoliosis of a 21-year-old male patient. E) Large paranasal sinuses of a 23-year-old male patient.

4.4 DISCUSSION

EPM1 is a rare disorder, and clinical research has been challenging because of the small number of cases worldwide. Consequently, there are few imaging studies of EPM1 patients. In the present study we had a unique opportunity to analyze the skeletal findings of 66 EPM1 patients. Here we report radiological findings of skeletal involvement in EPM1 that support a role for the CSTB protein as a modulator of bone metabolism.

EPM1 patients exhibited significant calvarial thickening in all measured cranial bones compared to the control group. The thickening was diffuse, involving the entire skull, and was most evident in the frontal, temporal and parietal bones. The skull thickness increased with age in EPM1 patients but not in healthy controls (Figure 7), suggesting that a lack of functional CSTB protein due to mutations in the *CSTB* gene affects the skeletal system throughout the patient's lifetime. A retrospective clinical study of 20 EPM1 patients demonstrated that the neurological symptoms in Unverricht-Lundborg disease progress over a limited period, with age-related apoptosis in selected neuronal populations (Magaudda et al. 2006). More experimental studies are needed to better understand CSTB protein function in human neuronal and skeletal systems.

It was suggested previously that hyperostosis frontalis interna (HFI) could explain the frontal bone thickening observed in EPM1 (Korja et al. 2007a). HFI is a sex- and age-dependent phenomenon of unknown etiology that is highly related to the hormonal changes that vary over a lifetime (Hershkovitz et al. 1999, Ross, Jantz & McCormick 1998). The overall prevalence of HFI is 5–12%, but it is notably higher among post-menopausal elderly women (40–60%). HFI was also seen in our group of healthy female controls (Figure 8). HFI is a general incidental finding that by itself does not cause significant

clinical disease (Hershkovitz et al. 1999). Accordingly, HFI can be considered as a separate, non-disease-related phenomenon. Our results confirm more generalized skull thickening in EPM1 patients that cannot be explained by HFI.

Human skull and cranial thickness have been investigated extensively. Early anthropological studies suggested that men have thicker skulls because of the size difference between men and women, but modern autopsy biopsy studies and one MRI study found no correlation between age, gender and body composition and thickness of the skull (excluding HFI) (Hershkovitz et al. 1999, Ross, Jantz & McCormick 1998, Hatipoglu et al. 2008, Lynnerup, Astrup & Sejrsen 2005). Contrary to these earlier studies, the men in our study tended to have thicker skulls than the women. The discrepancy between our results and those reported by others could be that we used different methods. Also, we used more measurement points, as well as more precise measurement points, than the previous studies.

Thickening of the skull is associated with many disorders, such as severe anemia, polycythemia vera, myelofibrosis, hyperparathyroidism and myeloproliferative diseases such as lymphoma, multiple myeloma and myelodysplasic syndromes (Ghanem et al. 2006, Nobauer, Uffmann 2005). These conditions were ruled out in our EPM1 patients. In addition, generalized thickening of the skull is associated with the use of an established anticonvulsant, phenytoin (Kattan 1970). A recent report describes skull thickening and cerebral atrophy after 13 years of phenytoin use (Chow, Szeto 2007). Indeed, 3 decades ago phenytoin was commonly used to treat epilepsy in Finland. We therefore evaluated whether the duration of phenytoin therapy correlated with skull thickness. Only two EPM1 patients had a history of long-term phenytoin therapy (≥10 years), while others reported short-term phenytoin use that ranged from one dose for status epilepticus up to 2 years. In this study, previous phenytoin use did not explain the skull thickening we observed in EPM1 patients (Table 7 and Figure 10).

Diffuse skull thickening and other skeletal changes are associated with a number of hereditary congenital bone disorders (Table 9). Interestingly, many of these disorders have neurological aspects, and many are extremely rare and occur only in certain populations, such as sclerosteosis among the Dutch settlers in Africa (Gardner et al. 2005). The genetic defects underlying many such disorders have been identified. For example, the role of cathepsin K in osteoclast function was discovered because of its association with pycnodysostosis (Gelb et al. 1996). Paget's disease is relatively common, and should be kept in mind when making a differential diagnosis of skull thickening. However, Paget's disease has a different clinical picture than EPM1, occurring in middle age (3–4% of those >40 years of age); in contrast, in EPM1 the thickening of the skull and other radiological findings are seen in all age groups.

Of the 61 EPM1 patients, 37 exhibited various bone abnormalities that were noted during a systematic evaluation of bone X-rays (Table 8, Figure 11). In EPM1 patients, the prevalence of both thoracic and lumbar spine scoliosis was 35%, which is a higher prevalence than in healthy age-matched subjects. The literature reports prevalence rates for scoliosis that vary from 1% among school children (Ueno et al. 2011), to 8.3% among US adults aged 25–74 years (Carter, Haynes 1987) and up to 35.5% among individuals older than 60 years (Hong et al. 2010). Scoliosis is also widespread in patients affected by the syndromes shown in Table 9. Large paranasal sinuses were observed in 27% of the EPM1 patients, a finding that is also reported in Dyke-Davidoff-Masson syndrome (Atalar, Icagasioglu & Tas 2007) (Table 9). Accessory ossicles of the foot were relatively common in the EPM1 patients, and the prevalence of os tibiale externum was remarkably high (68%) among EPM1 patients compared to the estimated prevalence of 4–21% in healthy individuals (Mellado et al. 2003). In addition, the EPM1 patients exhibited arachnodactyly,

vertebral abnormalities and other occasional bone findings.

The main limitation of the current study was its retrospective design. All patients prospectively underwent head MRI, but bone structure evaluation was limited to the clinical X-ray files that were available in the patients' medical files. Systematic prospective evaluation of skeletal changes in EPM1 patients was not possible due to radiation exposure concerns. However, there was a correlation between the number of bone abnormalities and the mean skull thickness in individual EPM1 patients; this correlation may have been statistically underestimated because the number of available x-ray files varied among the patients, and this may have influenced which skeletal changes we observed. Further, EPM1 patients may have more bone fractures than the healthy population. Traumatic skeletal changes were not evaluated in the present study. An excess of fractures could theoretically be associated with the movement disorder and epilepsy, as well as with the immobilization and reduced bone mineral density (Beerhorst et al. 2012). Unfortunately, EPM1 patients did not undergo bone mineral density measurements and bone turnover markers were not determined, which is a limitation of our study. These would have afforded more detailed information about the nature and severity of fractures, bone mass and bone mineral density in the patients with EPM1.

CSTB is an endogenous inhibitor of cysteine cathepsins, which are lysosomal proteases that promote apoptosis (Green et al. 1984, Leist, Jaattela 2001). Experiments show that CSTB has neuroprotective properties and that cathepsin B contributes to the pathophysiology of EPM1 (Pennacchio et al. 1998, Shannon et al. 2002, Houseweart et al. 2003, Lehtinen et al. 2009). Cathepsin K, a major cysteine protease in mature osteoclasts, has a critical role in bone resorption (Gelb et al. 1996, Saftig et al. 1998, Xia et al. 1999). *In vitro* study shows that CSTB is involved in bone resorption by regulating intracellular cathepsin K activity and that it protects osteoclasts from experimentally-induced apoptosis (Laitala-Leinonen et al. 2006). In mice, overexpression of cathepsin K increases the thickness and mineral density of diaphyseal cortical bone and increases the porosity of the diaphyseal cortex (Morko et al. 2005). In line with these findings, osteoporotic structures were observed in the head CT scans of the EPM1 patients in this study (Figure 9). Taken together, these data support the idea that a decrease in functional CSTB contributes to the skeletal phenotype of EPM1.

It has been shown that also human osteoblasts produce cathepsin K *in vitro* and the osteoblast-like cells function as matrix-degrading cells and can finalize the resorption phase before synthesizing new mineralized matrix (Mandelin et al. 2006, Mulari et al. 2004). Pycnodysostosis is a genetic deficiency of cathepsin K characterized by short stature, brittle bones and increased bone density. Contrary to these findings, delayed calvarial ossification and acro-osteolysis are also seen in pycnodysostosis (Gelb et al. 1996). This could be explained by the fact that the ossification of the human skull and the distal phalanges greatly differs from other skeletal structures. Further, impaired osteoclastic bone resorption in cathepsin-K-deficient mice results in the activation of osteoblastic cells to produce increased amounts of proteolytic enzymes *in vivo* (Kiviranta et al. 2005), and the overexpression of cathepsin K accelerates the resorption cycle and osteoblast differentiation (Morko et al. 2009). The detailed nature of cathepsin K activation is still poorly known and further studies are warranted to investigate whether osteoblastic cathepsin K has consequences in pycnodysostosis or the skeletal changes seen on EPM1 patients.

Loss of neurons plays a critical role in the pathophysiology of EPM1. From 2 months of age onwards, CSTB-deficient mice exhibit a severe loss of cerebellar granule cells as well as marked progressive loss of cerebellar volume and progressive atrophy of the cerebral cortex (Pennacchio et al. 1998, Tegelberg et al. 2012). Moreover, early and localized glial

activation precedes neuron loss, which first occurs within the cortex in the thalamocortical system and, subsequently, in the corresponding thalamic relay nucleus (Tegelberg et al. 2012). In addition, imaging studies in human EPM1 patients show mild to moderate cerebral and cerebellar atrophy in visual assessment, an MRI study shows loss of neuronal volume in the brainstem and motor cortex, and a VBM study shows thalamic atrophy (Koskenkorva et al. 2009, Chew et al. 2008, Mascalchi et al. 2002, Santoshkumar, Turnbull & Minassian 2008). In light of these findings, in the present study we hypothesized that thicker skulls would correspond to smaller brains. However, there was no significant statistical correlation between mean skull thickness and total ICV in the EPM1 patient group. The ANCOVA model (Table 7) showed a statistical correlation between ICV and mean skull thickness ($p=0.008$), but the regression coefficient for ICV as a predictor of mean skull thickness was small ($\beta=-0.004$). This may be because EPM1 selectively targets specific cells in certain brain structures while most of the neuronal architecture remains intact.

In conclusion, skull thickening and other specific skeletal findings in 66 EPM1 patients suggested that abnormal ossification of the skeleton is a universal feature of EPM1 that is associated with a defect in CSTB function. In order to gain a more complete understanding of the skeletal phenotype in EPM1, prospective evaluations of skeletal development, bone mineral density and fracture healing are required, as is molecular characterization of CSTB function in osteoclasts.

Table 9. Disorders with skeletal abnormalities: A review of the literature.

Dysplasia or Condition	**Reference**	**Method**	**No. of cases**	**Epidemiology**	**Involvement**	**Most common findings**	**Gene**	**Inheritance**
Paget's disease	Smith et al. 2002	Review	-	3-4% of the population over 40 years	Widespread osseus involvement related to the phase of disease	Lytic phase: Osteoporosis circumscripta. Blastic phase: diffuse sclerosis and calvarial thickening. Diffuse vertebral sclerosis, bowing in the spine results in scoliosis	*SQSTM1* *TNFRSF11B* *TNFRSF11A* *CSF1* *OPTN* *TM7SF4* *VCP* (Ralston, Layfield 2012)	AD:15 - 40%, Variable
Craniofacial fibrous dysplasia	Lisle et al. 2008	Review	-	Relatively common bone disorder	Face, skull base	Lesions in the skull base or face, generalized sclerotic involvement of the skull base, leontiasis ossea	*GNAS1* (Mangion et al. 2000)	Sporadic, Non-hereditary
Osteopetrosis	Cure et al. 2000	Brain MRI	47	ADO 1/20 000 ARE 1/250 000	Generalized bone disease	Diffuse sclerosis and thickening of the calvarium, skull base, spine and pelvis	At least 10 genes have been identified inc. *CLCN7* *TCIRG1* *OSTM1* (Del Fattore, Cappariello & Teti 2008)	AD, AR or X-linked recessive
Albers-Schonberg (Type II autosomal dominant) osteopetrosis	Benichou 2000 et al.	X-rays	42	1/20 000	Vertebral end-plates, iliac wings, skull base	Fractures, increased skull base density, hip osteoarthritis, thoracic or lumbar scoliosis, sandwich vertebraes	*CLCN7* (de Vernejoul, Schulz & Kornak 1993)	AD
McCune-Albright syndrome	Bulakbasi et al. 2008	MRI, CT	-	1-9/1 000 000	Face, base of the skull, Vertebrae	Widespread bone marrow involvement and enlargement of the skull and facial bones, scoliosis	*GNAS* (Weinstein et al. 1991)	Sporadic, Non-hereditary

Camurati-Engelmann disease	Janssens et al. 2006	Review CT, X-rays	100	Rare	Diaphyses of the long bones, pelvis, skull	Cortical thickening of the diaphyses of the longbones, extensive sclerosis and thickening of the calvaria, especially at the skull base	*TGFB1*	AD
Frontometa-physeal dysplasia	Morava et al. 2003	X-rays	6	Rare	Skull, face, vertebrae, extremities	Cranial hyperostosis, flared metaphyses, severe, progressive scoliosis	*FLNA* (Robertson et al. 2006)	X-linked dominant
Juvenile Paget's disease	Tau et al. 2004	X-rays	1	Rare	Generalized bone disease	Thickening and sclerosing of the skull, enlargement of bones and bone deformities, kyphoscoliosis, hyperlordosis	*TNFRSF11B* (Whyte et al. 2002)	AR
Osteopathia striata with cranial sclerosis	Magliulo et al. 2007	X-rays, CT, MRI	1	Rare, more than 100 reported cases	Skull, face, long bones	Hyperostosis of the cranial vault and increase in density of the cranial base	*FAM123B* (Jenkins et al. 2009)	X-linked dominant
Pycnodysostosis	Mills et al. 1988	X-rays	2	Rare	Generalized bone disease	Increased bone density and sclerosis with bone fragility, spondylolisthesis	*CSTK* (Gelb et al. 1996)	AR
Sclerosteosis	Gardner et al. 2005	Skull X-rays, DXA	25	Rare, condition occurs mainly in Afrikaners	Generalized bone disease	Progressive bone thickening and sclerosis of the skeleton, especially of the skull, thickening of the skull is also seen in (healthy) heterozygous carriers	*SOST* (Brunkow et al. 2001)	AR
Van Buchem disease	Vanhoenac ker et al. 2003	X-rays, CT	13	Rare, about 30 reported cases	Skull, mandible, ribs, clavicles, long bones	Symmetric thickening and hyperostosis of the calvaria, skull base, diaphyseal broadening	*SOST* *LRP5* (Staehling-Hampton et al. 2002)	AR
Dyke-Davidoff-Masson syndrome	Atalar et al. 2007	MRI, CT	19	Rare	Skull, face	Thickening of the skull, enlargement of the frontal sinuses	?	?

Craniodia-physeal dysplasia	Marden et al. 2004	MRI, CT	1	Rare	Craniofacial bones, tubular bones	Massive and progressive hyperostosis of the craniofacial bones	*SOST* (Kim et al. 2011)	Sporadic AD
Craniometa-physeal dysplasia	Lamazza et al. 2009	X-rays, CT	1	Rare	Skull, face, metaphyses of the long bones	Prominent craniofacial abnormalities, sclerosis of the skull bones, marked thickening of the cranium, scoliosis, Erlenmeyer flask deformity	*ANKH* (Reichenberger et al. 2001)	AD AR
Metaphyseal dysplasia (Pyle disease)	Beighton 1987	Review X-rays	-	Rare	Mild generalized bone disorder	Diffuse skull thickening, expansive metaphyses, genu valgum	unknown	AR (Raad, Beighton 1978)
Coffin-Lowry syndrome	Kondoh et al. 1998	MRI	1	Rare	Skull, face, skeleton	Thick calvarium, narrow intervertebral spaces, progressive kyphoscoliosis, drumstick shaped terminal phalanges	*RPS6KA3* (Field et al. 2006)	X-linked dominant
Hajdu-Cheney syndrome	O'Reilly et al. 1998	X-rays	1	Rare	Face, skull, vertebrae, limbs	Thickening of the skull vault, prominent occiput, multiple wormian bones, severe kyphoscoliosis, osteolysis of the terminal phalanges	*NOTHC2* (Simpson et al. 2011)	AD
Lenz-Majewski syndrome	Gorlin et al. 1983	X-rays	5	Rare	Generalized bone disease	Thickening of the calvaria, dwarfism, dense, thick bones, progressive sclerosis	unknown	AD
Large arteriovenous malformation	Govender et al. 2006	MRI, X-rays	1	Rare	Skull	Generalized skull vault thickening	-	-
Hyperostosis cranii ex vacuo	Di Preta et al. 1994	X-rays, CT	1	Rare	Skull	Dense irregular thickening of the skull base and all regions of the calvarium	-	-

AR: Autosomal recessive; AD: Autosomal dominant

5 Regional cortical thinning associates with neurocognitive profile in Unverricht-Lundborg disease (EPM1)

ABSTRACT

Objectives
Patients with Unverricht-Lundborg disease (progressive myoclonus epilepsy type 1, EPM1) display considerable variation in both clinical severity and neurocognitive manifestations even though they have a uniform genotype. Cortical thickness analysis (CTH) in MRI provides group-level structural information in neurological and neuropsychological disorders. The aim was to investigate the possible relationship between cortical thickness, disease severity and neurocognitive function in EPM1.

Methods
Sixty-three genetically verified EPM1 patients were clinically evaluated by using the Unified Myoclonus Rating Scale (UMRS) test panel. Patients were divided into three sub-groups according to their myoclonus in action score: Mild Disability (Action myoclonus scores 1−30; n=20); Moderate Disability (scores 31−59, n=21) and Severe Disability (scores ≥ 60; n=22). The cognitive performance of the patients was evaluated with a neuropsychological test battery, tailored to be suitable for EPM1. The patients underwent T1-weighted 3-dimensional MR imaging. The regional cortical thicknesses (CTH) were analysed and correlated to the neurocognitive profile.

Results
Intellectual functioning of the patients varied from high average to defective and correlated with the disease severity. Utilizing the CTH analysis, the EPM1 patients with the severe form of the disease had thinner cortex than patients with a milder form of the disease. The anatomical areas affected included Broca's and Wernicke's areas; fusiform gyrus; retrosplenial and perirhinal cortex (areas responsible for processing of verbal and complex visual data) and posterior cingulate and anterior prefrontal cortex (areas responsible for higher-order cognitive functions).

Conclusions
CTH analysis can supplement new information on visually normal MR images. The observed associations provide a structural neuroanatomical-biological basis for disease severity and cognitive decline in EPM1. A further evaluation will be needed to clarify the benefits of assessing CTH in individual EPM1 patients.

5.1 INTRODUCTION

Unverricht-Lundborg disease, progressive myoclonus epilepsy type 1 (EPM1, OMIM 254800) (Shahwan, Farrell & Delanty 2005) is a rare neurodegenerative disorder caused by mutations in the cystatin B encoding *CSTB* gene (Pennacchio et al. 1996, Lalioti et al. 1997, Joensuu, Lehesjoki & Kopra 2008). The age of onset in EPM1 is usually between 6–16 years and the first symptoms are stimulus-sensitive myoclonic jerks and tonic-clonic epileptic seizures. During the subsequent 5–10 years, symptoms progressively worsen and patients develop ataxia, intentional tremor, dysarthia and other signs of motor incoordination. Devastating myoclonias are the most disabling symptoms encountered during the disease. However, the clinical course and phenotype of the disease are heterogeneous. (Kälviäinen et al. 2008)

Cognitive function in patients with EPM1 has been found to be impaired, e.g., deficits in processing and executive functions and in working memory have been reported (Chew et al. 2008, Ferlazzo et al. 2009, Giovagnoli et al. 2009). Psychiatric disorders have been also described (Magaudda et al. 2006, Chew et al. 2008, Ferlazzo et al. 2009) although the presence of psychiatric problems in EPM1 has not been systematically assessed.

At the time of the EPM1 diagnosis, the qualitative MRI of the brain is usually interpreted as normal (Kälviäinen et al. 2008). However, volumetric/statistical analysis of the MR images of patients with EPM1 has revealed cerebral atrophy (Koskenkorva et al. 2009, Mascalchi et al. 2002). A previous cortical thickness analysis (CTH) study detected significant thinning of the cortical motor areas of patients with EPM1 and this was linked to the degree of the clinical severity of the myoclonus (Koskenkorva et al. 2012). CTH is a novel MR image analysis method that has been proposed to be a more sophisticated alternative to volumetric and voxel-based morphometry methods for measuring regional brain atrophy since it provides a direct quantitative index of regional thickness of the cerebral cortex (Lerch, Evans 2005, Lerch et al. 2005).

It is not understood why there are such wide clinical and neurocognitive variations in patients with EPM1 i.e. the heterogeneity of the phenotype. Though the primary genetic defect mutation in EPM1 is known, the actual pathological mechanisms leading to the symptoms remain unclear. By combining structural MRI data of the regional thickness of the cerebral cortex and quantitative results from neuropsychological evaluation, we aimed to determine whether cortical structures in specific brain areas could be linked to the cognitive impairments of the EPM1 patients.

5.2 PATIENTS AND METHODS

5.2.1 Subjects

Sixty-three genetically verified patients with EPM1 (35 men, 28 women; mean age 35.1 ± 10.9 years, range 16–64 years) participated a translational clinical and molecular genetics study organized by Kuopio Epilepsy Center, Kuopio University Hospital jointly with the Folkhälsan Institute of Genetics and Neuroscience Center, University of Helsinki; the patients were evaluated in 2006–2010. The ethical committee of Kuopio University Hospital approved the study protocol, and a written informed consent was obtained from all participants.

5.2.2 Clinical assessment of EPM1 patients

A neurologist performed the clinical evaluations. The medical histories of EPM1 patients were collected from medical records and by interviewing the patients and their relatives. EPM1 patients' clinical data is presented in Table 11. At the time of imaging and neuropsychological examination, all patients were treated with antiepileptic drugs (AEDs). The patients typically received a combination of at least two AEDs, titrated individually to maximally tolerated dosages (Table 10). With the exception of the oldest patient, all other 62 patients were receiving valproate. One patient had valproate acid monotherapy, 13 patients were being treated with 2 AEDs, 23 patients with 3 AEDs, 17 patients with 4 AED's, 8 patients with 5 AED's and 1 patient with 6 AED's.

The severity of myoclonus was used as a criterion for different subgroups, as the clearest marker of the disease progression. The Unified Myoclonus Rating Scale (UMRS) test panel was used for myoclonus severity evaluation as a part of the clinical examination. UMRS is a quantitative 74-item clinical rating instrument comprising 8 sections (Frucht et al. 2002). Patients' performances were recorded on video and the test sections were evaluated using a standard protocol. Myoclonus with action score (1–160) was used to evaluate the severity of myoclonus. The patients were subsequently classified into three disability groups according to the Myoclonus with Action scores: Mild Disability Group had scores 1–30; Moderate Disability Group had scores 31–59 and Severe Disability Group had scores ≥ 60.

Table 10. AEDs and dosages of patients with EPM1 received at time of neuropsychological testing.

Medication (mg/day)	**n**	**Mean ± SD**	**Range**
Valproate	62	1600 ± 650	300 – 3500
Clonazepam	49	4.4 ± 2.7	0.25 – 12
Levetiracetam	44	2290 ± 990	500 – 4000
Topimarate	14	270 ± 240	75 – 1000
Lamotrigine	12	210 ± 110	25 – 400
Piracetam	10	13680 ± 8060	2400 – 24000
Clobazam	3	30 ± 15	10 – 40
Other*	16		

*phenobarbital, pirimidone, zonisamide, diapam, nitrazepam, ethasuximide

5.2.3 Neuropsychological evaluation

Described in detail by Äikiä et al. (unpublished data), the neuropsychological evaluation consisted of measures for intellectual ability, verbal memory as well executive and psychomotor functions. Intellectual ability was assessed with six subtests of the Wechsler Adult Intelligence Scale Revised (WAIS-R) (Wechsler D 1981). Verbal and Performance Intelligence Quotients (VIQ and PIQ) were calculated. Verbal memory was assessed with a 15-word list learning test and story recall test, immediate and delayed memory were evaluated and percent retention scores were calculated. Executive functions were assessed

with the Trail Making test (TMT) and Stroop test. Psychomotor function was evaluated with Digit symbol test, alternating S-task and finger tapping. The neuropsychological test variables were converted into z-scores relative to the control group mean.

5.2.4 MR Imaging Acquisition Protocol and Data Analysis

The MR (1.5 T, Siemens Avanto, Erlangen, Germany) imaging protocol included T1- and T2- weighted and fluid attenuated inversion recovery sequences, and T1- weighted 3D images (magnetization-prepared rapid acquisition of gradient echo: TR 1980 ms, TE 3.09 ms, flip angle 15°, matrix 256 x 256, 176 sagittal sections with section thickness varying between 1.0 and 1.2 mm depending on the size of the head; in-slice resolution of 1.0 mm x 1.0 mm). A neuroradiologist (P.K) assessed all conventional images visually for focal abnormalities.

5.2.5 CTH analysis

CTH analysis was conducted by using the pipelining method developed in the McConnell Brain Imaging Centre, Montreal Neurologic Institute, McGill University, Montreal, Canada (http://www2.bic.mni.mcgill.ca/). First, the individual MR image volumes were spatially normalized to the standard template (Mazziotta et al. 2001), intensity inhomogeneities were corrected with the N3 algorithm (Sled, Zijdenbos & Evans 1998) and extracerebral voxels were removed with a stereotactic brain mask (Smith 2002). Then, the magnitude of the partial volume effect was estimated for each voxel (Tohka, Zijdenbos & Evans 2004) and brain tissue was divided into gray matter (GM), white matter (WM), and cerebrospinal fluid (CSF) by using the intensity-normalized stereotactic environment for classification of tissues (INSECT) algorithm (Zijdenbos 1998). The brains were automatically divided into two separate hemispheres and the inner and outer surfaces of the cortex were extracted by using the constrained Laplacian-based automated segmentation with a proximities (CLASP) algorithm (Kim et al. 2005) followed by identification of white matter surface (WMS) i.e. the surface between WM and GM, and gray matter surface (GMS) i.e. the surface between GM and CSF. First, CLASP formed the inner surface by expanding an ellipsoid polygon mesh to the shape of the WMS. GMS was modelled by further expanding the inner surface. The thickness of the cortex was defined with a t-link metric at each linked node as the distance between WMS and GMS and as a result a CTH map of 40,962 nodes per hemisphere was acquired (Lerch, Evans 2005). The thickness calculations were performed on each subject's native space and were then transformed back to the standard space for the group analysis. Finally, the data were smoothed with a 20-mm full width at half maximum diffusion smoothing kernel to improve the signal-to-noise ratio and statistical power (Chung, Taylor 2004).

5.2.6 Statistical analysis

Statistical analyses of CTH were performed according to the general linear model with Matlab R2007b (The MathWorks Inc., Natick, MA). Differences between Mild, Moderate and Severe Disability groups were tested by using a t test ($p < 0.05$), corrected for multiple comparisons with the FDR method. The correlations between the CTH values and the z-scores of the neuropsychological tests were tested in each node for all patients as one group. Correlations were calculated for the following neuropsychological variables: PIQ, VIQ; immediate and delayed verbal memory scores (six scores); executive function: (TMT, Stroop); and psychomotor function (alternating S-task, Digit symbol and finger tapping). Patients with missing test scores were excluded from the specific correlation analysis. In all CTH analysis, gender was used as a nuisance variable. As the age of the patient

significantly correlates with the duration of the disease, and the duration of the disease correlates with the clinical severity of the symptoms, age was not used as a nuisance variable. However, it has been shown that although age correlates negatively with CTH in both patients and controls, the cortical thinning follows regionally a more limited pattern in patients with EPM1 in comparison with healthy controls (Koskenkorva et al. 2012).

Other statistical analyses shown in Table 11 were performed with the statistical software SPSS 19.0 for Windows (IBM SPSS Inc., Chigaco, IL). Mann-Whitney U test was used to assess differences in clinical and demographical variables. Differences were considered statistically significant when $p < 0.05$.

Table 11. Demographical data of the EPM1 patients and three sub-groups according to the Myoclonus with Action scores: Mild Disability Group had scores 1−30; Moderate Disability Group had scores 31−59 and Severe Disability Group had scores ≥ 60.

	EPM1 patients mean ± std. dev. (range)	**Mild Disability Group**	**Moderate Disability Group**	**Severe Disability Group**	**Mild vs. Severe p**	**Mild vs. Moderate p**	**Moderate vs. severe p**
Number of subjects	63	20	21	22	-	-	-
Gender, male/female	35/28	12/8	10/11	13/9	-	-	-
Mean age	35.1 ± 10.9 (16 – 64)	30.4 ± 9.4	35.3 ± 12.7	39.1 ± 9.1	0.006	ns	ns
Onset age	10.4 ± 2.8 (6 – 25)	11.1 ± 2.0	11.2 ± 3.8	9.1 ± 1.6	0.001	ns	ns
Duration of the disease	24.4 ± 10.3 (4 – 44)	19.2 ± 9.1	23.6 ± 10.6	30.0 ± 8.5	0.001	ns	0.047
Education	11.5 ± 2.0 (8 – 15)[2]	12.3 ± 1.9	11.2 ± 2.1[1]	11.1 ± 1.8[1]	ns	ns	ns
Myoclonus with Action	48.3 ± 28.9 (2 – 122)	19.2 ± 7.3	40.1 ± 6.5	82.6 ± 16.7	0.000	0.000	0.000
Wheelchair-bound							
No	31	19	11	1	-	-	-
Occasionally	12	1	8	3			
Wheelchair bound	20	0	2	18			
Phenytoin use							
Never	39	14	15	10	-	-	-
Earlier temporarily/SE	19	4	5	10			
Unknown	5	2	1	2			
PIQ	75.1 ± 13.9 (50 – 119)	84.9 ± 14.1	75.5 ± 11.3	65.9 ± 9.4	0.000	0.040	0.004
VIQ	85.1 ± 14.7 (54 – 122)	92.5 ± 11.8	84.9 ± 16.9	78.5 ± 12.2	0.000	ns	ns

[1] Value missing from 1 patient, [2] value missing from 2 patients. SE = Status epilepticus.

5.3 RESULTS

Demographic and clinical data of the EPM1 patients are presented in Table 11. When assessed visually, no focal signal intensity abnormalities were found in the conventional MR images.

5.3.1 Cortical thickness and disease severity

The Severe Disability Group had statistically significantly thinner cortex values than the Mild Disability Group (Figure 12). In the regional analysis, widespread cortical thinning was observed in the primary and secondary visual cortices (BA17 &18), associative visual cortex (BA19), primary auditory and auditory association cortex (BA41 & 42), Broca's area i.e. pars opercularis (BA44) and pars triangularis (BA45), parts of Wernicke's area (BA22, 39 & 40), piriform cortex (BA27), fusiform gyrus (BA37), parts of primary gustatory cortex (BA43) and parts of posterior cingulate cortex (BA23 & 31). Retrosplenial regions of the cerebral cortex (BA26, 29, 30), perirhinal cortex (BA35), parts of primary somatosensory cortex (BA1 & 2) and primary motor cortex (BA4) displayed thinning particularly in the right but also on the left hemisphere. In addition, parts of the prefrontal cortex (BA9, 10 & 11) were affected. There was also thinning of the somatosensory association cortex (BA5) and posterior entorhinal cortex (BA28) in the left hemisphere.

No statistically significant differences in CTH were found in comparisons between Moderate and Severe Disability Groups or between the Mild and Moderate Disability Groups.

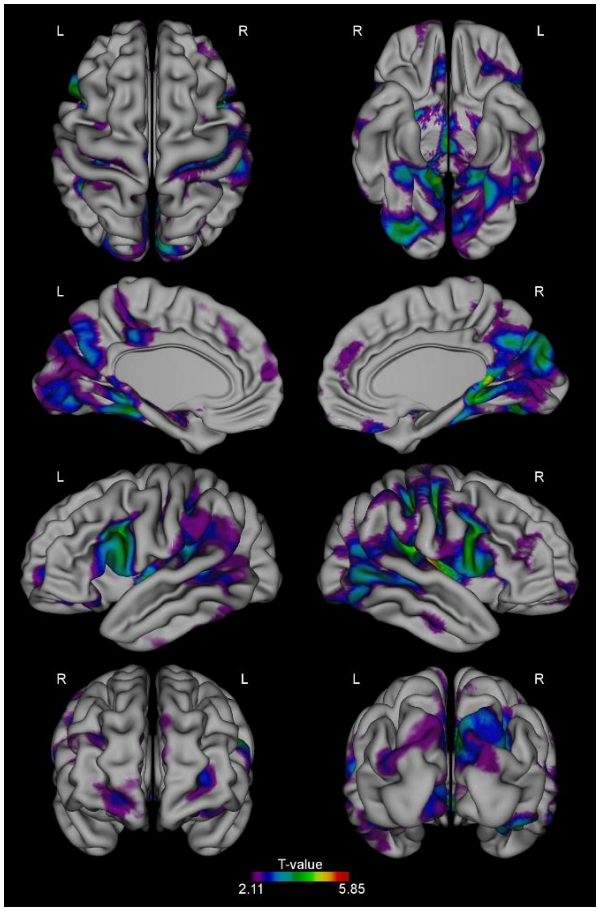

Figure 12. Statistical differences ($p < 0.05$, FDR corrected) in cortical thickness between Mild Disability Group and Severe Disability Group patients with EPM1. Severe Disability Group exhibits widespread cortical thinning compared to the Mild Disability Group.

5.3.2 Correlations between cortical thickness and neuropsychological test scores

In the correlation analysis between CTH and neuropsychological test scores, all the EPM1 patients were treated as one group. Test results of finger tapping and alternating S-task showed a significant positive correlation with CTH. The results of the correlation analyses are presented in Table 12 and illustrated in Figure 13 with respect to the finger tapping and in Figure 14 for the alternating S-task. PIQ, VIQ, Digit symbol and Verbal memory and Executive function tests did not reveal any significant correlation with cortical thickness in EPM1 patients.

Table 12. Cortical areas in the right and left hemisphere correlating with the finger-tapping and alternating S task z-scores.

Neuropsychological test	Regions of correlations in the right hemisphere	Regions of correlations in the left hemisphere
Finger-tapping (Figure 13)	A part of primary somatosensory cortex (BA2)	
		A small part of somatosensory association cortex (BA5)
	Frontal eye fields (BA8)	Frontal eye fields (BA8)
	A small part of frontopolar cortex (BA10)	Frontopolar cortex (BA10)
	A part of orbitofrontal cortex (BA11)	
	Parts of secondary visual cortex (BA18)	
	Small parts of superior temporal area (BA22)	Small parts of Wernicke's area (BA22)
	Parts of posterior cingulate cortex (BA23 & 31)	Parts of posterior cingulate cortex (BA23 & 31)
	Retrosplenial cortex (BA26, 29, 30)	Parts of retrosplenial cortex (BA26, 29, 30)
	Piriform cortex (BA27)	
	Perirhinal cortex (BA35)	Perirhinal cortex (BA35)
	Primary auditory and auditory association cortex (BA41 & 42)	Primary auditory and auditory association cortex (BA41 & 42)
	Parts of pars opercularis (BA44)	A part of Broca's area (BA44 & 45)
		Parts of orbitofrontal cortex (BA 47)
Alternating S task (Figure 14)	A small part of primary somatosensory cortex (BA2, superior postcentral sulcus)	
		A small part of frontal eye fields (BA 8)
	Primary visual cortex (BA17)	Parts of primary visual cortex (BA17)
	Parts of secondary visual cortex (BA18)	Parts of secondary visual cortex (BA18)
	A small part of superior temporal area (BA22)	A small part of Wernicke's area (BA22)
	Retrosplenial cortex (BA26, 29, 30)	
	Perirhinal cortex (BA35)	
		Parts of Broca's area (BA44, 45)

BA = Brodmann area

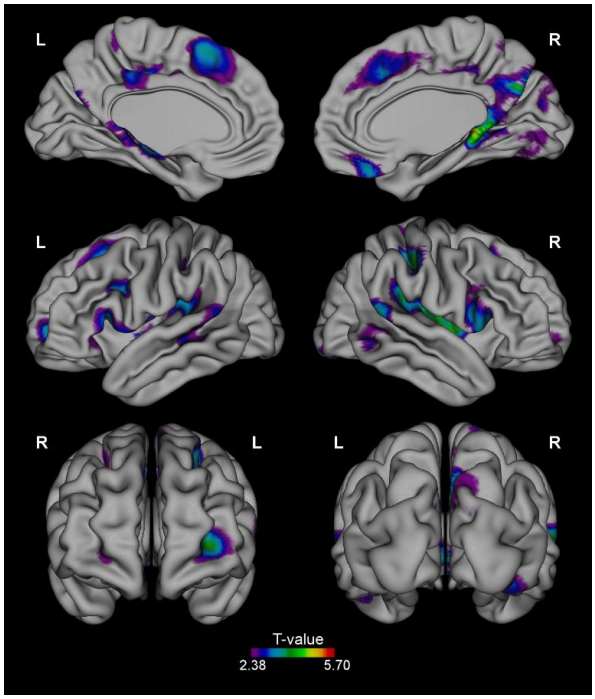

Figure 13. Correlation between cortical thickness and performance in finger-tapping test in patients with EPM1 (n=57). CTH and Z-scores of finger-tapping test were positively correlated ($p < 0.05$, FDR corrected).

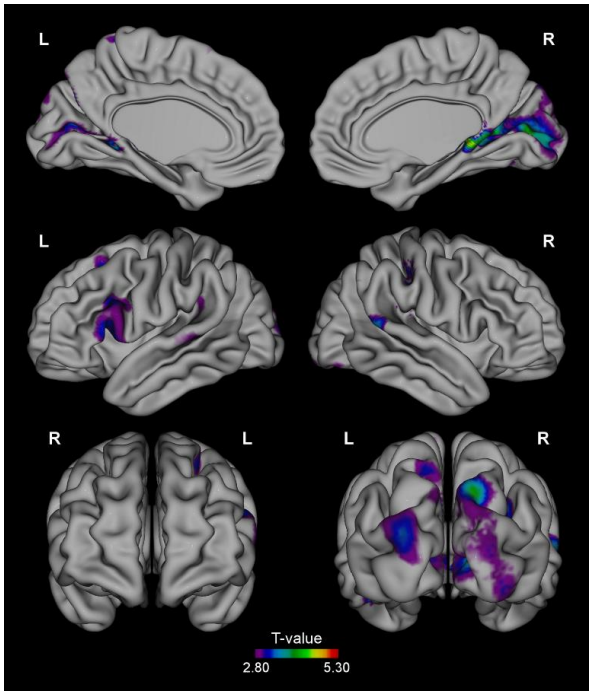

Figure 14. Correlation between cortical thickness and performance in alternating S-task in patients with EPM1 (n=55). CTH and Z-scores of alternating S-task were positively correlated ($p < 0.05$, FDR corrected).

5.4 DISCUSSION

This study indicates that there is a structural background to the neurocognitive decline experienced by the patients with EPM1. The phenotype of our patients is carefully described by Hyppönen et al. including comprehensive clinical findings of the Finnish patients with EPM1 (unpublished data). The main neuropsychological findings of the patients have been described by Äikiä et al. (unpublished data). The subjects with a severe phenotype displayed extensive thinning in several cortical areas; areas that are considered important in higher-level cognitive functions. Previous studies have revealed that the decline in cognitive function in patients with EPM1 occurred in parallel with the extent of general disability however with significant individual variation (Chew et al. 2008, Ferlazzo et al. 2009, Giovagnoli et al. 2009). This is the first study to describe an association between a local structural damage and cognitive impairment in EPM1. CTH was able to reveal mild cortical atrophy, not visible on conventional visual assessment of brain MRI; these pathological disturbances may explain the subnormal performance of the patients in various neuropsychological tasks.

5.4.1 Areas of cortical thinning in severe form of EPM1

Studies with modern group-level neuroimaging methods have been able to reveal gray matter volume reduction and diffuse cortical thinning particularly in the motor, sensory,

visual and auditory cortices (Koskenkorva et al. 2009, Koskenkorva et al. 2012). In our study, the subgroup of EPM1 patients with the severe form of disease displayed widespread thinning of the cerebral cortex in comparison with the subgroup with only mild disability; the sensory, visual and auditory cortices were the areas most severely affected (Fig. 12). In addition, brain regions for language functions (i.e., Broca's and Wernicke's areas) were thinner in patients with more severe EPM1. The cortical thinning present in the Broca's area could at least partly account for the development of dysarthria which typically is encountered some years after the diagnosis.

The retrosplenial cortex was thinner particularly in the right hemisphere in the severe EPM1 subgroup. The retrosplenial cortex (BA26, 29, 30) projecting to the anterior thalamic nuclei and hippocampus is involved in episodic and spatial memory, navigation, imagination and planning for the future (Vann, Aggleton & Maguire 2009). Neurocognitive studies and case reports have indicated that patients with damaged retrosplenial cortex suffer spatial orientation deficits and experience difficulty in acquiring new visual information (Maguire 2001). The posterior cingulate cortex was also thinner in patients with severe EPM1. The posterior cingulate cortex (BA23, 31) is a part of the default mode network, a set of brain regions that are highly active during rest, and it is believed to generate spontaneous thoughts during mind-wandering (Buckner, Andrews-Hanna & Schacter 2008).

Posterior parts of perirhinal cortex (BA35) were bilaterally thinner in patients with severe EPM1. The perirhinal cortex contributes to higher-order visual perception and complex conjunctions of objects and storage of visual data in the memory (Murray, Bussey & Saksida 2007). The fusiform gyrus (BA37) was bilaterally thinner in patients with more severe EPM1. The fusiform gyrus is known to be involved in the perception of faces (Kanwisher, McDermott & Chun 1997) but it also has highly selective neural populations for recognition of non-facial objects (Grill-Spector, Sayres & Ress 2006). The piriform cortex (BA27) was bilaterally thinner in patients with severe EPM1. The piriform cortex is a highly seizure-prone region (Piredda, Gale 1985).

5.4.2 Anatomical correlates of distinct neuropsychological test results

Correlations were found between psychomotor function test scores (finger tapping and alternating S-task) and the thickness of cortical areas that process visual data: Finger tapping correlated positively with the CTH especially in areas involved in higher-order visual perception as previously mentioned (BA26, 29, 30, 35) and also with frontal eye fields (BA8). The performance scores in Finger tapping correlated also with the CTH in prefrontal cortex: frontopolar cortex (BA10) particularly on the left; and orbitofrontal cortex on the right (BA11) and left (BA47) (Figure 13). In addition to motor functions, the frontopolar cortex is involved in the executive system including decision making (Koechlin, Hyafil 2007, Ramnani, Owen 2004). Furthermore, orbitofrontal cortex is thought to be involved in decision making, expected reward situations and associative learning (Schoenbaum et al. 2011).

We did not detect any statistically significant correlations in cortical thickness with other cognitive measures such as verbal memory or executive function parameters. This may be due to the fact that several patients with severe disability could not perform the executive function tests and had to be excluded from these analyses. There were also no correlations found between cortical thickness and PIQ and VIQ which is to be expected due to the complex nature of these cognitive measures. In general, the statistical significance of CTH analyses requires a reasonably large group size and/or a homogeneous group. Since the EPM1 patient group is rather heterogeneous with regards

to the severity of the symptoms, the reduction in group size due to missing test scores might have affected the statistical significance and reduced to some extent the reliability of the results.

It has to be stressed that in EPM1 patients the structural alterations are restricted not only to cerebral cortex but also extend to deep gray matter and white matter (Koskenkorva et al. 2009, Manninen et al. 2013). Thus, the cortical findings could not be expected to comprehensively account for all aspects of the neurocognitive impairment experienced by patients with EPM1.

The statistical analyses in our study are also complicated by the fact that the age of the patient, duration of the disease, clinical severity of the symptoms and CTH are all mutually correlated. The only way to eliminate the possible effect of age in the present results would have been to evaluate similar groups in terms of age, sex and duration of the disease but this was not possible due to the inherently small study population. However, it has been shown that although age correlates with CTH in both healthy controls and patients with EPM1, the regional distribution of thinning is more limited in EPM1 (Koskenkorva et al. 2012). The onset of EPM1 is in early childhood or late adolescence with the peak occurring around 12–13 years (Genton 2010), thus the cortical areas maturing before and after onset may behave differently.

Recently, a CTH study of patients with intractable focal epilepsy and childhood onset epilepsy detected a reduced WM and parietal lobe thickness in valproate users vs. non-users (Pardoe, Berg & Jackson 2013). In EPM1, valproate is the drug of choice and its use is started as soon as the disease is diagnosed. Thus, valproate is used as the main AED virtually in all patients with EPM1 (Kälviäinen et al. 2008). However, a recent translational study detected analogous WM degeneration in *Cstb*-deficient (*Cstb*$^{-/-}$) mice and patients with EPM1 (Manninen et al. 2013). Furthermore, neuronal loss and progressive thinning of the cortex are also present in *Cstb*-deficient mice (Tegelberg et al. 2012). Although the possible effects of valproate cannot be omitted in our patient population they do not alone explain the cortical thinning in patients with EPM1.

5.5 CONCLUSION

The current study is the first to report associations between cortical thinning and cognitive functions in EPM1. Although visually interpreted MRI typically remains normal, CTH not only revealed abnormalities but these were also correlated to poor neuropsychological performance. Patients with a severe form of EPM1 have extensively thinner cortices than patients with a mild form of the disease. The brain areas that process verbal and complex visual data or those involved in higher order cognitive functions become particularly affected in patients with severe EPM1 providing an anatomical-biological background for the link between the severity of disability and cognitive decline in EPM1. The basis for the heterogeneity of the disease remains unclear. Future research will determine whether CTH analysis will prove helpful in the prognostic assessment in individual patients with EPM1 e.g. in newly diagnosed patients.

6 3D texture analysis reveals imperceptible MRI textural alterations in the thalamus and putamen in progressive myoclonic epilepsy type 1, EPM1

ABSTRACT

Progressive myoclonic epilepsy type 1 (EPM1) is an autosomal recessively inherited neurodegenerative disorder characterized by young onset age, myoclonus and tonic-clonic epileptic seizures. At the time of diagnosis, the visual assessment of the brain MRI is usually normal, with no major changes found later. Therefore, we utilized texture analysis (TA) to characterize and classify the underlying properties of the affected brain tissue by means of 3D texture features.

Sixteen genetically verified patients with EPM1 and 16 healthy controls were included in the study. TA was performed upon 3D volumes of interest that were placed bilaterally in the thalamus, amygdala, hippocampus, caudate nucleus and putamen.

Compared to the healthy controls, EPM1 patients had significant textural differences especially in the thalamus and right putamen. The most significantly differing texture features included parameters that measure the complexity and heterogeneity of the tissue, such as the co-occurrence matrix-based entropy and angular second moment, and also the run-length matrix-based parameters of gray-level non-uniformity, short run emphasis and long run emphasis.

This study demonstrates the usability of 3D TA for extracting additional information from MR images. Textural alterations which suggest complex, coarse and heterogeneous appearance were found bilaterally in the thalamus, supporting the previous literature on thalamic pathology in EPM1. The observed putamenal involvement is a novel finding. Our results encourage further studies on the clinical applications, feasibility, reproducibility and reliability of 3D TA.

6.1 INTRODUCTION

Progressive myoclonic epilepsy type 1 or Unverricht-Lundborg disease (EPM1, ULD, OMIM 254800) is the most common type of progressive myoclonic epilepsy (Shahwan, Farrell & Delanty 2005). It is an autosomal recessively inherited neurodegenerative disorder caused by mutations in the cystatin B gene (*CSTB*) (Pennacchio et al. 1996, Lalioti et al. 1997, Lafreniere et al. 1997). EPM1 in Finland has an incidence of 1:20 000 births per year, with about 200 diagnosed cases (Norio, Koskiniemi 1979), but it is also prevalent elsewhere in the Baltic Sea region and in the Western Mediterranean area. Sporadic cases of EPM1 have been reported worldwide (Kälviäinen et al. 2008).

The first symptoms of EPM1 are commonly stimulus-sensitive myoclonic jerks and generalized tonic-clonic epileptic seizures. Neurological examination is initially normal, but patients later develop intention tremor, dysarthria, ataxia and poor coordination, thus subsequently one-third of EPM1 patients become severely incapacitated and wheelchair bound. Alternatively, the clinical symptoms can be so mild that there is a delay in the diagnosis and patients may manage well. (Kälviäinen et al. 2008) Mild cognitive

impairment and slow decline in intellectual level over time have been reported (Kälviäinen et al. 2008, Chew et al. 2008, Ferlazzo et al. 2009, Lehesjoki, Koskiniemi 1999).

MRI findings of the patients with EPM1 remain sparse. At the time of diagnosis, MRI of the brain is usually normal (Kälviäinen et al. 2008). However, changes in MRI, such as mild to moderate cerebral and/or cerebellar atrophy, loss of neuronal volume in the brainstem and high intensity signal changes in the basal ganglia have been reported as well (Chew et al. 2008, Mascalchi et al. 2002, Santoshkumar, Turnbull & Minassian 2008, Korja et al. 2010). Recently modern group level MRI analysis methods have revealed loss of gray matter volume in cortical motor areas (voxel-based morphometry, VBM), and atrophy of the sensorimotor, visual and auditory cortices (cortical thickness analysis, CTH) in EPM1 patients (Koskenkorva et al. 2009, Koskenkorva et al. 2012) while abnormal findings could not be detected in visual assessments. Loss of gray matter volume in the thalamus has also been reported in one VBM study (Koskenkorva et al. 2009), paralleling a PET study indicating dopamine depletion in the thalamostriatal area in four EPM1 patients (Korja et al. 2007b).

Although the human visual system can discriminate different textures, the capacity of human vision to detect and discriminate between complex higher-order textures is limited (Julesz 1973). Texture analysis (TA) is a method to evaluate the position of signal features i.e. pixels/voxels, and their gray-level intensity, distribution and relationships in a digital image (Castellano et al. 2004). TA presents texture features as mathematical parameters, which could characterize the properties of the underlying tissue. These features can be described as, for example, fine, coarse, smooth, or irregular (Haralick 1973). Previously, texture analysis techniques have been used two-dimensionally in medical imaging of multiple sclerosis, brain tumours and brain injuries (Castellano et al. 2004, Holli et al. 2010c, Kassner, Thornhill 2010). In epilepsy research, TA has been applied in temporal lobe epilepsy, focal cortical dysplasia and juvenile myoclonic epilepsy (JME) (Yu et al. 2001, Bonilha et al. 2003, Jafari-Khouzani et al. 2010, Alegro et al. 2012, Antel et al. 2003, Bernasconi et al. 2001, de Oliveira et al. 2013).

Theoretically, three-dimensional (3D) texture analysis provides more comprehensive data analysis of biological tissue texture properties and enables calculation of texture parameters in several directions. However, the literature on 3D TA applications in brain research is still sparse (Zhang et al. 2012, Kovalev, Kruggel & von Cramon 2003, Mahmoud-Ghoneim et al. 2003, Chen et al. 2007, Kocinski et al. 2012, Georgiadis et al. 2009).

Patients with EPM1 seem to provide a suitable population to assess the feasibility of novel image analysis techniques to detect possible subtle changes in the brain that are not evident upon visual assessment. The specific aim of this study is to investigate possible imperceptible structural differences in the thalamus and other deep gray matter tissue in patients with EPM1 via comparison with healthy controls by using three-dimensional MRI-based texture analysis. Further, we want to determine whether the possible texture changes correlate with EPM1 patients' clinical symptoms and neuropsychological findings.

6.2 PATIENTS AND METHODS

6.2.1 Subjects

EPM1 patients were evaluated at Kuopio University Hospital during the period 2006 − 2010. The study was jointly administered by the Folkhälsan Institute of Genetics and Neuroscience Center at the University of Helsinki. The patients had either participated in an earlier molecular genetics study or were referred to the Kuopio Epilepsy Center during the study. The ethics committee at the Kuopio University Hospital approved the study and written informed consent was obtained from all participants.

The original EPM1 study group comprised 66 EPM1 patients. In all cases, MR images were obtained using a T1-weighted 3D MPRAGE sequence. Due to slight differences in updated scanner versions, technical difficulties, and slightly different slice thicknesses in some of the controls due to differences in head size, slight modifications in the parameters and resolutions were observed. Consequently, 16 genetically verified EPM1 patients (10 male, mean age of 31.0 ± 10.9 years, range 18 − 51 years) and 16 healthy controls (8 men, mean age of 35.2 ± 12.0 years, range 19 − 52 years) shared identical MPRAGE sequence details and were included in the 3D TA study.

6.2.2 Clinical assessment of patients with EPM1

Of the EPM1 patients, 13 were homozygous for the dodecamer expansion mutation, while 3 were compound heterozygous for the expansion mutations. The mean onset age was 9.6 ± 1.9 years (range 5 − 12 years) and the mean duration of the disorder at the time of the study was 21.4 ± 10.2 years (range 8 − 41 years). All of the EPM1 patients were treated with antiepileptic drugs (AEDs). Valproate was in use in all 16 patients and was augmented with levetiracetam (n = 10), clonazepam (n = 10), topimarate (n = 3) piracetam (n = 4), lamotrigine (n = 5), clopazam (n = 1) or other AEDs (n = 5). The medical histories of EPM1 patients were confirmed from medical records and by interviewing the patients and their relatives. A Unified Myoclonus Rating Scale (UMRS) test panel was performed as part of the clinical patient evaluation. UMRS is a quantitative, 74-item clinical rating instrument comprising 8 sections (Frucht et al. 2002). The patients were video-recorded and evaluated by using the standard protocol. Higher UMRS scores indicate more severe myoclonus.

Neuropsychological assessments were performed by an experienced neuropsychologist (M.Ä). General intellectual ability was assessed with the Wechsler Adult Intelligence Scale Revised (WAIS-R) (Wechsler D 1981), and verbal and performance Intelligence Quotients (VIQ, PIQ) were estimated.

6.2.3 MR image acquisition

The EPM1 patients and healthy control subjects underwent MRI of the brain (1.5 T, Siemens Magnetom Avanto, Erlangen, Germany) using a birdcage Tx/Rx head coil. T1-weighted 3-dimensional images (MPRAGE, TR 1980 ms, TE 3.93 ms, flip angle 15°, matrix 256 x 256, 176 sagittal slices, slice thickness 1.0 mm, in-slice resolution of 1.0 mm x 1.0 mm) were used for regional 3D TA.

6.2.4 Texture analysis and volumes of interest definition

TA was performed with the software package MaZda (MaZda 4.60 3D, Institute of Electronics, Technical University of Lodz, Poland) (Szczypinski et al. 2009, Hajek et al. 2006) specially designed for texture analysis by Materka and co-workers as a part of the European COST B11 and the following COST B21 programs.

Spherical volumes of interest (VOI) were manually placed bilaterally on each region of interest in the deep gray matter structures (thalamus, putamen, caudate nucleus,

hippocampus and amygdala; Figure 15). The VOIs were carefully placed to avoid any overlap with other anatomical structures or cerebrospinal fluid. The 3D VOI placement was done manually by two observers (S.S. and K.H.).

Image gray level intensity normalization was performed with method limiting image intensities in the range [μ-3σ, μ+3σ], where μ is the mean gray level value and σ the standard deviation. This method has been shown to intensify differences between two classes when comparing image intensity normalization methods in texture classification (Collewet, Strzelecki & Mariette 2004).

A total of 223 texture parameters were calculated based on the histogram, gradient, run-length matrix and co-occurrence matrix (Table 13) (Szczypinski et al. 2009, Hajek et al. 2006). Run-length matrix parameters were calculated in four directions: horizontal (0°), vertical (90°), 45° and 135°, and co-occurrence matrix parameters were calculated in three distances of 1, 2 and 3 voxels in each 3D spatial co-ordinate directions were considered. All of these texture features were calculated for each VOI.

Table 13. Texture features used in the study.

Histogram	**Absolute gradient**	**Co-occurrence matrix**	**Run-length matrix**
Mean	Mean	Angular second moment	Run-length non-uniformity
Variance	Variance	Contrast	Gray-level non-uniformity
Skewness	Skewness	Correlation	Long run emphasis
Kurtosis	Kurtosis	Sum of squares	Short run emphasis
Percentiles 1-, 10-, 50-, 90-, 99-%	Percentage of pixels with non-zero gradient	Inverse difference moment	Fraction image in runs
		Sum average	
		Sum variance	
		Sum entropy	
		Difference variance	
		Difference entropy	

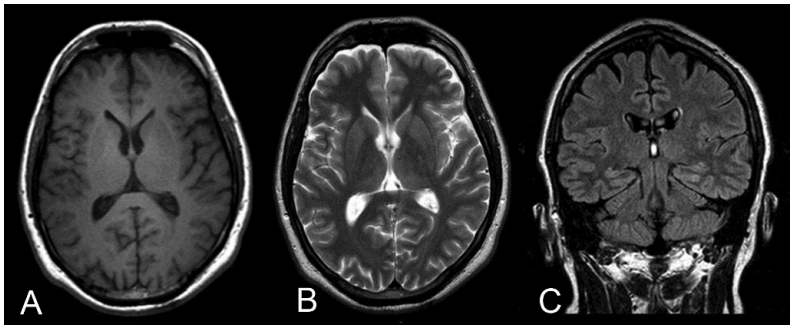

Figure 15. Illustrative A) T1-weighted, B) T2-weighted and C) FLAIR images from a 34 year old male patient with EPM1. Mild frontoparietal cortical atrophy can be suspected but there are no visible focal abnormalities.

6.2.5 Statistical analysis

Statistical analyses were performed with SPSS 19.0 (IBM SPSS, Chicago, Illinois). P-values under 0.05 were considered statistically significant. Because of the small group size and skewed distributions, nonparametric statistical tests were used. The Mann-Whitney U test was used to evaluate the raw TA parameters to describe the textural difference between EPM1 patients and controls on each VOI. All 223 raw texture parameters were statistically tested to find out how many and which of the 223 parameters differed statistically.

The texture parameters were calculated in several directions and pixel distances, mean value for different pixel distances, and directions were calculated for six texture parameters (Table 13) and for correlation analysis of four texture parameters (entropy, angular second moment, short run emphasis, long run emphasis). Thus, the Spearman correlation coefficient was used to assess any correlations between the mean values of the four texture parameters and the clinical parameters (myoclonus in action score, age, duration of the disease, PIQ and VIQ).

To test the reproducibility of the TA, 10 control subjects were drawn by two observers. The intraclass correlation coefficient (ICC) with a 95% confidence interval, coefficient of variation (CV) and paired samples t-test were calculated. Co-occurrence parameters from one voxel distance (1, 0, 0) i.e., all together 1320 numerical values per observer were involved in the reproducibility analysis.

Table 14. Texture features that differed most between the patients with EPM1 and healthy controls.

	Patient		Control		
	Mean	**SD**	**Mean**	**SD**	**p**
Histogram-based parameters					
Mean 3D					
VOI1, right thalamus	677.71	24.03	664.88	22.06	0.152
VOI2, left thalamus	682.10	23.13	658.23	21.71	0.004
VOI9, right putamen	631.92	21.25	653.66	24.70	0.016
Variance 3D					
VOI1, right thalamus	1571.64	353.99	1148.05	204.36	0.001
VOI2, left thalamus	1500.03	215.39	1113.45	160.68	0.000
VOI9, right putamen	682.85	226.09	542.93	127.31	0.050
Co-occurence-based parameters					
Mean of angular second moment					
VOI1, right thalamus	5.55×10^{-4}	1.42×10^{-5}	5.76×10^{-4}	1.52×10^{-5}	0.001
VOI2, left thalamus	5.57×10^{-4}	1.05×10^{-5}	5.79×10^{-4}	1.21×10^{-5}	0.000
VOI9, right putamen	9.06×10^{-3}	2.96×10^{-4}	9.38×10^{-3}	3.14×10^{-4}	0.006
Mean of entropy					
VOI1, right thalamus	3.28	8.50×10^{-3}	3.27	8.61×10^{-3}	0.001
VOI2, left thalamus	3.28	6.03×10^{-3}	3.27	6.93×10^{-3}	0.000
VOI9, right putamen	2.11	1.04×10^{-2}	2.09	1.24×10^{-2}	0.005
Run-length matrix-based parameters					
Mean of short run emphasis					
VOI1, right thalamus	9.91×10^{-1}	7.84×10^{-4}	9.90×10^{-1}	1.14×10^{-3}	0.000
VOI2, left thalamus	9.91×10^{-1}	1.53×10^{-3}	9.90×10^{-1}	1.42×10^{-3}	0.042
VOI9, right putamen	9.93×10^{-1}	2.46×10^{-3}	9.91×10^{-1}	3.30×10^{-3}	0.101
Mean of long run emphasis					
VOI1, right thalamus	1.035	3.30×10^{-3}	1.042	4.63×10^{-3}	0.000
VOI2, left thalamus	1.038	6.18×10^{-3}	1.043	5.72×10^{-3}	0.026
VOI9, right putamen	1.029	1.02×10^{-2}	1.037	1.38×10^{-2}	0.109
Run-length non-uniformity					
VOI1, right thalamus	1381.49	7.98	1372.74	13.29	0.046
VOI2, left thalamus	1377.92	10.98	1369.90	17.78	0.050
VOI9, right putamen	140.79	2.49	137.49	3.45	0.002
Gray-level non-uniformity					
VOI1, right thalamus	11.41	1.00	12.95	1.21	0.001
VOI2, left thalamus	11.48	0.70	13.14	0.99	0.000
VOI9, right putamen	2.58	0.34	2.74	0.18	0.032

Mean 3D and Variance 3D are single texture features whereas co-occurrence and run-length matrix-based parameters are the mean of each texture feature

6.3 RESULTS

The demographic and clinical data of patients with EPM1 are presented in Table 15. When assessed visually by experienced neuroradiologists (P.K. and R.V.), no focal signal intensity abnormalities were found (Figures 15 and 16).

Table 15. Demographic data of 16 EPM1 patients.

	n	Mean ± SD	Range
Sex, M/F	10/6		
Age, y		31.0 ± 10.9	18 – 51
Age at EPM1 onset, y		9.6 ± 1.9	5 – 12
Duration of disease, y		21.4 ± 10.2	8 – 41
UMRS: Myoclonus with Action		49.1 ± 25.8	12 – 92
Wheelchair use, no/occasionally/wheelchair bound	9/4/3		
Number of AED's in use, 2/3/4/5	5/5/5/1		
Phenytoin use, never/earlier temporarily/unknown	9/6/1		
VIQ		82.4 ± 12.4	62 – 102
PIQ		70.4 ± 13.1	52 – 94

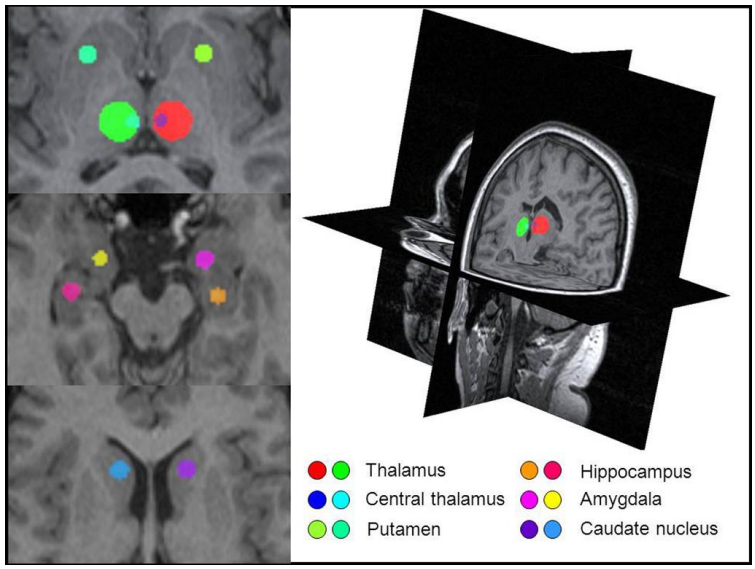

Figure 16. Volumes of interests and a three-dimensional view of the brain in MaZda. Image slices from a T1-weighted 3D image package illustrating the volumes of interest in a 19 year old female patient. There is no focal pathology or atrophy visible. VOIs are placed bilaterally in the thalamus, hippocampi, amygdalae, caudate nuclei and putamen.

6.3.1 Reproducibility

Reproducibility of 3D TA proved to be excellent. There were no statistically significant differences (p=0.738) between Observer 1 and Observer 2 in the values of co-occurrence (1, 0, 0) parameters. ICC was excellent (0.990). The CV was 1.90 for Observer 1, and 1.89 for Observer 2.

6.3.2 Regional texture parameters differing between patients and control subjects

The regional differences in texture parameters (n=223) were evaluated by the number of TA parameters with statistically significant differences between EPM1 patients and healthy controls (Table 16). The largest number of significant differences between EPM1 patients and healthy controls were found in the VOIs of the thalamus (Table 16) and were based on co-occurrence matrix, in particular the following parameters: angular second moment, entropy, sum variance and sum average (Table 17). The values of entropy were higher in patients than in healthy controls whereas the angular second moment feature acted in the opposite direction (Table 14).

The thalamus also differed in the histogram-based features including variance and mean as EPM1 patients had higher values than healthy controls. Furthermore, the run-length matrix-based parameters also differed between patients and controls (Table 18). The values of short run emphasis were larger in patients than in healthy controls, whilst values of long run emphasis features acted in the opposite direction (Table 14). Values indicating gray-level non-uniformity were smaller in patients than in controls and vice versa with run-length non-uniformity (Table 14).

In addition to the thalamus bilaterally, the right putamen provided statistically differing texture features between EPM1 patients and healthy controls (Tables 16 and 14). Again, significant differences were found in histogram-, co-occurrence matrix- and run-length matrix-based parameters. No major differences were found between EPM1 patients and healthy controls in the left putamen, hippocampi, amygdalae or caudate nuclei.

Table 16. Volumes of interest (VOI) with number and percentages of statistically significantly different texture parameters from a total of 223 texture parameters between EPM1 patients and healthy controls.

Region	Volume of VOI (mm^3)	Number of statistically significant different parameters	%
VOI 1, Right side of the thalamus	1437	62	28%
VOI 2, Left side of the thalamus	1437	83	37%
VOI 3, Right central thalamus	66	27	12%
VOI 4, Left central thalamus	66	12	5%
VOI 5, Right amygdala	144	15	7%
VOI 6, Left amygdala	144	11	5%
VOI 7, Right hippocampus	144	4	0.5%
VOI 8, Left hippocampus	144	11	5%
VOI 9, Right putamen	144	59	26%
VOI 10, Left putamen	144	10	1%
VOI 11, Right caudate nucleus	144	7	3%
VOI 12, Left caudate nucleus	144	16	7%

Table 17. The number of differing co-occurence based texture parameters ($p<0.05$) between EPM1 patients and healthy controls in the thalamus and putamen in three distances in all five evaluated directions (maximal number = 15 parameters).

	Thalamus (right side)	**Thalamus (left side)**	**Putamen right**	**Putamen left**
Angular second moment	**14/15**	**15/15**	6/15	1/15
Entropy	**14/15**	**15/15**	**9/15**	0/15
Sum average	**7/15**	1/15	2/15	0/15
Sum variance	1/15	**8/15**	0/15	0/15
Sum entropy	3/15	3/15	5/15	0/15
Sum of squares	4/15	0/15	4/15	1/15
Contrast	1/15	6/15	1/15	1/15
Correlation	1/15	6/15	0/15	0/15

Table 18. The directions of differing run-length-based texture parameters ($p<0.05$) between EPM1 patients and healthy controls in the thalamus and putamen.

	Thalamus (right side)	**Thalamus (left side)**	**Putamen right**	**Putamen left**
Long run emphasis	Horizontal	Horizontal	135°	45°
	135°	Vertical		
Short run emphasis	Horizontal	Vertical	135°	45°
	135°			
Run-length non-uniformity	135°	Horizontal	Horizontal	–
		Vertical	45°	
			135°	
Gray-level non-uniformity	All degrees	All degrees	All degrees	–

6.3.3 Correlations between TA and clinical parameters

The myoclonus in action score correlated significantly with the angular second moment values in the left side of the thalamus (VOI2, r=0.542, p=0.030) and tended to correlate with values from the right side of the thalamus (VOI1, r=0,440, p=0.088). A tendency for inverse correlation was observed between the myoclonus in action score and the entropy values both in the right side of the thalamus (r= -0.442, p=0.087) and left side of the thalamus (r= -0.495, p=0.051). No correlations were found between the texture parameters in the thalamus and age, duration of the disorder, PIQ and VIQ. In the right putamen, the VIQ score significantly correlated with the entropy values (r= -0.498, p=0.050) and angular second moment values (r=0.514, p= 0.042). No correlations were found between the texture parameters in the right putamen and myoclonus in action score, age, duration of the disorder or PIQ.

6.4 DISCUSSION

The present study shows that MRI-based texture analysis reveals imperceptible alterations in EPM1 patients, especially in the thalamus. Three dimensional TA is a novel method for the analysis of MR images of the brain, and according to our results, 3D TA is able to provide subtle information of the structures of deep gray matter in EPM1 patients that could not be detected by direct visual inspection of the images. The TA changes were demonstrated by statistical analysis of the pixel gray level distributions in the volumes of interest in the anatomical structures analysed.

In our study we used 3D texture analysis, a more advanced technique than reported in most of the previous TA studies (Castellano et al. 2004). Studies of TA in epilepsy are sparse but have evaluated hippocampal abnormalities in temporal lobe epilepsy) (Yu et al. 2001, Bonilha et al. 2003, Jafari-Khouzani et al. 2010, Alegro et al. 2012) and observed subtle lesions of cortex in focal cortical dysplasia (Antel et al. 2003, Bernasconi et al. 2001). Recently, 2D texture analysis based on co-occurrence matrix was able to detect tissue alterations in the right side of the thalamus in JME, and both caudate nuclei and the thalamus in Machado-Joseph disease, a rare neurodegenerative disorder characterized by ataxia and motorical dysfunction (de Oliveira et al. 2013, de Oliveira et al. 2012)

The present TA study detected significantly different thalamic texture features in EPM1 patients compared to healthy controls. This is in line with imaging and experimental studies that have previously suggested thalamic and possible dopaminergic pathology in EPM1 (Koskenkorva et al. 2009, Mervaala et al. 1990, Mascalchi et al. 2002, Korja et al. 2007b, Franceschetti et al. 2007, Tegelberg et al. 2012). The thalamus is a relay centre between subcortical areas and the cerebral cortex, and it has multiple sensory and motor functions, along with the regulation of awareness, attention, memory and language (Smythies 1997, Buchel et al. 1998, Johnson, Ojemann 2000). Lesions confined to the thalamus have been associated with asterixis (Lee, Marsden 1994), and hemorrhages restricted to the region lateralis of the thalamus lead to a cheiro-oral syndrome (Shintani, Tsuruoka & Shiigai 2000) or choreiform and dystonic movements associated with myorhythmia (Lera et al. 2000). Lesions of both thalamus and basal ganglia are related to dystonia (Lee et al. 1994). Similar clinical symptoms are seen in both EPM1 patients (Kälviäinen et al. 2008) and *Cstb*-deficient mice (Pennacchio et al. 1998) in the shape of ataxia, apraxia, dysarthia and involuntary asynchronous myoclonic jerks that occur mainly in the proximal muscles of the extremities.

The most significantly different parameters in the thalami of EPM1 patients compared to controls were the second-order co-occurrence matrix-based parameters, especially angular second moment and entropy values. Angular second moment is a measure of

homogeneity as it measures the monotony of gray level transition in an image texture. The observed higher value of this feature in control individuals indicates that the intensity varies less in the VOI and the VOI is more homogenous than in EPM1 patients. Entropy indicates the complexity and randomness within the VOI. When the image is not texturally uniform then the value of entropy is larger (Haralick 1973). In other words, our results indicate that the thalamus may be structurally more complex and heterogenous in EPM1.

We also observed differences in first-order histogram-based parameters and higher-order RLM-based parameters. Histogram-based statistics assess the global distribution of pixels/voxels with specific gray level tones (Castellano et al. 2004). Several statistical properties can be calculated from the histogram. The mean is the average intensity level of the image, variance assesses the roughness of an image, skewness describes the histogram symmetry and kurtosis describes the flatness of the histogram. We found that EPM1 patients had higher values of variance in the thalamus than those of the control group, thus the thalamic texture in EPM1 patients is rougher than that of healthy controls.

RLM-based parameters assess the number of runs when two or more pixels/voxels have the same value in a present direction, and they describe the coarseness or smoothness of an image (Galloway 1975). Gray-level non-uniformity calculates how uniformly the runs are distributed among the gray levels; smaller values indicate that the distribution of runs is more uniform. The value of short run emphasis is larger in more coarse images and the value of long run emphasis is larger in smoother images. In the present study, the short run emphasis features were larger in the thalami of EPM1 patients than in healthy controls, indicating a more coarse thalamic texture.

Put together, the observed differences in variance, angular second moment, entropy and short run emphasis features indicate that the texture of the thalamus may be more complex, rough and coarse in EPM1 patients than in healthy controls.

The putamen together with the caudate nucleus and nucleus accumbens form the striatum, which is a major part of the basal ganglia. Basal ganglia are a part of the extrapyramidal motor system involved in cognition, emotion and motivation (Herrero, Barcia & Navarro 2002). The anterior parts of the striatum, including the putamen, are essential for learning, attention, planning (Graybiel 2005, Bellebaum et al. 2008) and verbal working memory (Dahlin et al. 2008), where dopamine plays an essential role in neurotransmission (Brooks 2006). Putamenal pathology is related to movement disorders that also contain cognitive features, for example Parkinson's disease and Huntington's disease (Turner, Desmurget 2010). Interestingly, microstructural and volumetric abnormalities of the putamen have also been observed in juvenile myoclonic epilepsy (Keller et al. 2011)which shares similar clinical characteristics with EPM1.

Our results indicated that the right putamen had significantly different texture parameters in EPM1 patients when compared to the healthy controls. The most significantly different parameters were the same as those found in the thalamus bilaterally; co-occurrence matrix based angular second moment and entropy. The VIQ correlated negatively with entropy and positively with angular second moment values in the right putamen, indicating that the smaller the VIQ score, the more complex the texture in the right putamen. There was no correlation between myoclonus in action scores and entropy in the putamen of either hemisphere. Our VOI included the anterior, mainly rostrodorsal (associative) part of the putamen that is involved in learning new motor tasks, whereas the posterior caudoventral (sensorimotor) part of putamen is more involved in storage and execution of learned tasks (Jueptner et al. 1997, Lehericy et al. 2005). The parallel textural alterations in the thalamus and right putamen are an interesting finding. Initially, basal ganglia-thalamocortical circuitry was considered to be

involved only in the control of movement but nowadays these structures are also regarded to be part of higher-order behavioral control (Herrero, Barcia & Navarro 2002, DeLong, Wichmann 2009).

Memory problems are not main symptoms in EPM1 (Genton 2010, Magaudda et al. 2006) and previous imaging studies have not revealed any hippocampal abnormalities. In agreement with the previous studies, we found no major textural differences in the hippocampi, amygdalae or caudate nuclei between the EPM1 patients and healthy controls.

Our study has some limitations. The original study population had in part been scanned with slightly different MR imaging parameters. Since we wanted to make sure the different imaging parameters do not affect the TA results, our identical MRI data for TA remained relatively small. Further, some of the original patient imaging data could not be included in the texture analysis because of the suboptimal image quality caused by myoclonic movement artefacts. Finally, 16 patients and 16 controls from the original study population shared the identical imaging protocol and were included in the present TA study. The restrictions in the data collection reflect the fact that TA is still an experimental method with many limitations, including its potential sensitivity to slight differences in different scanners, coils and imaging protocols, complicating its routine clinical use and prohibiting data comparisons between institutions.

To conclude, three dimensional TA proved to be a feasible method to obtain imperceptible quantitative individual information from MR images of the brain in EPM1. Patients with EPM1 exhibit more coarse and heterogeneous texture in thalamus and right putamen. The textural differences observed in the present study parallel the previous imaging, neuropathological, and molecular genetics studies of thalamic involvement in EPM1. Textural alterations in the right putamen is a novel finding. Our results indicate that the changes in both the thalamus and putamen may play an important role in the pathophysiology of EPM1. Further studies in larger patient materials will show whether 3D TA could be a relevant tool for clinical applications.

7 General discussion

EPM1 is a progressive neurodegenerative disorder with no specific cure. Although mutations in the CSTB gene are responsible for the primary defect in EPM1, the exact pathogenesis of the disorder remains unknown. Clinical research in EPM1 has been challenging due to small number of cases worldwide. Consequently, there are few imaging studies of EPM1 patients. In the present study, both the skeletal and cerebral abnormalities of EPM1 patients were assessed and combined to the clinical and neuropsychological data of the patients.

7.1 SKELETAL FINDINGS IN EPM1

Previously, three studies have documented bone findings in patients with EPM1. Koskiniemi et al. first described thickening of the skull and thoracic scoliosis in patients with in early 1970's (Koskiniemi et al. 1974) when phenytoin was commonly used as a treatment in PMEs. A case report of a patient with two rare genetic disorders, both EPM1 and myotonic dystrophy, exhibited thickening of the skull and with large frontal sinus in MRI but no focal pathology in the brain parenchyma (Nokelainen et al. 2000) similarly to the findings of EPM1 patients in the present study. Lately, thickening of the calvarium in four patients with EPM1 was interpreted as hyperostosis frontalis interna (HFI) (Korja et al. 2007a). In molecular genetic studies, CSTB and Cathepsin K have been shown to be interconnected in vitro leading to the altered osteoclast bone resorption activity (Laitala-Leinonen et al. 2006). Reflecting to the previous studies, in the present study systematic analysis of head MRI and skeletal radiographs revealed more generalized skull thickening in EPM1 patients and scoliosis and an increased prevalence of abnormal skeletal findings that was not explained by the HFI, former phenytoin use, Paget's disease or other conditions such as severe anaemia or hyperparathyroidism. Both scoliosis and accessory ossicles were common and the prevalences were higher than given in literature (Carter, Haynes 1987, Hong et al. 2010, Ueno et al. 2011, Mellado et al. 2003). Taken together, skeletal findings suggest that abnormal ossification of the skeleton is a universal feature of EPM1 which may be associated with a defect in CSTB function.

7.2 REGIONAL CORTICAL THINNING AND COGNITION IN EPM1

As previously shown, the compound heterozygous individuals exhibit a more severe form of the disorder (Koskenkorva et al. 2011, Canafoglia et al. 2012). However, most of the patients with EPM1 are homozygous. In spite of uniform genotype, the severity of the symptoms, myoclonus and neurocognitive function is variable among patients with EPM1.

By combining the neuropsychological data with CTH in homozygous patients with EPM1, we found that the patients with a more severe form of the disease had thinner cortex compared to them with a milder form of the disease. The anatomical areas responsible for processing of verbal and complex visual data, and areas responsible for higher-order cognitive functions were affected. Parallel cortical thinning has been observed in mice already at a young age (Tegelberg et al. 2012). Furthermore, in mice cortical atrophy precedes the loss of neurons in corresponding thalamic relay nucleus.
Previous studies have shown that sensorimotor cortex is affected in patients with EPM1 compared to the healthy controls (Koskenkorva et al. 2009, Koskenkorva et al. 2012). The severity of myoclonus was used as a criterion for different subgroups in the present CTH study as well. The most interesting finding in CTH was that although the myoclonus and

motor dysfunction is a peculiar character in EPM1, there were no major differences in sensorimotor cortical areas between the three severity sub-groups. Thus, it can be suggested that the sensorimotor cortices are simirlarly damaged in EPM1. Whereas, the subtle changes in more limited cortical areas result in the heterogeneity of the cognitive function and severity in symptoms in patients with EPM1.

The verbal memory has been found to be the least affected cognitive domain in Finnish patients with EPM1 (unpublished data). No correlations were found between the verbal memory scores and CTH as well as no major textural differences in hippocampi between the EPM1 patients and healthy controls in TA study. This is similar to the previous imaging studies and that the memory problems are not the main symptoms in EPM1 (Genton 2010, Magaudda et al. 2006).

7.3 SUBTLE TEXTURAL ALTERATIONS IN EPM1

TA detected significant differing texture features especially in the thalamus of EPM1 patients compared to the healthy controls. Also right putamen was significantly affected that is a novel finding. Thalamus is a relay center between subcortical areas and the cerebral cortex, and it has multiple functions both in sensory and motor aspects, along with the regulation of awareness, attention, memory and language (Smythies 1997, Buchel et al. 1998, Johnson, Ojemann 2000). Both the myoclonus, mice studies and previous imaging finding in patients with EPM1 support the role of the thalamus in the pathophysiology of EPM1 (Koskenkorva et al. 2009, Mascalchi et al. 2002, Korja et al. 2007b, Korja et al. 2010, Manninen et al. 2013, Franceschetti et al. 2007, Tegelberg et al. 2012). Thalamus is a fascinating part of the brain in regards to EPM1, and possible dopaminergic defect in thalamus should be further studied. As previously proposed dopamine may have a role in the pathophysiology of EPM1 (Mervaala et al. 1990, Korja et al. 2007b).

In addition, the TA study demonstrates that three dimensional TA is a feasible method to obtain imperceptible quantitative information from MR images of the brain. However, there were also some limitations including slightly different MR imaging parameters and artefacts due the suboptimal image quality caused by the myoclonic movement artefact. The restrictions in the data collection reflect the fact that TA is still an experimental method with many limitations. This includes its potential sensitivity to slight differences in different scanners, coils and imaging protocols complicating its routine clinical use and prohibiting data comparisons between institutions. However, TA is already applied in different fields of industry and this study further demonstrates that it can be applied in MRI as well. Further studies in larger patient materials will show its potential in clinical imaging.

Thus far, it has been shown that patients with EPM1 have widespread alterations both in cortical and subcortical areas not limited only to the motor areas. The human brain is complex and there are still many mysteries to investigate. Seldomly, one area of the brain is purely involved in a motor, sensory or cognitive system but these all functions are layered and transposed into the greater whole. More commonly, damages are not restricted to the certain areas of the brain. In other words, all these aspects are united which create every patient's individual symptoms. Today, when individual treatments are increasingly topical issues, it would be essential to use tailored medication by the distinctive characteristics of the patients. For example, to be able to predict the progression of the disease. Modern image analysis can be one tool in this characterization along with genetic testing and other biomarkers.

To conclude, as seen in EPM1, the evaluation of human brain in current routine MR images is not sufficient to show subtle changes of the brain. Still more data is needed

about the normal age- and sex-related changes and effects of genetic factors on brain. Future research may support the development of more automated MR image analysis methods to evaluate patients' brain individually, and could be applied in routine clinical practice.

8 Conclusions

I Patients with EPM1 had thickening of the skull and an increased prevalence of abnormal findings in skeletal radiographs. Skeletal findings in EPM1 are suggested to be connected to defective cystatin B function.

II Patients with a more severe form of the disorder exhibit more widespread cortical thinning compared to the patients with milder form of the disease. Areas involved in higher-order cognitive function were particularly affected providing a structural neuroanatomical-biological basis for disease severity and cognitive decline in EPM1.

III TA detected subtle textural changes in EPM1 patients especially in thalamus and right putamen. TA has potential in MR image analysis while still being an experimental method with its limitations recognized in this study.

9 References

Adams, J.E. 2013, "Advances in bone imaging for osteoporosis", *Nature reviews. Endocrinology,* vol. 9, no. 1, pp. 28-42.

Alegro, M.D., Silva, A.V., Bando, S.Y., Lopes, R.D., Martins de Castro, L.H., Hungtsu, W., Moreira-Filho, C.A. & Amaro, E.,Jr 2012, "Texture analysis of high resolution MRI allows discrimination between febrile and afebrile initial precipitating injury in mesial temporal sclerosis", *Magnetic resonance in medicine,* vol. 68 no. 5. pp. 1647-53.

Allman, J.M., Hakeem, A., Erwin, J.M., Nimchinsky, E. & Hof, P. 2001, "The anterior cingulate cortex. The evolution of an interface between emotion and cognition", *Annals of the New York Academy of Sciences,* vol. 935, pp. 107-117.

Altaf, F., Gibson, A., Dannawi, Z. & Noordeen, H. 2013, "Adolescent idiopathic scoliosis", *BMJ (Clinical research ed.),* vol. 346, pp. f2508.

Amiez, C. & Petrides, M. 2009, "Anatomical organization of the eye fields in the human and non-human primate frontal cortex", *Progress in neurobiology,* vol. 89, no. 2, pp. 220-230.

Antel, S.B., Collins, D.L., Bernasconi, N., Andermann, F., Shinghal, R., Kearney, R.E., Arnold, D.L. & Bernasconi, A. 2003, "Automated detection of focal cortical dysplasia lesions using computational models of their MRI characteristics and texture analysis", *NeuroImage,* vol. 19, no. 4, pp. 1748-1759.

Arnsten, A.F. 2009, "Stress signalling pathways that impair prefrontal cortex structure and function", *Nature reviews. Neuroscience,* vol. 10, no. 6, pp. 410-422.

Ashburner, J., Csernansky, J.G., Davatzikos, C., Fox, N.C., Frisoni, G.B. & Thompson, P.M. 2003, "Computer-assisted imaging to assess brain structure in healthy and diseased brains", *Lancet neurology,* vol. 2, no. 2, pp. 79-88.

Atalar, M.H., Icagasioglu, D. & Tas, F. 2007, "Cerebral hemiatrophy (Dyke-Davidoff-Masson syndrome) in childhood: clinicoradiological analysis of 19 cases", *Pediatrics international: official journal of the Japan Pediatric Society,* vol. 49, no. 1, pp. 70-75.

Bassuk, A.G., Wallace, R.H., Buhr, A., Buller, A.R., Afawi, Z., Shimojo, M., Miyata, S., Chen, S., Gonzalez-Alegre, P., Griesbach, H.L., Wu, S., Nashelsky, M., Vladar, E.K., Antic, D., Ferguson, P.J., Cirak, S., Voit, T., Scott, M.P., Axelrod, J.D., Gurnett, C., Daoud, A.S., Kivity, S., Neufeld, M.Y., Mazarib, A., Straussberg, R., Walid, S., Korczyn, A.D., Slusarski, D.C., Berkovic, S.F. & El-Shanti, H.I. 2008, "A homozygous mutation in human PRICKLE1 causes an autosomal-recessive progressive myoclonus epilepsy-ataxia syndrome", *American Journal of Human Genetics,* vol. 83, no. 5, pp. 572-581.

Bear, M.F., Connor, B.W. & Paradiso, M.A. (eds) 2007, "Neuroscience, Exploring the Brain", 3rd edn, *Lippincott Williams & Wilkins, USA.*

Beerhorst, K., Schouwenaars, F.M., Tan, I.Y. & Aldenkamp, A.P. 2012, "Epilepsy: fractures and the role of cumulative antiepileptic drug load", *Acta Neurologica Scandinavica,* vol. 125, no. 1, pp. 54-59.

Beighton, P. 1987, "Pyle disease (metaphyseal dysplasia)", *Journal of medical genetics,* vol. 24, no. 6, pp. 321-324.

Bellebaum, C., Koch, B., Schwarz, M. & Daum, I. 2008, "Focal basal ganglia lesions are associated with impairments in reward-based reversal learning", *Brain: a journal of neurology,* vol. 131, no. Pt 3, pp. 829-841.

Benchenane, K., Tiesinga, P.H. & Battaglia, F.P. 2011, "Oscillations in the prefrontal cortex: a gateway to memory and attention", *Current opinion in neurobiology,* vol. 21, no. 3, pp. 475-485.

Benichou, O.D., Laredo, J.D. & de Vernejoul, M.C. 2000, "Type II autosomal dominant osteopetrosis (Albers-Schonberg disease): clinical and radiological manifestations in 42 patients", *Bone,* vol. 26, no. 1, pp. 87-93.

Berkovic, S.F., Mazarib, A., Walid, S., Neufeld, M.Y., Manelis, J., Nevo, Y., Korczyn, A.D., Yin, J., Xiong, L., Pandolfo, M., Mulley, J.C. & Wallace, R.H. 2005, "A new clinical and molecular form of Unverricht-Lundborg disease localized by homozygosity mapping", *Brain: a journal of neurology,* vol. 128, no. Pt 3, pp. 652-658.

Bernasconi, A., Antel, S.B., Collins, D.L., Bernasconi, N., Olivier, A., Dubeau, F., Pike, G.B., Andermann, F. & Arnold, D.L. 2001, "Texture analysis and morphological processing of magnetic resonance imaging assist detection of focal cortical dysplasia in extra-temporal partial epilepsy", *Annals of Neurology,* vol. 49, no. 6, pp. 770-775.

Bonilha, L., Kobayashi, E., Castellano, G., Coelho, G., Tinois, E., Cendes, F. & Li, L.M. 2003, "Texture analysis of hippocampal sclerosis", *Epilepsia,* vol. 44, no. 12, pp. 1546-1550.

Brooks, D.J. 2006, "Dopaminergic action beyond its effects on motor function: imaging studies", *Journal of neurology,* vol. 253 Suppl 4, pp. IV8-15.

Brunkow, M.E., Gardner, J.C., Van Ness, J., Paeper, B.W., Kovacevich, B.R., Proll, S., Skonier, J.E., Zhao, L., Sabo, P.J., Fu, Y., Alisch, R.S., Gillett, L., Colbert, T., Tacconi, P., Galas, D., Hamersma, H., Beighton, P. & Mulligan, J. 2001, "Bone dysplasia sclerosteosis results from loss of the SOST gene product, a novel cystine knot-containing protein", *American Journal of Human Genetics,* vol. 68, no. 3, pp. 577-589.

Buchel, C., Josephs, O., Rees, G., Turner, R., Frith, C.D. & Friston, K.J. 1998, "The functional anatomy of attention to visual motion. A functional MRI study", *Brain: a journal of neurology,* vol. 121 (Pt 7), no. Pt 7, pp. 1281-1294.

Buckner, R.L., Andrews-Hanna, J.R. & Schacter, D.L. 2008, "The brain's default network: anatomy, function, and relevance to disease", *Annals of the New York Academy of Sciences,* vol. 1124, pp. 1-38.

Bulakbasi, N., Bozlar, U., Karademir, I., Kocaoglu, M. & Somuncu, I. 2008, "CT and MRI in the evaluation of craniospinal involvement with polyostotic fibrous dysplasia in McCune-Albright syndrome", *Diagnostic and interventional radiology (Ankara, Turkey),* vol. 14, no. 4, pp. 177-181.

Burgener, F.A., Kormano, M. & Pudas, T. (eds) 2008, "Differential Diagnosis in Conventional Radiology", *Thieme, New York, NY, USA.*

Calabrese, M., Rinaldi, F., Mattisi, I., Grossi, P., Favaretto, A., Atzori, M., Bernardi, V., Barachino, L., Romualdi, C., Rinaldi, L., Perini, P. & Gallo, P. 2010, "Widespread

cortical thinning characterizes patients with MS with mild cognitive impairment", *Neurology,* vol. 74, no. 4, pp. 321-328.

Canafoglia, L., Gennaro, E., Capovilla, G., Gobbi, G., Boni, A., Beccaria, F., Viri, M., Michelucci, R., Agazzi, P., Assereto, S., Coviello, D.A., Di Stefano, M., Rossi Sebastiano, D., Franceschetti, S. & Zara, F. 2012, "Electroclinical presentation and genotype-phenotype relationships in patients with Unverricht-Lundborg disease carrying compound heterozygous CSTB point and indel mutations", *Epilepsia,* vol. 53, no. 12, pp. 2120-2127.

Carter, O.D. & Haynes, S.G. 1987, "Prevalence rates for scoliosis in US adults: results from the first National Health and Nutrition Examination Survey", *International journal of epidemiology,* vol. 16, no. 4, pp. 537-544.

Castellano, G., Bonilha, L., Li, L.M. & Cendes, F. 2004, "Texture analysis of medical images", *Clinical radiology,* vol. 59, no. 12, pp. 1061-1069.

Chen, W., Giger, M.L., Li, H., Bick, U. & Newstead, G.M. 2007, "Volumetric texture analysis of breast lesions on contrast-enhanced magnetic resonance images", *Magnetic resonance in medicine,* vol. 58, no. 3, pp. 562-571.

Chew, N.K., Mir, P., Edwards, M.J., Cordivari, C., Martino, D., Schneider, S.A., Kim, H.T., Quinn, N.P. & Bhatia, K.P. 2008, "The natural history of Unverricht-Lundborg disease: a report of eight genetically proven cases", *Movement disorders: official journal of the Movement Disorder Society,* vol. 23, no. 1, pp. 107-113.

Chien, Y.P. 1974, "Recognition of X-Ray Picture Patterns", *Systems, Man and Cybernetics, IEEE Transactions on,* vol. 4, pp. 145.

Chow, K.M. & Szeto, C.C. 2007, "Cerebral atrophy and skull thickening due to chronic phenytoin therapy", *CMAJ: Canadian Medical Association journal = journal de l'Association medicale canadienne,* vol. 176, no. 3, pp. 321-323.

Chung, M. & Taylor, J. 2004, "Diffusion smoothing on brain surface via finite element method.", *IEEE International Symposium on Biomedical Imagining: Macro to Nano,* Vol. 1, pp. 425-435.

Cohen, M.M.,Jr 2006, "The new bone biology: pathologic, molecular, and clinical correlates", *American journal of medical genetics. Part A,* vol. 140, no. 23, pp. 2646-2706.

Collewet, G., Strzelecki, M. & Mariette, F. 2004, "Influence of MRI acquisition protocols and image intensity normalization methods on texture classification", *Magnetic resonance imaging,* vol. 22, no. 1, pp. 81-91.

Corbett, M.A., Schwake, M., Bahlo, M., Dibbens, L.M., Lin, M., Gandolfo, L.C., Vears, D.F., O'Sullivan, J.D., Robertson, T., Bayly, M.A., Gardner, A.E., Vlaar, A.M., Korenke, G.C., Bloem, B.R., de Coo, I.F., Verhagen, J.M., Lehesjoki, A.E., Gecz, J. & Berkovic, S.F. 2011, "A mutation in the Golgi Qb-SNARE gene GOSR2 causes progressive myoclonus epilepsy with early ataxia", *American Journal of Human Genetics,* vol. 88, no. 5, pp. 657-663.

Cure, J.K., Key, L.L., Goltra, D.D. & VanTassel, P. 2000, "Cranial MR imaging of osteopetrosis", *AJNR. American journal of neuroradiology,* vol. 21, no. 6, pp. 1110-1115.

Dabbs, K., Jones, J., Seidenberg, M. & Hermann, B. 2009, "Neuroanatomical correlates of cognitive phenotypes in temporal lobe epilepsy", *Epilepsy & behavior: E&B,* vol. 15, no. 4, pp. 445-451.

Dahlin, E., Neely, A.S., Larsson, A., Backman, L. & Nyberg, L. 2008, "Transfer of learning after updating training mediated by the striatum", *Science (New York, N.Y.),* vol. 320, no. 5882, pp. 1510-1512.

Damasio, A.R. & Geschwind, N. 1984, "The neural basis of language", *Annual Review of Neuroscience,* vol. 7, pp. 127-147.

de Haan, G.J., Halley, D.J., Doelman, J.C., Geesink, H.H., Augustijn, P.B., Jager-Jongkind, A.D., Majoie, M., Bader, A.J., Leliefeld-Ten Doeschate, L.A., Deelen, W.H., Bertram, E., Lehesjoki, A.E. & Lindhout, D. 2004, "Univerricht-Lundborg disease: underdiagnosed in the Netherlands", *Epilepsia,* vol. 45, no. 9, pp. 1061-1063.

de Oliveira, M.S., Betting, L.E., Mory, S.B., Cendes, F. & Castellano, G. 2013, "Texture analysis of magnetic resonance images of patients with juvenile myoclonic epilepsy", *Epilepsy & behavior: E&B,* vol. 27, no. 1, pp. 22-28.

de Oliveira, M.S., D'Abreu, A., Franca, M.C.,Jr, Lopes-Cendes, I., Cendes, F. & Castellano, G. 2012, "MRI-texture analysis of corpus callosum, thalamus, putamen, and caudate in Machado-Joseph disease", *Journal of neuroimaging: official journal of the American Society of Neuroimaging,* vol. 22, no. 1, pp. 46-52.

de Vernejoul, M.C., Schulz, A. & Kornak, U. 1993, "CLCN7-Related Osteopetrosis" in *GeneReviews(R)*, eds. R.A. Pagon, M.P. Adam, H.H. Ardinger et al., *University of Washington, Seattle, Seattle (WA).*

Del Fattore, A., Cappariello, A. & Teti, A. 2008, "Genetics, pathogenesis and complications of osteopetrosis", *Bone,* vol. 42, no. 1, pp. 19-29.

DeLong, M. & Wichmann, T. 2009, "Update on models of basal ganglia function and dysfunction", *Parkinsonism & related disorders,* vol. 15 Suppl 3, pp. S237-40.

Di Preta, J.A., Powers, J.M. & Hicks, D.G. 1994, "Hyperostosis cranii ex vacuo: a rare complication of shunting for hydrocephalus", *Human pathology,* vol. 25, no. 5, pp. 545-547.

Dibbens, L.M., Michelucci, R., Gambardella, A., Andermann, F., Rubboli, G., Bayly, M.A., Joensuu, T., Vears, D.F., Franceschetti, S., Canafoglia, L., Wallace, R., Bassuk, A.G., Power, D.A., Tassinari, C.A., Andermann, E., Lehesjoki, A.E. & Berkovic, S.F. 2009, "SCARB2 mutations in progressive myoclonus epilepsy (PME) without renal failure", *Annals of Neurology,* vol. 66, no. 4, pp. 532-536.

Dijk, J.M. & Tijssen, M.A. 2010, "Management of patients with myoclonus: available therapies and the need for an evidence-based approach", *Lancet neurology,* vol. 9, no. 10, pp. 1028-1036.

Duvernoy, H.M. 1999, *The Human Brain,* Springer-Verlag, Vienna, Austria.

Eldridge, R., Iivanainen, M., Stern, R., Koerber, T. & Wilder, B.J. 1983, ""Baltic" myoclonus epilepsy: hereditary disorder of childhood made worse by phenytoin", *Lancet,* vol. 2, no. 8354, pp. 838-842.

Ferlazzo, E., Gagliano, A., Calarese, T., Magaudda, A., Striano, P., Cortese, L., Cedro, C., Laguitton, V., Bramanti, P., Carbonaro, M., Albachiara, A., Fragassi, N., Italiano, D.,

Sessa, E., Coppola, A. & Genton, P. 2009, "Neuropsychological findings in patients with Unverricht-Lundborg disease", *Epilepsy & behavior: E&B,* vol. 14, no. 3, pp. 545-549.

Ferlazzo, E., Magaudda, A., Striano, P., Vi-Hong, N., Serra, S. & Genton, P. 2007, "Long-term evolution of EEG in Unverricht-Lundborg disease", *Epilepsy research,* vol. 73, no. 3, pp. 219-227.

Field, M., Tarpey, P., Boyle, J., Edkins, S., Goodship, J., Luo, Y., Moon, J., Teague, J., Stratton, M.R., Futreal, P.A., Wooster, R., Raymond, F.L. & Turner, G. 2006, "Mutations in the RSK2(RPS6KA3) gene cause Coffin-Lowry syndrome and nonsyndromic X-linked mental retardation", *Clinical genetics,* vol. 70, no. 6, pp. 509-515.

Fischl, B. & Dale, A.M. 2000, "Measuring the thickness of the human cerebral cortex from magnetic resonance images", *Proceedings of the National Academy of Sciences of the United States of America,* vol. 97, no. 20, pp. 11050-11055.

Fjell, A.M., Westlye, L.T., Amlien, I., Espeseth, T., Reinvang, I., Raz, N., Agartz, I., Salat, D.H., Greve, D.N., Fischl, B., Dale, A.M. & Walhovd, K.B. 2009a, "High consistency of regional cortical thinning in aging across multiple samples", *Cerebral cortex (New York, N.Y.: 1991),* vol. 19, no. 9, pp. 2001-2012.

Fjell, A.M., Westlye, L.T., Amlien, I., Espeseth, T., Reinvang, I., Raz, N., Agartz, I., Salat, D.H., Greve, D.N., Fischl, B., Dale, A.M. & Walhovd, K.B. 2009b, "Minute effects of sex on the aging brain: a multisample magnetic resonance imaging study of healthy aging and Alzheimer's disease", *The Journal of neuroscience: the official journal of the Society for Neuroscience,* vol. 29, no. 27, pp. 8774-8783.

Franceschetti, S., Sancini, G., Buzzi, A., Zucchini, S., Paradiso, B., Magnaghi, G., Frassoni, C., Chikhladze, M., Avanzini, G. & Simonato, M. 2007, "A pathogenetic hypothesis of Unverricht-Lundborg disease onset and progression", *Neurobiology of disease,* vol. 25, no. 3, pp. 675-685.

Frucht, S.J., Leurgans, S.E., Hallett, M. & Fahn, S. 2002, "The Unified Myoclonus Rating Scale", *Advances in Neurology,* vol. 89, pp. 361-376.

Funahashi, S. 2006, "Prefrontal cortex and working memory processes", *Neuroscience,* vol. 139, no. 1, pp. 251-261.

Galloway, M. 1975, "Texture analysis using gray level run lengths", *Computer graphics and image processing,* vol. 4, pp. 172-179.

Ganeshan, B., Goh, V., Mandeville, H.C., Ng, Q.S., Hoskin, P.J. & Miles, K.A. 2013, "Non-small cell lung cancer: histopathologic correlates for texture parameters at CT", *Radiology,* vol. 266, no. 1, pp. 326-336.

Ganeshan, B., Miles, K.A., Young, R.C., Chatwin, C.R., Gurling, H.M. & Critchley, H.D. 2010, "Three-dimensional textural analysis of brain images reveals distributed grey-matter abnormalities in schizophrenia", *European radiology,* vol. 20, no. 4, pp. 941-948.

Gardner, J.C., van Bezooijen, R.L., Mervis, B., Hamdy, N.A., Lowik, C.W., Hamersma, H., Beighton, P. & Papapoulos, S.E. 2005, "Bone mineral density in sclerosteosis; affected individuals and gene carriers", *The Journal of clinical endocrinology and metabolism,* vol. 90, no. 12, pp. 6392-6395.

Gelb, B.D., Shi, G.P., Chapman, H.A. & Desnick, R.J. 1996, "Pycnodysostosis, a lysosomal disease caused by cathepsin K deficiency", *Science (New York, N.Y.),* vol. 273, no. 5279, pp. 1236-1238.

Genton, P. 2010, "Unverricht-Lundborg disease (EPM1)", *Epilepsia,* vol. 51 Suppl 1, pp. 37-39.

Georgiadis, P., Cavouras, D., Kalatzis, I., Glotsos, D., Athanasiadis, E., Kostopoulos, S., Sifaki, K., Malamas, M., Nikiforidis, G. & Solomou, E. 2009, "Enhancing the discrimination accuracy between metastases, gliomas and meningiomas on brain MRI by volumetric textural features and ensemble pattern recognition methods", *Magnetic resonance imaging,* vol. 27, no. 1, pp. 120-130.

Ghanem, N., Lohrmann, C., Engelhardt, M., Pache, G., Uhl, M., Saueressig, U., Kotter, E. & Langer, M. 2006, "Whole-body MRI in the detection of bone marrow infiltration in patients with plasma cell neoplasms in comparison to the radiological skeletal survey", *European radiology,* vol. 16, no. 5, pp. 1005-1014.

Giovagnoli, A.R., Canafoglia, L., Reati, F., Raviglione, F. & Franceschetti, S. 2009, "The neuropsychological pattern of Unverricht-Lundborg disease", *Epilepsy research,* vol. 84, no. 2-3, pp. 217-223.

Gogtay, N., Giedd, J.N., Lusk, L., Hayashi, K.M., Greenstein, D., Vaituzis, A.C., Nugent, T.F.,3rd, Herman, D.H., Clasen, L.S., Toga, A.W., Rapoport, J.L. & Thompson, P.M. 2004, "Dynamic mapping of human cortical development during childhood through early adulthood", *Proceedings of the National Academy of Sciences of the United States of America,* vol. 101, no. 21, pp. 8174-8179.

Goldstein, R.Z. & Volkow, N.D. 2011, "Dysfunction of the prefrontal cortex in addiction: neuroimaging findings and clinical implications", *Nature reviews. Neuroscience,* vol. 12, no. 11, pp. 652-669.

Gorlin, R.J. & Whitley, C.B. 1983, "Lenz-Majewski syndrome", *Radiology,* vol. 149, no. 1, pp. 129-131.

Govender, P., Byrne, A., Lyburn, I.D. & Torreggiani, W.C. 2006, "Generalized skull vault thickening in association with a large arteriovenous malformation", *Australasian Radiology,* vol. 50, no. 1, pp. 66-67.

Graybiel, A.M. 2005, "The basal ganglia: learning new tricks and loving it", *Current opinion in neurobiology,* vol. 15, no. 6, pp. 638-644.

Green, R.L. & Ostrander, R.L. (eds) 2009, "Neuroanatomy for students of behavioral disorders", *W. W. Norton & Company, Inc., New York, NY, United States of America.*

Green, G.D., Kembhavi, A.A., Davies, M.E. & Barrett, A.J. 1984, "Cystatin-like cysteine proteinase inhibitors from human liver", *The Biochemical journal,* vol. 218, no. 3, pp. 939-946.

Greenblatt, S.H. 1995, "Phrenology in the science and culture of the 19th century", *Neurosurgery,* vol. 37, no. 4, pp. 790-804; discussion 804-5.

Grill-Spector, K., Sayres, R. & Ress, D. 2006, "High-resolution imaging reveals highly selective nonface clusters in the fusiform face area", *Nature neuroscience,* vol. 9, no. 9, pp. 1177-1185.

Gutierrez-Galve, L., Flugel, D., Thompson, P.J., Koepp, M.J., Symms, M.R., Ron, M.A. & Foong, J. 2012, "Cortical abnormalities and their cognitive correlates in patients with temporal lobe epilepsy and interictal psychosis", *Epilepsia,* vol. 53, no. 6, pp. 1077-1087.

Hajek, M., Dezortova, M., Materka, A. & Lerski, R. 2006, "Texture analysis for magnetic resonance imaging", *Med4publishing, Prague.*

Hall, E.L., Kruger, R.P., Dwyer III, S.J., Hall, D.L., McLaren, R.W. & Lodwick, G.S. 1971, "Survey of preprocessing and feature extraction techniques for radiographic images", *IEEE Transactions on Computers,* vol. C-20, no. 9, pp. 1032-1044.

Haltia, M. & Goebel, H.H. 2012, "The neuronal ceroid-lipofuscinoses: A historical introduction", *Biochimica et biophysica acta,* vol. 1832, No. 11, pp. 1795-1800.

Haralick, R.M. 1973, "Textural features for image classification", *IEEE transactions on systems, man, and cybernetics,* vol. SMC-3 (Nov. 1973), pp. 610-621.

Haralick, R.M. 1979, "Statistical and structural approaches to texture", *Proceedings of the IEEE,* vol. 67, No. 5, pp. 786-804.

Harrison, L. 2011, "Clinical Applicability of MRI Texture Analysis", *Acta Universitatis Tamperensis, Tampere University Press*; 1640.

Hartikainen, P., Räsänen, J., Julkunen, V., Niskanen, E., Hallikainen, M., Kivipelto, M., Vanninen, R., Remes, A.M. & Soininen, H. 2012, "Cortical thickness in frontotemporal dementia, mild cognitive impairment, and Alzheimer's disease", *Journal of Alzheimer's disease: JAD,* vol. 30, no. 4, pp. 857-874.

Hatipoglu, H.G., Ozcan, H.N., Hatipoglu, U.S. & Yuksel, E. 2008, "Age, sex and body mass index in relation to calvarial diploe thickness and craniometric data on MRI", *Forensic science international,* vol. 182, no. 1-3, pp. 46-51.

Herculano-Houzel, S. 2012, "The remarkable, yet not extraordinary, human brain as a scaled-up primate brain and its associated cost", *Proceedings of the National Academy of Sciences of the United States of America,* vol. 109 Suppl 1, pp. 10661-10668.

Herlidou-Meme, S., Constans, J.M., Carsin, B., Olivie, D., Eliat, P.A., Nadal-Desbarats, L., Gondry, C., Le Rumeur, E., Idy-Peretti, I. & de Certaines, J.D. 2003, "MRI texture analysis on texture test objects, normal brain and intracranial tumors", *Magnetic resonance imaging,* vol. 21, no. 9, pp. 989-993.

Herrero, M.T., Barcia, C. & Navarro, J.M. 2002, "Functional anatomy of thalamus and basal ganglia", *Child's nervous system: ChNS: official journal of the International Society for Pediatric Neurosurgery,* vol. 18, no. 8, pp. 386-404.

Hershkovitz, I., Greenwald, C., Rothschild, B.M., Latimer, B., Dutour, O., Jellema, L.M. & Wish-Baratz, S. 1999, "Hyperostosis frontalis interna: an anthropological perspective", *American Journal of Physical Anthropology,* vol. 109, no. 3, pp. 303-325.

Holli, K. 2011, "Texture Analysis as a Tool for Tissue Characterization in Clinical MRI" *Tampere University of Technology*. Publication; 988.

Holli, K., Lääperi, A.L., Harrison, L., Luukkaala, T., Toivonen, T., Ryymin, P., Dastidar, P., Soimakallio, S. & Eskola, H. 2010a, "Characterization of breast cancer types by texture analysis of magnetic resonance images", *Academic Radiology,* vol. 17, no. 2, pp. 135-141.

Holli, K.K., Harrison, L., Dastidar, P., Wäljas, M., Liimatainen, S., Luukkaala, T., Ohman, J., Soimakallio, S. & Eskola, H. 2010b, "Texture analysis of MR images of patients with mild traumatic brain injury", *BMC medical imaging,* vol. 10, pp. 8.

Holli, K.K., Wäljas, M., Harrison, L., Liimatainen, S., Luukkaala, T., Ryymin, P., Eskola, H., Soimakallio, S., Ohman, J. & Dastidar, P. 2010c, "Mild traumatic brain injury: tissue texture analysis correlated to neuropsychological and DTI findings", *Academic Radiology,* vol. 17, no. 9, pp. 1096-1102.

Hong, J.Y., Suh, S.W., Modi, H.N., Hur, C.Y., Song, H.R. & Park, J.H. 2010, "The prevalence and radiological findings in 1347 elderly patients with scoliosis", *The Journal of bone and joint surgery.British volume,* vol. 92, no. 7, pp. 980-983.

Houseweart, M.K., Pennacchio, L.A., Vilaythong, A., Peters, C., Noebels, J.L. & Myers, R.M. 2003, "Cathepsin B but not cathepsins L or S contributes to the pathogenesis of Unverricht-Lundborg progressive myoclonus epilepsy (EPM1)", *Journal of neurobiology,* vol. 56, no. 4, pp. 315-327.

Iivanainen, M. & Himberg, J.J. 1982, "Valproate and clonazepam in the treatment of severe progressive myoclonus epilepsy", *Archives of Neurology,* vol. 39, no. 4, pp. 236-238.

Jafari-Khouzani, K., Elisevich, K., Patel, S., Smith, B. & Soltanian-Zadeh, H. 2010, "FLAIR signal and texture analysis for lateralizing mesial temporal lobe epilepsy", *NeuroImage,* vol. 49, no. 2, pp. 1559-1571.

Janssens, K., Vanhoenacker, F., Bonduelle, M., Verbruggen, L., Van Maldergem, L., Ralston, S., Guanabens, N., Migone, N., Wientroub, S., Divizia, M.T., Bergmann, C., Bennett, C., Simsek, S., Melancon, S., Cundy, T. & Van Hul, W. 2006, "Camurati-Engelmann disease: review of the clinical, radiological, and molecular data of 24 families and implications for diagnosis and treatment", *Journal of medical genetics,* vol. 43, no. 1, pp. 1-11.

Järvinen, M. & Rinne, A. 1982, "Human spleen cysteineproteinase inhibitor. Purification, fractionation into isoelectric variants and some properties of the variants", *Biochimica et biophysica acta,* vol. 708, no. 2, pp. 210-217.

Jenkins, Z.A., van Kogelenberg, M., Morgan, T., Jeffs, A., Fukuzawa, R., Pearl, E., Thaller, C., Hing, A.V., Porteous, M.E., Garcia-Minaur, S., Bohring, A., Lacombe, D., Stewart, F., Fiskerstrand, T., Bindoff, L., Berland, S., Ades, L.C., Tchan, M., David, A., Wilson, L.C., Hennekam, R.C., Donnai, D., Mansour, S., Cormier-Daire, V. & Robertson, S.P. 2009, "Germline mutations in WTX cause a sclerosing skeletal dysplasia but do not predispose to tumorigenesis", *Nature genetics,* vol. 41, no. 1, pp. 95-100.

Joensuu, T., Lehesjoki, A.E. & Kopra, O. 2008, "Molecular background of EPM1-Unverricht-Lundborg disease", *Epilepsia,* vol. 49, no. 4, pp. 557-563.

Johnson, M.D. & Ojemann, G.A. 2000, "The role of the human thalamus in language and memory: evidence from electrophysiological studies", *Brain and cognition,* vol. 42, no. 2, pp. 218-230.

Jueptner, M., Frith, C.D., Brooks, D.J., Frackowiak, R.S. & Passingham, R.E. 1997, "Anatomy of motor learning. II. Subcortical structures and learning by trial and error", *Journal of neurophysiology,* vol. 77, no. 3, pp. 1325-1337.

Julesz, B. 1973, "Inability of humans to discriminate betwen visual textures that agree second-order statistics: Revisited.", *Perception,* vol. 2(4), pp. 391-405.

Julkunen, V., Niskanen, E., Muehlboeck, S., Pihlajamäki, M., Könönen, M., Hallikainen, M., Kivipelto, M., Tervo, S., Vanninen, R., Evans, A. & Soininen, H. 2009, "Cortical thickness analysis to detect progressive mild cognitive impairment: a reference to Alzheimer's disease", *Dementia and geriatric cognitive disorders,* vol. 28, no. 5, pp. 404-412.

Juntu, J., Sijbers, J., De Backer, S., Rajan, J. & Van Dyck, D. 2010, "Machine learning study of several classifiers trained with texture analysis features to differentiate benign from malignant soft-tissue tumors in T1-MRI images", *Journal of magnetic resonance imaging: JMRI,* vol. 31, no. 3, pp. 680-689.

Kaizer, H. 1955, "A quantification of textures on aerial photographs", *Boston University Research Laboratories, Boston, MA,* Technical note 221.

Kanwisher, N., McDermott, J. & Chun, M.M. 1997, "The fusiform face area: a module in human extrastriate cortex specialized for face perception", *The Journal of neuroscience: the official journal of the Society for Neuroscience,* vol. 17, no. 11, pp. 4302-4311.

Karvonen, M.K., Kaasinen, V., Korja, M. & Marttila, R.J. 2010, "Ropinirole diminishes myoclonus and improves writing and postural balance in an ULD patient", *Movement disorders: official journal of the Movement Disorder Society,* vol. 25, no. 4, pp. 520-521.

Kassner, A. & Thornhill, R.E. 2010, "Texture analysis: a review of neurologic MR imaging applications", *AJNR. American journal of neuroradiology,* vol. 31, no. 5, pp. 809-816.

Kato, H., Kanematsu, M., Zhang, X., Saio, M., Kondo, H., Goshima, S. & Fujita, H. 2007, "Computer-aided diagnosis of hepatic fibrosis: preliminary evaluation of MRI texture analysis using the finite difference method and an artificial neural network", *AJR. American journal of roentgenology,* vol. 189, no. 1, pp. 117-122.

Kattan, K.R. 1970, "Calvarial thickening after Dilantin medication", *The American Journal of Roentgenology, Radium Therapy, and Nuclear Medicine,* vol. 110, no. 1, pp. 102-105.

Kaur, G., Mohan, P., Pawlik, M., DeRosa, S., Fajiculay, J., Che, S., Grubb, A., Ginsberg, S.D., Nixon, R.A. & Levy, E. 2010, "Cystatin C rescues degenerating neurons in a cystatin B-knockout mouse model of progressive myoclonus epilepsy", *The American journal of pathology,* vol. 177, no. 5, pp. 2256-2267.

Keller, S.S., Ahrens, T., Mohammadi, S., Moddel, G., Kugel, H., Ringelstein, E.B. & Deppe, M. 2011, "Microstructural and volumetric abnormalities of the putamen in juvenile myoclonic epilepsy", *Epilepsia,* vol. 52, no. 9, pp. 1715-1724.

Keppler, D. 2006, "Towards novel anti-cancer strategies based on cystatin function", *Cancer letters,* vol. 235, no. 2, pp. 159-176.

Kestilä, M., Ikonen, E. & Lehesjoki, A.E. 2010, "Finnish disease heritage", *Duodecim; lääketieteellinen aikakauskirja,* vol. 126, no. 19, pp. 2311-2320.

Khiari, H.M., Franceschetti, S., Jovic, N., Mrabet, A. & Genton, P. 2009, "Death in Unverricht-Lundborg disease", *Neurological sciences: official journal of the Italian Neurological Society and of the Italian Society of Clinical Neurophysiology,* vol. 30, no. 4, pp. 315-318.

Kim, J.S., Singh, V., Lee, J.K., Lerch, J., Ad-Dab'bagh, Y., MacDonald, D., Lee, J.M., Kim, S.I. & Evans, A.C. 2005, "Automated 3-D extraction and evaluation of the inner and outer cortical surfaces using a Laplacian map and partial volume effect classification", *NeuroImage,* vol. 27, no. 1, pp. 210-221.

Kim, S.J., Bieganski, T., Sohn, Y.B., Kozlowski, K., Semenov, M., Okamoto, N., Kim, C.H., Ko, A.R., Ahn, G.H., Choi, Y.L., Park, S.W., Ki, C.S., Kim, O.H., Nishimura, G., Unger, S., Superti-Furga, A. & Jin, D.K. 2011, "Identification of signal peptide domain SOST mutations in autosomal dominant craniodiaphyseal dysplasia", *Human genetics,* vol. 129, no. 5, pp. 497-502.

Kiviranta, R., Morko, J., Alatalo, S.L., NicAmhlaoibh, R., Risteli, J., Laitala-Leinonen, T. & Vuorio, E. 2005, "Impaired bone resorption in cathepsin K-deficient mice is partially compensated for by enhanced osteoclastogenesis and increased expression of other proteases via an increased RANKL/OPG ratio", *Bone,* vol. 36, no. 1, pp. 159-172.

Kiviranta, R., Morko, J., Uusitalo, H., Aro, H.T., Vuorio, E. & Rantakokko, J. 2001, "Accelerated turnover of metaphyseal trabecular bone in mice overexpressing cathepsin K", *Journal of bone and mineral research: the official journal of the American Society for Bone and Mineral Research,* vol. 16, no. 8, pp. 1444-1452.

Kocinski, M., Klepaczko, A., Materka, A., Chekenya, M. & Lundervold, A. 2012, "3D image texture analysis of simulated and real-world vascular trees", *Computer methods and programs in biomedicine,* vol. 107, no. 2, pp. 140-154.

Koechlin, E. & Hyafil, A. 2007, "Anterior prefrontal function and the limits of human decision-making", *Science (New York, N.Y.),* vol. 318, no. 5850, pp. 594-598.

Koenigs, M., Young, L., Adolphs, R., Tranel, D., Cushman, F., Hauser, M. & Damasio, A. 2007, "Damage to the prefrontal cortex increases utilitarian moral judgements", *Nature,* vol. 446, no. 7138, pp. 908-911.

Kolb, B. & Whishaw, I.Q. 2009, "Fundamentals of Human Neuropsychology", *Worth Publishers, New York, NY, USA.*

Kondoh, T., Matsumoto, T., Ochi, M., Sukegawa, K. & Tsuji, Y. 1998, "New radiological finding by magnetic resonance imaging examination of the brain in Coffin-Lowry syndrome", *Journal of human genetics,* vol. 43, no. 1, pp. 59-61.

Kopitar-Jerala, N. 2006, "The role of cystatins in cells of the immune system", *FEBS letters,* vol. 580, no. 27, pp. 6295-6301.

Korja, M., Ferlazzo, E., Soilu-Hänninen, M., Magaudda, A., Marttila, R., Genton, P. & Parkkola, R. 2010, "T2-weighted high-intensity signals in the basal ganglia as an interesting image finding in Unverricht-Lundborg disease", *Epilepsy research,* vol. 88, no. 1, pp. 87-91.

Korja, M., Kaasinen, V., Lamusuo, S., Marttila, R.J. & Parkkola, R. 2007a, "Hyperostosis frontalis interna as a novel finding in Unverricht-Lundborg disease", *Neurology,* vol. 68, no. 13, pp. 1077-1078.

Korja, M., Kaasinen, V., Lamusuo, S., Parkkola, R., Nagren, K. & Marttila, R.J. 2007b, "Substantial thalamostriatal dopaminergic defect in Unverricht-Lundborg disease", *Epilepsia,* vol. 48, no. 9, pp. 1768-1773.

Koskenkorva, P., Hyppönen, J., Äikiä, M., Mervaala, E., Kiviranta, T., Eriksson, K., Lehesjoki, A.E., Vanninen, R. & Kälviäinen, R. 2011, "Severer phenotype in Unverricht-Lundborg disease (EPM1) patients compound heterozygous for the dodecamer repeat expansion and the c.202C>T mutation in the CSTB gene", *Neurodegenerative diseases,* vol. 8, no. 6, pp. 515-522.

Koskenkorva, P., Khyuppenen, J., Niskanen, E., Könönen, M., Bendel, P., Mervaala, E., Lehesjoki, A.E., Kälviäinen, R. & Vanninen, R. 2009, "Motor cortex and thalamic atrophy in Unverricht-Lundborg disease: voxel-based morphometric study", *Neurology,* vol. 73, no. 8, pp. 606-611.

Koskenkorva, P., Niskanen, E., Hyppönen, J., Könönen, M., Mervaala, E., Soininen, H., Kälviäinen, R. & Vanninen, R. 2012, "Sensorimotor, Visual, and Auditory Cortical Atrophy in Unverricht-Lundborg Disease Mapped with Cortical Thickness Analysis", *AJNR. American journal of neuroradiology,* vol 33, no. 5, pp. 878-883.

Koskiniemi, M., Donner, M., Majuri, H., Haltia, M. & Norio, R. 1974, "Progressive myoclonus epilepsy. A clinical and histopathological study", *Acta Neurologica Scandinavica,* vol. 50, no. 3, pp. 307-332.

Koskiniemi, M., Toivakka, E. & Donner, M. 1974, "Progressive myoclonus epilepsy. Electroencephalographical findings", *Acta Neurologica Scandinavica,* vol. 50, no. 3, pp. 333-359.

Kovalev, V.A., Kruggel, F. & von Cramon, D.Y. 2003, "Gender and age effects in structural brain asymmetry as measured by MRI texture analysis", *NeuroImage,* vol. 19, no. 3, pp. 895-905.

Kravitz, D.J., Saleem, K.S., Baker, C.I. & Mishkin, M. 2011, "A new neural framework for visuospatial processing", *Nature reviews.Neuroscience,* vol. 12, no. 4, pp. 217-230.

Krubitzer, L.A. & Seelke, A.M. 2012, "Cortical evolution in mammals: the bane and beauty of phenotypic variability", *Proceedings of the National Academy of Sciences of the United States of America,* vol. 109 Suppl 1, pp. 10647-10654.

Kuhn, S., Kaufmann, C., Simon, D., Endrass, T., Gallinat, J. & Kathmann, N. 2012, "Reduced thickness of anterior cingulate cortex in obsessive-compulsive disorder", *Cortex; a journal devoted to the study of the nervous system and behavior,* vol. 49, no. 8, pp. 2178-2185.

Kuperberg, G.R., Broome, M.R., McGuire, P.K., David, A.S., Eddy, M., Ozawa, F., Goff, D., West, W.C., Williams, S.C., van der Kouwe, A.J., Salat, D.H., Dale, A.M. & Fischl, B. 2003, "Regionally localized thinning of the cerebral cortex in schizophrenia", *Archives of General Psychiatry,* vol. 60, no. 9, pp. 878-888.

Kälviäinen, R. 2007, "Nuoruusiän myoklonusepilepsia", *Epilepsialiitto, Helsinki.*

Kälviäinen, R., Khyuppenen, J., Koskenkorva, P., Eriksson, K., Vanninen, R. & Mervaala, E. 2008, "Clinical picture of EPM1-Unverricht-Lundborg disease", *Epilepsia,* vol. 49, no. 4, pp. 549-556.

Lafreniere, R.G., Rochefort, D.L., Chretien, N., Rommens, J.M., Cochius, J.I., Kälviäinen, R., Nousiainen, U., Patry, G., Farrell, K., Soderfeldt, B., Federico, A., Hale, B.R., Cossio, O.H., Sorensen, T., Pouliot, M.A., Kmiec, T., Uldall, P., Janszky, J., Pranzatelli, M.R., Andermann, F., Andermann, E. & Rouleau, G.A. 1997, "Unstable insertion in the 5'

flanking region of the cystatin B gene is the most common mutation in progressive myoclonus epilepsy type 1, EPM1", *Nature genetics,* vol. 15, no. 3, pp. 298-302.

Laitala-Leinonen, T., Rinne, R., Saukko, P., Väänänen, H.K. & Rinne, A. 2006, "Cystatin B as an intracellular modulator of bone resorption", *Matrix biology: journal of the International Society for Matrix Biology,* vol. 25, no. 3, pp. 149-157.

Lalioti, M.D., Scott, H.S., Buresi, C., Rossier, C., Bottani, A., Morris, M.A., Malafosse, A. & Antonarakis, S.E. 1997, "Dodecamer repeat expansion in cystatin B gene in progressive myoclonus epilepsy", *Nature,* vol. 386, no. 6627, pp. 847-851.

Lamazza, L., Messina, A., D'Ambrosio, F., Spink, M. & De Biase, A. 2009, "Craniometaphyseal dysplasia: a case report", *Oral surgery, oral medicine, oral pathology, oral radiology, and endodontics,* vol. 107, no. 5, pp. e23-7.

Landis, J.R. & Koch, G.G. 1977, "The measurement of observer agreement for categorical data", *Biometrics,* vol. 33, no. 1, pp. 159-174.

Lee, M.S. & Marsden, C.D. 1994, "Movement disorders following lesions of the thalamus or subthalamic region", *Movement disorders: official journal of the Movement Disorder Society,* vol. 9, no. 5, pp. 493-507.

Lee, M.S., Rinne, J.O., Ceballos-Baumann, A., Thompson, P.D. & Marsden, C.D. 1994, "Dystonia after head trauma", *Neurology,* vol. 44, no. 8, pp. 1374-1378.

Lehericy, S., Benali, H., Van de Moortele, P.F., Pelegrini-Issac, M., Waechter, T., Ugurbil, K. & Doyon, J. 2005, "Distinct basal ganglia territories are engaged in early and advanced motor sequence learning", *Proceedings of the National Academy of Sciences of the United States of America,* vol. 102, no. 35, pp. 12566-12571.

Lehesjoki, A.E. & Koskiniemi, M. 1999, "Progressive myoclonus epilepsy of Unverricht-Lundborg type", *Epilepsia,* vol. 40 Suppl 3, pp. 23-28.

Lehesjoki, A.E., Koskiniemi, M., Sistonen, P., Miao, J., Hastbacka, J., Norio, R. & de la Chapelle, A. 1991, "Localization of a gene for progressive myoclonus epilepsy to chromosome 21q22", *Proceedings of the National Academy of Sciences of the United States of America,* vol. 88, no. 9, pp. 3696-3699.

Lehtinen, M.K., Tegelberg, S., Schipper, H., Su, H., Zukor, H., Manninen, O., Kopra, O., Joensuu, T., Hakala, P., Bonni, A. & Lehesjoki, A.E. 2009, "Cystatin B deficiency sensitizes neurons to oxidative stress in progressive myoclonus epilepsy, EPM1", *The Journal of neuroscience : the official journal of the Society for Neuroscience,* vol. 29, no. 18, pp. 5910-5915.

Leist, M. & Jaattela, M. 2001, "Triggering of apoptosis by cathepsins", *Cell death and differentiation,* vol. 8, no. 4, pp. 324-326.

Lera, G., Scipioni, O., Garcia, S., Cammarota, A., Fischbein, G. & Gershanik, O. 2000, "A combined pattern of movement disorders resulting from posterolateral thalamic lesions of a vascular nature: a syndrome with clinico-radiologic correlation", *Movement disorders: official journal of the Movement Disorder Society,* vol. 15, no. 1, pp. 120-126.

Lerch, J.P. & Evans, A.C. 2005, "Cortical thickness analysis examined through power analysis and a population simulation", *NeuroImage,* vol. 24, no. 1, pp. 163-173.

Lerch, J.P., Pruessner, J.C., Zijdenbos, A., Hampel, H., Teipel, S.J. & Evans, A.C. 2005, "Focal decline of cortical thickness in Alzheimer's disease identified by computational neuroanatomy", *Cerebral cortex (New York, N.Y.: 1991),* vol. 15, no. 7, pp. 995-1001.

Levy, B.J. & Wagner, A.D. 2011, "Cognitive control and right ventrolateral prefrontal cortex: reflexive reorienting, motor inhibition, and action updating", *Annals of the New York Academy of Sciences,* vol. 1224, pp. 40-62.

Lieuallen, K., Pennacchio, L.A., Park, M., Myers, R.M. & Lennon, G.G. 2001, "Cystatin B-deficient mice have increased expression of apoptosis and glial activation genes", *Human molecular genetics,* vol. 10, no. 18, pp. 1867-1871.

Link, T.M., Majumdar, S., Grampp, S., Guglielmi, G., van Kuijk, C., Imhof, H., Glueer, C. & Adams, J.E. 1999, "Imaging of trabecular bone structure in osteoporosis", *European radiology,* vol. 9, no. 9, pp. 1781-1788.

Lisle, D.A., Monsour, P.A. & Maskiell, C.D. 2008, "Imaging of craniofacial fibrous dysplasia", *Journal of medical imaging and radiation oncology,* vol. 52, no. 4, pp. 325-332.

Luders, E., Narr, K.L., Thompson, P.M., Rex, D.E., Woods, R.P., Deluca, H., Jancke, L. & Toga, A.W. 2006, "Gender effects on cortical thickness and the influence of scaling", *Human brain mapping,* vol. 27, no. 4, pp. 314-324.

Ly, M., Motzkin, J.C., Philippi, C.L., Kirk, G.R., Newman, J.P., Kiehl, K.A. & Koenigs, M. 2012, "Cortical thinning in psychopathy", *The American Journal of Psychiatry,* vol. 169, no. 7, pp. 743-749.

Lynnerup, N., Astrup, J.G. & Sejrsen, B. 2005, "Thickness of the human cranial diploe in relation to age, sex and general body build", *Head & face medicine,* vol. 1, pp. 13.

Lyoo, C.H., Ryu, Y.H. & Lee, M.S. 2011, "Cerebral cortical areas in which thickness correlates with severity of motor deficits of Parkinson's disease", *Journal of neurology,* vol. 258, no. 10, pp. 1871-1876.

Magaudda, A., Ferlazzo, E., Nguyen, V.H. & Genton, P. 2006, "Unverricht-Lundborg disease, a condition with self-limited progression: long-term follow-up of 20 patients", *Epilepsia,* vol. 47, no. 5, pp. 860-866.

Magliulo, G., Parrotto, D., Zicari, A.M., Zappala, D., Lo Mele, L., Primicerio, P. & Marini, M. 2007, "Osteopathia striata-cranial sclerosis: otorhinolaryngologic clinical presentation and radiologic findings", *American Journal of Otolaryngology,* vol. 28, no. 1, pp. 59-63.

Maguire, E.A. 2001, "The retrosplenial contribution to human navigation: a review of lesion and neuroimaging findings", *Scandinavian Journal of Psychology,* vol. 42, no. 3, pp. 225-238.

Mahmoud-Ghoneim, D., Toussaint, G., Constans, J.M. & de Certaines, J.D. 2003, "Three dimensional texture analysis in MRI: a preliminary evaluation in gliomas", *Magnetic resonance imaging,* vol. 21, no. 9, pp. 983-987.

Mandelin, J., Hukkanen, M., Li, T.F., Korhonen, M., Liljeström, M., Sillat, T., Hanemaaijer, R., Salo, J., Santavirta, S. & Konttinen, Y.T. 2006, "Human osteoblasts produce cathepsin K", *Bone,* vol. 38, no. 6, pp. 769-777.

Mangion, J., Edkins, S., Goss, A.N., Stratton, M.R. & Flanagan, A.M. 2000, "Familial craniofacial fibrous dysplasia: absence of linkage to GNAS1 and the gene for cherubism", *Journal of medical genetics,* vol. 37, no. 11, pp. E37.

Manninen, O., Koskenkorva, P., Lehtimäki, K.K., Hyppönen, J., Könönen, M., Laitinen, T., Kalimo, H., Kopra, O., Kälviäinen, R., Gröhn, O., Lehesjoki, A.E. & Vanninen, R. 2013, "White Matter Degeneration with Unverricht-Lundborg Progressive Myoclonus Epilepsy: A Translational Diffusion-Tensor Imaging Study in Patients and Cystatin B-Deficient Mice", *Radiology,* vol. 269, no.1, pp. 232-239.

Manninen, O., Laitinen, T., Lehtimäki, K.K., Tegelberg, S., Lehesjoki, A.E., Gröhn, O. & Kopra, O. 2014, "Progressive volume loss and white matter degeneration in cstb-deficient mice: a diffusion tensor and longitudinal volumetry MRI study", *PloS one,* vol. 9, no. 3, pp. e90709.

Marden, F.A. & Wippold, F.J.,2nd 2004, "MR imaging features of craniodiaphyseal dysplasia", *Pediatric radiology,* vol. 34, no. 2, pp. 167-170.

Mascalchi, M., Michelucci, R., Cosottini, M., Tessa, C., Lolli, F., Riguzzi, P., Lehesjoki, A.E., Tosetti, M., Villari, N. & Tassinari, C.A. 2002, "Brainstem involvement in Unverricht-Lundborg disease (EPM1): An MRI and (1)H MRS study", *Neurology,* vol. 58, no. 11, pp. 1686-1689.

Materka, A. & Strzelecki, M. 1998, "Texture Analysis Methods – A Review", *Technical University of Iodz, Institute of Electronics, COST B11 Report.*

May, H., Peled, N., Dar, G., Cohen, H., Abbas, J., Medlej, B. & Hershkovitz, I. 2011, "Hyperostosis frontalis interna: criteria for sexing and aging a skeleton", *International journal of legal medicine,* vol. 125, no. 5, pp. 669-673.

Mayerhoefer, M.E., Schima, W., Trattnig, S., Pinker, K., Berger-Kulemann, V. & Ba-Ssalamah, A. 2010, "Texture-based classification of focal liver lesions on MRI at 3.0 Tesla: a feasibility study in cysts and hemangiomas", *Journal of magnetic resonance imaging: JMRI,* vol. 32, no. 2, pp. 352-359.

Mazarib, A., Xiong, L., Neufeld, M.Y., Birnbaum, M., Korczyn, A.D., Pandolfo, M. & Berkovic, S.F. 2001, "Unverricht-Lundborg disease in a five-generation Arab family: instability of dodecamer repeats", *Neurology,* vol. 57, no. 6, pp. 1050-1054.

Mazziotta, J., Toga, A., Evans, A., Fox, P., Lancaster, J., Zilles, K., Woods, R., Paus, T., Simpson, G., Pike, B., Holmes, C., Collins, L., Thompson, P., MacDonald, D., Iacoboni, M., Schormann, T., Amunts, K., Palomero-Gallagher, N., Geyer, S., Parsons, L., Narr, K., Kabani, N., Le Goualher, G., Boomsma, D., Cannon, T., Kawashima, R. & Mazoyer, B. 2001, "A probabilistic atlas and reference system for the human brain: International Consortium for Brain Mapping (ICBM)", *Philosophical transactions of the Royal Society of London. Series B, Biological sciences,* vol. 356, no. 1412, pp. 1293-1322.

McGinnis, S.M., Brickhouse, M., Pascual, B. & Dickerson, B.C. 2011, "Age-related changes in the thickness of cortical zones in humans", *Brain topography,* vol. 24, no. 3-4, pp. 279-291.

Mellado, J.M., Ramos, A., Salvado, E., Camins, A., Danus, M. & Sauri, A. 2003, "Accessory ossicles and sesamoid bones of the ankle and foot: imaging findings, clinical

significance and differential diagnosis", *European radiology,* vol. 13 Suppl 4, pp. L164-77.

Mervaala, E., Andermann, F., Quesney, L.F. & Krelina, M. 1990, "Common dopaminergic mechanism for epileptic photosensitivity in progressive myoclonus epilepsies", *Neurology,* vol. 40, no. 1, pp. 53-56.

Mills, K.L. & Johnston, A.W. 1988, "Pycnodysostosis", *Journal of medical genetics,* vol. 25, no. 8, pp. 550-553.

Morava, E., Illes, T., Weisenbach, J., Karteszi, J. & Kosztolanyi, G. 2003, "Clinical and genetic heterogeneity in frontometaphyseal dysplasia: severe progressive scoliosis in two families", *American journal of medical genetics. Part A,* vol. 116A, no. 3, pp. 272-277.

Morko, J., Kiviranta, R., Hurme, S., Rantakokko, J. & Vuorio, E. 2005, "Differential turnover of cortical and trabecular bone in transgenic mice overexpressing cathepsin K", *Bone,* vol. 36, no. 5, pp. 854-865.

Morko, J., Kiviranta, R., Mulari, M.T., Ivaska, K.K., Väänänen, H.K., Vuorio, E. & Laitala-Leinonen, T. 2009, "Overexpression of cathepsin K accelerates the resorption cycle and osteoblast differentiation in vitro", *Bone,* vol. 44, no. 4, pp. 717-728.

Moulard, B., Genton, P., Grid, D., Jeanpierre, M., Ouazzani, R., Mrabet, A., Morris, M., LeGuern, E., Dravet, C., Mauguiere, F., Utermann, B., Baldy-Moulinier, M., Belaidi, H., Bertran, F., Biraben, A., Ali Cherif, A., Chkili, T., Crespel, A., Darcel, F., Dulac, O., Geny, C., Humbert-Claude, V., Kassiotis, P., Buresi, C. & Malafosse, A. 2002, "Haplotype study of West European and North African Unverricht-Lundborg chromosomes: evidence for a few founder mutations", *Human genetics,* vol. 111, no. 3, pp. 255-262.

Mulari, M.T., Qu, Q., Härkönen, P.L. & Väänänen, H.K. 2004, "Osteoblast-like cells complete osteoclastic bone resorption and form new mineralized bone matrix in vitro", *Calcified tissue international,* vol. 75, no. 3, pp. 253-261.

Murray, E.A., Bussey, T.J. & Saksida, L.M. 2007, "Visual perception and memory: a new view of medial temporal lobe function in primates and rodents", *Annual Review of Neuroscience,* vol. 30, pp. 99-122.

Narayan, V.M., Narr, K.L., Kumari, V., Woods, R.P., Thompson, P.M., Toga, A.W. & Sharma, T. 2007, "Regional cortical thinning in subjects with violent antisocial personality disorder or schizophrenia", *The American Journal of Psychiatry,* vol. 164, no. 9, pp. 1418-1427.

Ng, F., Ganeshan, B., Kozarski, R., Miles, K.A. & Goh, V. 2013, "Assessment of primary colorectal cancer heterogeneity by using whole-tumor texture analysis: contrast-enhanced CT texture as a biomarker of 5-year survival", *Radiology,* vol. 266, no. 1, pp. 177-184.

Nobauer, I. & Uffmann, M. 2005, "Differential diagnosis of focal and diffuse neoplastic diseases of bone marrow in MRI", *European Journal of Radiology,* vol. 55, no. 1, pp. 2-32.

Nokelainen, P., Heiskala, H., Lehesjoki, A.E. & Kaski, M. 2000, "A patient with 2 different repeat expansion mutations", *Archives of Neurology,* vol. 57, no. 8, pp. 1199-1203.

Norio, R. & Koskiniemi, M. 1979, "Progressive myoclonus epilepsy: genetic and nosological aspects with special reference to 107 Finnish patients", *Clinical genetics,* vol. 15, no. 5, pp. 382-398.

O'Doherty, J.P. 2011, "Contributions of the ventromedial prefrontal cortex to goal-directed action selection", *Annals of the New York Academy of Sciences,* vol. 1239, pp. 118-129.

O'Reilly, M.A. & Shaw, D.G. 1994, "Hajdu-Cheney syndrome", *Annals of the Rheumatic Diseases,* vol. 53, no. 4, pp. 276-279.

Pardoe, H.R., Berg, A.T. & Jackson, G.D. 2013, "Sodium valproate use is associated with reduced parietal lobe thickness and brain volume", *Neurology,* vol. 80, no. 20, pp. 1895-1900.

Parmeggiani, A., Lehesjoki, A.E., Carelli, V., Posar, A., Santi, A., Santucci, M., Gobbi, G., Pini, A. & Rossi, P.G. 1997, "Familial Unverricht-Lundborg disease: a clinical, neurophysiologic, and genetic study", *Epilepsia,* vol. 38, no. 6, pp. 637-641.

Paus, T. 2001, "Primate anterior cingulate cortex: where motor control, drive and cognition interface", *Nature reviews.Neuroscience,* vol. 2, no. 6, pp. 417-424.

Pennacchio, L.A., Bouley, D.M., Higgins, K.M., Scott, M.P., Noebels, J.L. & Myers, R.M. 1998, "Progressive ataxia, myoclonic epilepsy and cerebellar apoptosis in cystatin B-deficient mice", *Nature genetics,* vol. 20, no. 3, pp. 251-258.

Pennacchio, L.A., Lehesjoki, A.E., Stone, N.E., Willour, V.L., Virtaneva, K., Miao, J., D'Amato, E., Ramirez, L., Faham, M., Koskiniemi, M., Warrington, J.A., Norio, R., de la Chapelle, A., Cox, D.R. & Myers, R.M. 1996, "Mutations in the gene encoding cystatin B in progressive myoclonus epilepsy (EPM1)", *Science (New York, N.Y.),* vol. 271, no. 5256, pp. 1731-1734.

Piredda, S. & Gale, K. 1985, "A crucial epileptogenic site in the deep prepiriform cortex", *Nature,* vol. 317, no. 6038, pp. 623-625.

Raad, M.S. & Beighton, P. 1978, "Autosomal recessive inheritance of metaphyseal dysplasia (Pyle disease)", *Clinical genetics,* vol. 14, no. 5, pp. 251-256.

Rachner, T.D., Khosla, S. & Hofbauer, L.C. 2011, "Osteoporosis: now and the future", *Lancet,* vol. 377, no. 9773, pp. 1276-1287.

Raine, A., Laufer, W.S., Yang, Y., Narr, K.L., Thompson, P. & Toga, A.W. 2012, "Increased executive functioning, attention, and cortical thickness in white-collar criminals", *Human brain mapping,* vol. 33, no. 12, pp. 2932-2940.

Ralston, S.H. & Layfield, R. 2012, "Pathogenesis of Paget disease of bone", *Calcified tissue international,* vol. 91, no. 2, pp. 97-113.

Ramnani, N. & Owen, A.M. 2004, "Anterior prefrontal cortex: insights into function from anatomy and neuroimaging", *Nature Reviews Neuroscience,* vol. 5, pp. 184-194.

Reichenberger, E., Tiziani, V., Watanabe, S., Park, L., Ueki, Y., Santanna, C., Baur, S.T., Shiang, R., Grange, D.K., Beighton, P., Gardner, J., Hamersma, H., Sellars, S., Ramesar, R., Lidral, A.C., Sommer, A., Raposo do Amaral, C.M., Gorlin, R.J., Mulliken, J.B. & Olsen, B.R. 2001, "Autosomal dominant craniometaphyseal dysplasia is caused by mutations in the transmembrane protein ANK", *American Journal of Human Genetics,* vol. 68, no. 6, pp. 1321-1326.

Rinne, R., Saukko, P., Järvinen, M. & Lehesjoki, A.E. 2002, "Reduced cystatin B activity correlates with enhanced cathepsin activity in progressive myoclonus epilepsy", *Annals of Medicine,* vol. 34, no. 5, pp. 380-385.

Robbins, T.W. & Arnsten, A.F. 2009, "The neuropsychopharmacology of fronto-executive function: monoaminergic modulation", *Annual Review of Neuroscience,* vol. 32, pp. 267-287.

Robertson, S.P., Jenkins, Z.A., Morgan, T., Ades, L., Aftimos, S., Boute, O., Fiskerstrand, T., Garcia-Minaur, S., Grix, A., Green, A., Der Kaloustian, V., Lewkonia, R., McInnes, B., van Haelst, M.M., Mancini, G., Illes, T., Mortier, G., Newbury-Ecob, R., Nicholson, L., Scott, C.I., Ochman, K., Brozek, I., Shears, D.J., Superti-Furga, A., Suri, M., Whiteford, M., Wilkie, A.O. & Krakow, D. 2006, "Frontometaphyseal dysplasia: mutations in FLNA and phenotypic diversity", *American journal of medical genetics. Part A,* vol. 140, no. 16, pp. 1726-1736.

Roivainen, R., Karvonen, M.K. & Puumala, T. 2014, "Seizure control in Unverricht-Lundborg disease: a single-centre study", *Epileptic disorders: international epilepsy journal with videotape,* vol. 16, no. 2, pp. 191-195.

Ross, A.H., Jantz, R.L. & McCormick, W.F. 1998, "Cranial thickness in American females and males", *Journal of forensic sciences,* vol. 43, no. 2, pp. 267-272.

Saftig, P., Hunziker, E., Wehmeyer, O., Jones, S., Boyde, A., Rommerskirch, W., Moritz, J.D., Schu, P. & von Figura, K. 1998, "Impaired osteoclastic bone resorption leads to osteopetrosis in cathepsin-K-deficient mice", *Proceedings of the National Academy of Sciences of the United States of America,* vol. 95, no. 23, pp. 13453-13458.

Sakagami, M. & Pan, X. 2007, "Functional role of the ventrolateral prefrontal cortex in decision making", *Current opinion in neurobiology,* vol. 17, no. 2, pp. 228-233.

Salat, D.H., Buckner, R.L., Snyder, A.Z., Greve, D.N., Desikan, R.S., Busa, E., Morris, J.C., Dale, A.M. & Fischl, B. 2004, "Thinning of the cerebral cortex in aging", *Cerebral cortex (New York, N.Y.: 1991),* vol. 14, no. 7, pp. 721-730.

Santoshkumar, B., Turnbull, J. & Minassian, B.A. 2008, "Unverricht-Lundborg progressive myoclonus epilepsy in Oman", *Pediatric neurology,* vol. 38, no. 4, pp. 252-255.

Schoenbaum, G., Takahashi, Y., Liu, T.L. & McDannald, M.A. 2011, "Does the orbitofrontal cortex signal value?", *Annals of the New York Academy of Sciences,* vol. 1239, pp. 87-99.

Shahwan, A., Farrell, M. & Delanty, N. 2005, "Progressive myoclonic epilepsies: a review of genetic and therapeutic aspects", *Lancet neurology,* vol. 4, no. 4, pp. 239-248.

Shannon, P., Pennacchio, L.A., Houseweart, M.K., Minassian, B.A. & Myers, R.M. 2002, "Neuropathological changes in a mouse model of progressive myoclonus epilepsy: cystatin B deficiency and Unverricht-Lundborg disease", *Journal of neuropathology and experimental neurology,* vol. 61, no. 12, pp. 1085-1091.

Shaw, P., Lerch, J.P., Pruessner, J.C., Taylor, K.N., Rose, A.B., Greenstein, D., Clasen, L., Evans, A., Rapoport, J.L. & Giedd, J.N. 2007, "Cortical morphology in children and adolescents with different apolipoprotein E gene polymorphisms: an observational study", *Lancet neurology,* vol. 6, no. 6, pp. 494-500.

She, R. & Szakacs, J. 2004, "Hyperostosis frontalis interna: case report and review of literature", *Annals of Clinical and Laboratory Science,* vol. 34, no. 2, pp. 206-208.

Shields, W.D. 2004, "Diagnosis of infantile spasms, Lennox-Gastaut syndrome, and progressive myoclonic epilepsy", *Epilepsia,* vol. 45 Suppl 5, pp. 2-4.

Shintani, S., Tsuruoka, S. & Shiigai, T. 2000, "Pure sensory stroke caused by a cerebral hemorrhage: clinical-radiologic correlations in seven patients", *AJNR. American journal of neuroradiology,* vol. 21, no. 3, pp. 515-520.

Sikiö, M., Holli, K.K., Harrison, L.C., Ruottinen, H., Rossi, M., Helminen, M.T., Ryymin, P., Paalavuo, R., Soimakallio, S., Eskola, H.J., Elovaara, I. & Dastidar, P. 2011, "Parkinson's disease: interhemispheric textural differences in MR images", *Academic Radiology,* vol. 18, no. 10, pp. 1217-1224.

Simpson, M.A., Irving, M.D., Asilmaz, E., Gray, M.J., Dafou, D., Elmslie, F.V., Mansour, S., Holder, S.E., Brain, C.E., Burton, B.K., Kim, K.H., Pauli, R.M., Aftimos, S., Stewart, H., Kim, C.A., Holder-Espinasse, M., Robertson, S.P., Drake, W.M. & Trembath, R.C. 2011, "Mutations in NOTCH2 cause Hajdu-Cheney syndrome, a disorder of severe and progressive bone loss", *Nature genetics,* vol. 43, no. 4, pp. 303-305.

Sled, J.G., Zijdenbos, A.P. & Evans, A.C. 1998, "A nonparametric method for automatic correction of intensity nonuniformity in MRI data", *IEEE Transactions on Medical Imaging,* vol. 17, no. 1, pp. 87-97.

Smith, E.E. & Jonides, J. 1999, "Storage and executive processes in the frontal lobes", *Science (New York, N.Y.),* vol. 283, no. 5408, pp. 1657-1661.

Smith, S.E., Murphey, M.D., Motamedi, K., Mulligan, M.E., Resnik, C.S. & Gannon, F.H. 2002, "From the archives of the AFIP. Radiologic spectrum of Paget disease of bone and its complications with pathologic correlation", *Radiographics: a review publication of the Radiological Society of North America, Inc,* vol. 22, no. 5, pp. 1191-1216.

Smith, S.M. 2002, "Fast robust automated brain extraction", *Human brain mapping,* vol. 17, no. 3, pp. 143-155.

Smythies, J. 1997, "The functional neuroanatomy of awareness: with a focus on the role of various anatomical systems in the control of intermodal attention", *Consciousness and cognition,* vol. 6, no. 4, pp. 455-481.

Sowell, E.R., Peterson, B.S., Kan, E., Woods, R.P., Yoshii, J., Bansal, R., Xu, D., Zhu, H., Thompson, P.M. & Toga, A.W. 2007, "Sex differences in cortical thickness mapped in 176 healthy individuals between 7 and 87 years of age", *Cerebral cortex (New York, N.Y.: 1991),* vol. 17, no. 7, pp. 1550-1560.

Staehling-Hampton, K., Proll, S., Paeper, B.W., Zhao, L., Charmley, P., Brown, A., Gardner, J.C., Galas, D., Schatzman, R.C., Beighton, P., Papapoulos, S., Hamersma, H. & Brunkow, M.E. 2002, "A 52-kb deletion in the SOST-MEOX1 intergenic region on 17q12-q21 is associated with van Buchem disease in the Dutch population", *American Journal of Medical Genetics,* vol. 110, no. 2, pp. 144-152.

Szczypinski, P.M., Strzelecki, M., Materka, A. & Klepaczko, A. 2009, "MaZda--a software package for image texture analysis", *Computer methods and programs in biomedicine,* vol. 94, no. 1, pp. 66-76.

Tai, K.K. & Truong, D.D. 2005, "Post-hypoxic myoclonus induces Fos expression in the reticular thalamic nucleus and neurons in the brainstem", *Brain research,* vol. 1059, no. 2, pp. 122-128.

Tau, C., Mautalen, C., Casco, C., Alvarez, V. & Rubinstein, M. 2004, "Chronic idiopathic hyperphosphatasia: normalization of bone turnover with cyclical intravenous pamidronate therapy", *Bone,* vol. 35, no. 1, pp. 210-216.

Tegelberg, S. 2013, "Early pathological changes in the mouse model for progressive myoclonus epilepsy of Unverricht-Lundborg type, EPM1", *University of Helsinki.*

Tegelberg, S., Kopra, O., Joensuu, T., Cooper, J.D. & Lehesjoki, A.E. 2012, "Early Microglial Activation Precedes Neuronal Loss in the Brain of the Cstb-/- Mouse Model of Progressive Myoclonus Epilepsy, EPM1", *Journal of neuropathology and experimental neurology,* vol. 71, no. 1, pp. 40-53.

Thambisetty, M., Wan, J., Carass, A., An, Y., Prince, J.L. & Resnick, S.M. 2010, "Longitudinal changes in cortical thickness associated with normal aging", *NeuroImage,* vol. 52, no. 4, pp. 1215-1223.

Tohka, J., Zijdenbos, A. & Evans, A. 2004, "Fast and robust parameter estimation for statistical partial volume models in brain MRI", *NeuroImage,* vol. 23, no. 1, pp. 84-97.

Tosun, D., Caplan, R., Siddarth, P., Seidenberg, M., Gurbani, S., Toga, A.W. & Hermann, B. 2011a, "Intelligence and cortical thickness in children with complex partial seizures", *NeuroImage,* vol. 57, no. 2, pp. 337-345.

Tosun, D., Siddarth, P., Toga, A.W., Hermann, B. & Caplan, R. 2011b, "Effects of childhood absence epilepsy on associations between regional cortical morphometry and aging and cognitive abilities", *Human brain mapping,* vol. 32, no. 4, pp. 580-591.

Tourassi, G.D. 1999, "Journey toward computer-aided diagnosis: role of image texture analysis", *Radiology,* vol. 213, no. 2, pp. 317-320.

Tuceryan, M. & Jain, A.K. 1998, "The Handbook of Pattern Recognition and Computer Vision (2nd Edition)", eds. C. H. Chen, L. F. Pau, P. S. P. Wang, pp. 207-248. *World Scientific Publishing Co.*

Turner, R.S. & Desmurget, M. 2010, "Basal ganglia contributions to motor control: a vigorous tutor", *Current opinion in neurobiology,* vol. 20, no. 6, pp. 704-716.

Ueno, M., Takaso, M., Nakazawa, T., Imura, T., Saito, W., Shintani, R., Uchida, K., Fukuda, M., Takahashi, K., Ohtori, S., Kotani, T. & Minami, S. 2011, "A 5-year epidemiological study on the prevalence rate of idiopathic scoliosis in Tokyo: school screening of more than 250,000 children", *Journal of orthopaedic science: official journal of the Japanese Orthopaedic Association,* vol. 16, no. 1, pp. 1-6.

van Kaick, G. & Delorme, S. 2005, "Computed tomography in various fields outside medicine", *European radiology,* vol. 15 Suppl 4, pp. D74-81.

Vanhoenacker, F.M., Balemans, W., Tan, G.J., Dikkers, F.G., De Schepper, A.M., Mathysen, D.G., Bernaerts, A. & Hul, W.V. 2003, "Van Buchem disease: lifetime evolution of radioclinical features", *Skeletal radiology,* vol. 32, no. 12, pp. 708-718.

Vann, S.D., Aggleton, J.P. & Maguire, E.A. 2009, "What does the retrosplenial cortex do?", *Nature reviews. Neuroscience,* vol. 10, no. 11, pp. 792-802.

Virtaneva, K., D'Amato, E., Miao, J., Koskiniemi, M., Norio, R., Avanzini, G., Franceschetti, S., Michelucci, R., Tassinari, C.A., Omer, S., Pennacchio, L.A., Myers, R.M., Dieguez-Lucena, J.L., Krahe, R., de la Chapelle, A. & Lehesjoki, A.E. 1997, "Unstable

minisatellite expansion causing recessively inherited myoclonus epilepsy, EPM1", *Nature genetics,* vol. 15, no. 4, pp. 393-396.

Vuorinen, M., Kåreholt, I., Julkunen, V., Spulber, G., Niskanen, E., Paajanen, T., Soininen, H., Kivipelto, M. & Solomon, A. 2013, "Changes in vascular factors 28 years from midlife and late-life cortical thickness", *Neurobiology of aging,* vol. 34, no. 1, pp. 100-109.

Wallis, J.D. & Kennerley, S.W. 2011, "Contrasting reward signals in the orbitofrontal cortex and anterior cingulate cortex", *Annals of the New York Academy of Sciences,* vol. 1239, pp. 33-42.

Wechsler, D. 1981, "WAIS-R Manual", *Psychological Corp., New York, NY.*

Weinstein, L.S., Shenker, A., Gejman, P.V., Merino, M.J., Friedman, E. & Spiegel, A.M. 1991, "Activating mutations of the stimulatory G protein in the McCune-Albright syndrome", *The New England journal of medicine,* vol. 325, no. 24, pp. 1688-1695.

Whyte, M.P., Obrecht, S.E., Finnegan, P.M., Jones, J.L., Podgornik, M.N., McAlister, W.H. & Mumm, S. 2002, "Osteoprotegerin deficiency and juvenile Paget's disease", *The New England journal of medicine,* vol. 347, no. 3, pp. 175-184.

Xia, L., Kilb, J., Wex, H., Li, Z., Lipyansky, A., Breuil, V., Stein, L., Palmer, J.T., Dempster, D.W. & Bromme, D. 1999, "Localization of rat cathepsin K in osteoclasts and resorption pits: inhibition of bone resorption and cathepsin K-activity by peptidyl vinyl sulfones", *Biological chemistry,* vol. 380, no. 6, pp. 679-687.

Yang, D.S., Stavrides, P., Mohan, P.S., Kaushik, S., Kumar, A., Ohno, M., Schmidt, S.D., Wesson, D., Bandyopadhyay, U., Jiang, Y., Pawlik, M., Peterhoff, C.M., Yang, A.J., Wilson, D.A., St George-Hyslop, P., Westaway, D., Mathews, P.M., Levy, E., Cuervo, A.M. & Nixon, R.A. 2011, "Reversal of autophagy dysfunction in the TgCRND8 mouse model of Alzheimer's disease ameliorates amyloid pathologies and memory deficits", *Brain: a journal of neurology,* vol. 134, no. Pt 1, pp. 258-277.

Yin, H.H. & Knowlton, B.J. 2006, "The role of the basal ganglia in habit formation", *Nature reviews. Neuroscience,* vol. 7, no. 6, pp. 464-476.

Yu, O., Mauss, Y., Namer, I.J. & Chambron, J. 2001, "Existence of contralateral abnormalities revealed by texture analysis in unilateral intractable hippocampal epilepsy", *Magnetic resonance imaging,* vol. 19, no. 10, pp. 1305-1310.

Zesiewicz, T.A., Shaw, J.D., Allison, K.G., Staffetti, J.S., Okun, M.S. & Sullivan, K.L. 2013, "Update on treatment of essential tremor", *Current treatment options in neurology,* vol. 15, no. 4, pp. 410-423.

Zhang, J., Yu, C., Jiang, G., Liu, W. & Tong, L. 2012, "3D texture analysis on MRI images of Alzheimer's disease", *Brain imaging and behavior,* vol. 6, no. 1, pp. 61-69.

Zhang, Y. 2012, "MRI texture analysis in multiple sclerosis", *International journal of biomedical imaging,* vol. 2012, Article ID 762804.

Zijdenbos, A. 1998, "Automated quantification of MS lesions in 3D MRI brain data sets; validitation of INSECT", *Medical Image Computing and Computer Assisted Intervention – MICCAI, 1496,* pp. 439-448.

Zilles, K. & Amunts, K. 2010, "Centenary of Brodmann's map – conception and fate", *Nature reviews. Neuroscience,* vol. 11, no. 2, pp. 139-145.

Sanna Suoranta

Skeletal and Neuroradiological Findings Related to Unverricht-Lundborg Disease (EPM1)

EPM1 is a rare progressive neurodegenerative disorder with no specific cure. Mutations in the CSTB gene are responsible for the primary defect in EPM1. The study revealed that EPM1 patients exhibit thickening of the skull and various bone abnormalities that link the CSTB mutation to bone metabolism. In visual assessment of MR images, focal brain abnormalities were not found but cortical thickness analysis (CTH) and texture analysis (TA) revealed subtle brain changes in patients with EPM1

UNIVERSITY OF EASTERN FINLAND

Publications of the University of Eastern Finland

Dissertations in Health Sciences

ISBN 978-952-61-1706-5